区域气候–化学–生态耦合模式与模拟

王体健 徐北瑶 马丹阳 谢南洪 张芊 宋荣
南京大学大气科学学院

2023.7.27，南京

报告提纲

- 研究背景
- 模式发展
- 应用研究
- 总结展望

空气污染与气候系统的相互作用

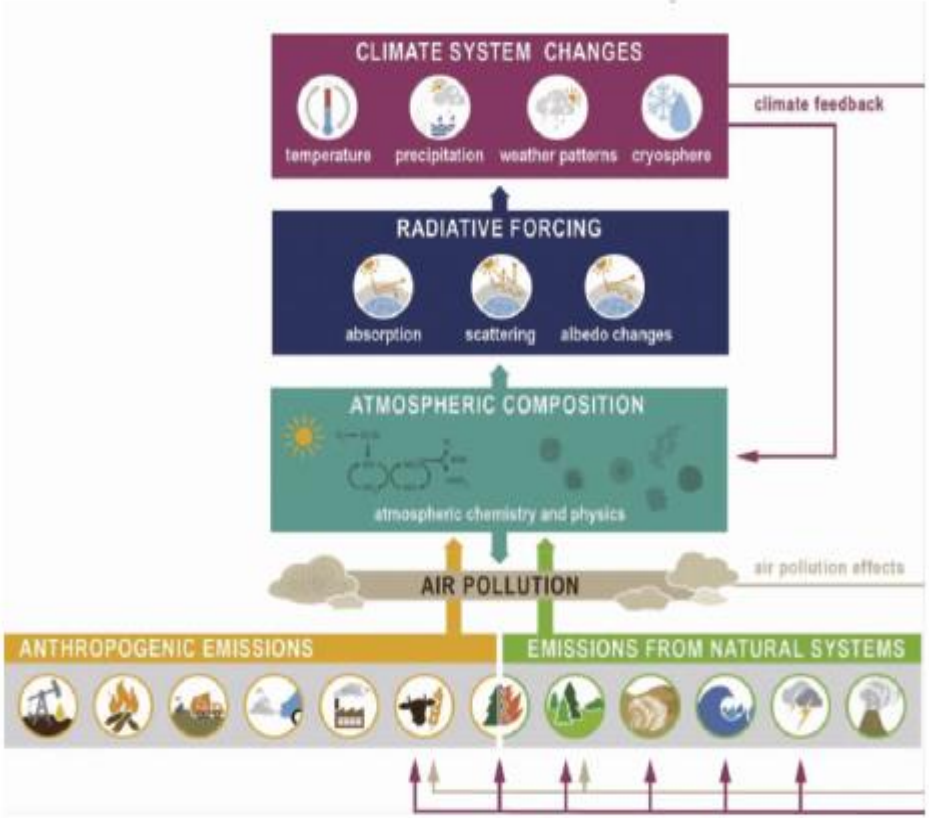

图 1　空气污染与气候系统的相互作用(来源: IPCC AR6 WGI 报告,图 6.1)

IPCC AR6　　(廖宏，2021)

会经济协调发展的重要研究领域。大气中短寿命的化学物质臭氧和气溶胶(大气中液态或固态的颗粒物)对人体健康和生态系统有着直接的危害,是当前空气污染治理的主要对象(UNEP and WMO, 2011)。同时这些化学物质还是仅次于长寿命温室气体(二氧化碳、氧化亚氮等)影响气候变化的重要大气成分。对流层臭氧是温室气体,引起气候增暖。气溶胶吸收、散射短波和长波辐射(气溶胶-辐射相互作用),还作为云凝结核影响云的辐射特性、云的生命史及降水特性(气溶胶-云相互作用),从而导致气候变化。

气候变化可通过影响物理、化学和生物过程从而对大气污染物产生影响。气象条件变化改变大气污染物的传输(通过大气阻塞事件的发生和持续时间、大气边界层的通风条件、平流层-对流层交换(STE)等方式)、二次污染物的化学反应速率以及降水对气溶胶的湿清除,对大气污染物浓度有很大的影响(Hou et al.,2018)。气候变化也影响动态植被以及相应的 BVOCs 排放。

空气污染和气候变化对作物的影响

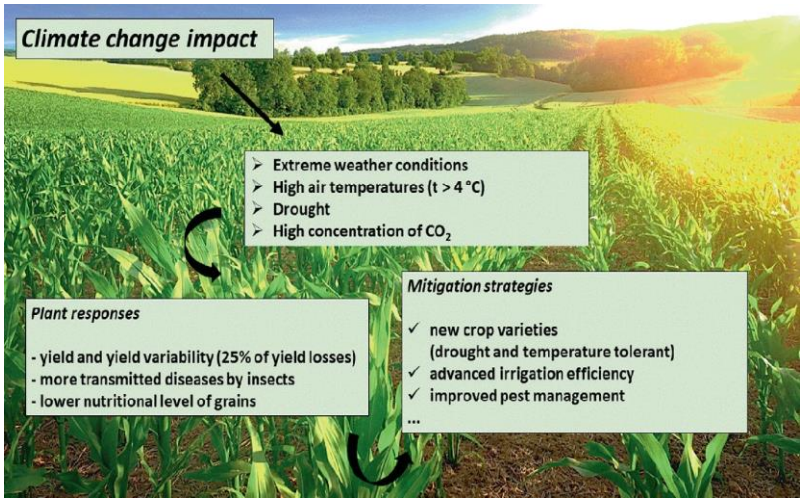

（Žarković and Radovanović, 2022）

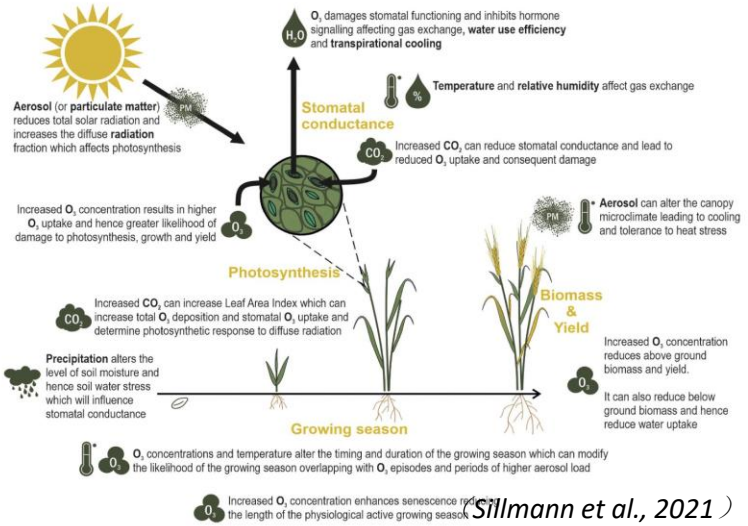

（Sillmann et al., 2021）

✓ 气候变化：通过温度升高、降水模式、极端天气和气候事件频率和CO_2浓度变化等影响作物产量和品质。

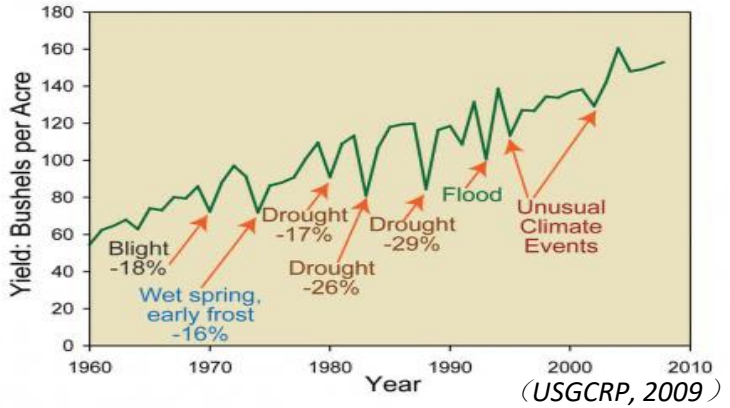

（USGCRP, 2009）

✓ 空气污染：O_3进入叶片气孔导致作物功能性叶片受损， $PM_{2.5}$通过改变辐射、降水等影响光合作用。

（Tian et al. 2016）

Chapter 8: Anthropogenic and Natural Radiative Forcing

Coordinating Lead Authors: Gunnar Myhre (Norway), Drew Shindell (USA)

Lead Authors: François-Marie Bréon (France), William Collins (UK), Jan Fuglestvedt (Norway), Jianping Huang (China), Dorothy Koch (USA), Jean-François Lamarque (USA), David Lee (UK), Blanca Mendoza (Mexico), Teruyuki Nakajima (Japan), Alan Robock (USA), Graeme Stephens (USA), Toshihiko Takemura (Japan), Hua Zhang (China)

Contributing Authors: Olivier Boucher (France), Stig B. Dalsoren (Norway), John S. Daniel (USA), Piers Forster (UK), Claire Granier (France), Joanna Haigh (UK), Øivind Hodnebrog (Norway), Jed O. Kaplan (Switzerland/Belgium/USA), Brian C. O'Neill (USA), Claus J. Nielsen (Norway), George Marston (UK), Glen P. Peters (Norway), Julia Pongratz (Germany), Michael Prather (USA), Venkatachalam Ramaswamy (USA), Raphael Roth (Switzerland), Leon Rotstayn (Australia), Steven J. Smith (USA), David Stevenson (UK), Jean-Paul Vernier (USA), Paul Young (USA), Oliver Wild (UK), Borgar Aamaas (Norway)

Review Editors: Daniel Jacob (USA), A.R. Ravishankara (USA), Keith Shine (UK)

Date of Draft: 7 June 2013

Table of Contents:

AR1
1994

AR2
1996

AR3
2001

AR4
2007

AR5
2013

AR6
2021

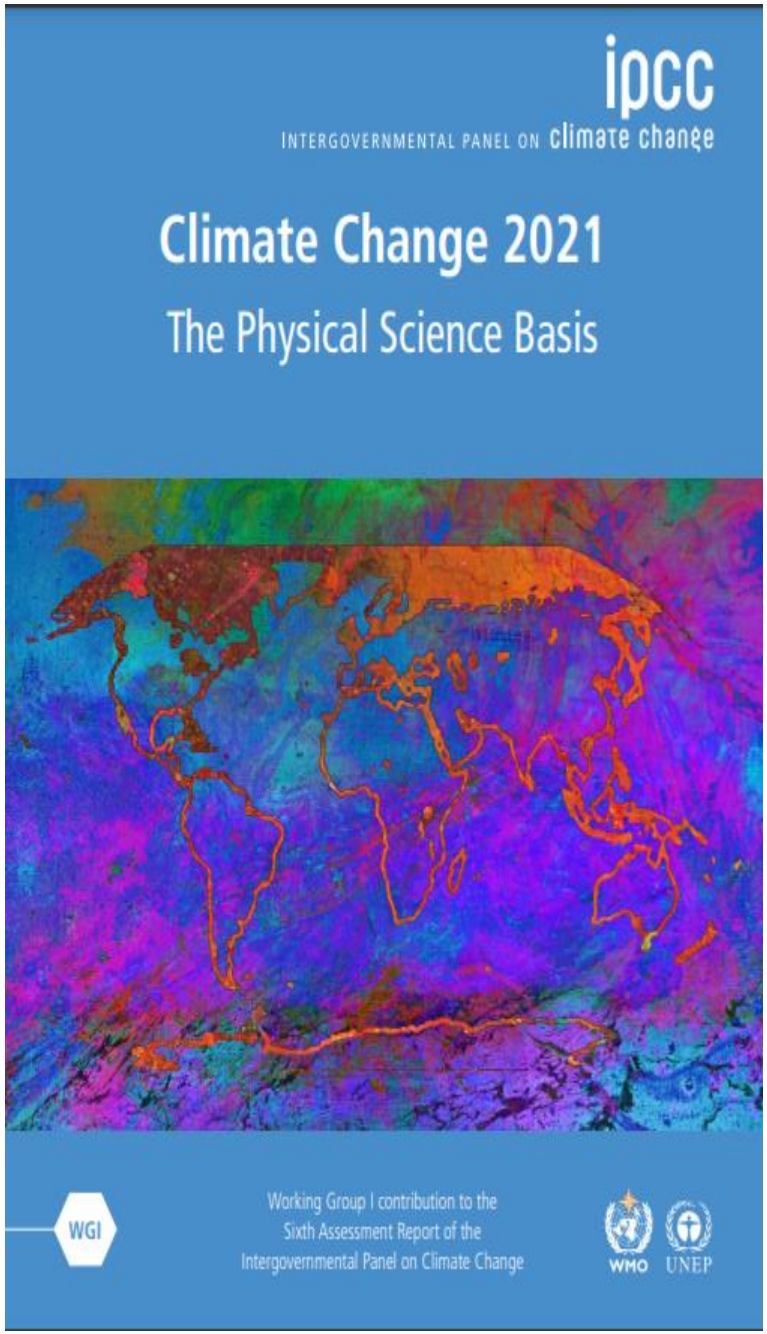

DOI: 10.12006/j.issn.1673-1719.2021.191

张华，王菲，赵树云，等．IPCC AR6 报告解读：地球能量收支、气候反馈和气候敏感度 [J]. 气候变化研究进展，2021, 17 (6): 691-698

Zhang H, Wang F, Zhao S Y, *et al*. Earth's energy budget, climate feedbacks, and climate sensitivity [J]. Climate Change Research, 2021, 17 (6): 691-698

IPCC AR6 报告解读：地球能量收支、气候反馈和气候敏感度

张 华[1,2,3]，王 菲[2,1]，赵树云[3,2]，谢 冰[4]

1 中国气象科学研究院灾害天气国家重点实验室，北京 100081；
2 南京信息工程大学气象灾害预报预警与评估协同创新中心，南京 210044；
3 中国地质大学环境学院大气科学系，武汉 430078；
4 中国气象局－南京大学气候预测研究联合实验室，北京 100081

摘 要：文中对 IPCC 第六次评估报告（AR6）第一工作组（WGI）报告的第七章关于地球能量收支、气候反馈和气候敏感度中的重要内容进行了凝练，并简要总结该方面的最新研究成果和结论。评估显示，自工业革命以来，人类活动造成的有效辐射强迫（ERF）为 2.72 [1.96 ~ 3.48] W/m^2，其中，均匀混合温室气体的贡献为 3.32 [3.03 ~ 3.61] W/m^2，气溶胶的贡献为 −1.1 [−1.7 ~ −0.4] W/m^2。净的气候反馈参数为 −1.16 [−1.81 ~ −0.51] W/(m^2·℃)，云仍然是气候反馈整体不确定性的最大来源。平衡态气候敏感度（ECS）和瞬态气候响应（TCR）可用于评估全球平均地表气温对强迫的响应，是衡量全球气候响应的有效手段。ECS 和 TCR 的最佳估计分别为 3.0 [2.0 ~ 5.0]℃和 1.8 [1.2 ~ 2.4]℃。

关键词：有效辐射强迫（ERF），气候反馈，平衡态气候敏感度（ECS），瞬态气候响应（TCR）

1750—2019年不同因子的有效辐射强迫的变化和不确定性（置信区间5%~95%）

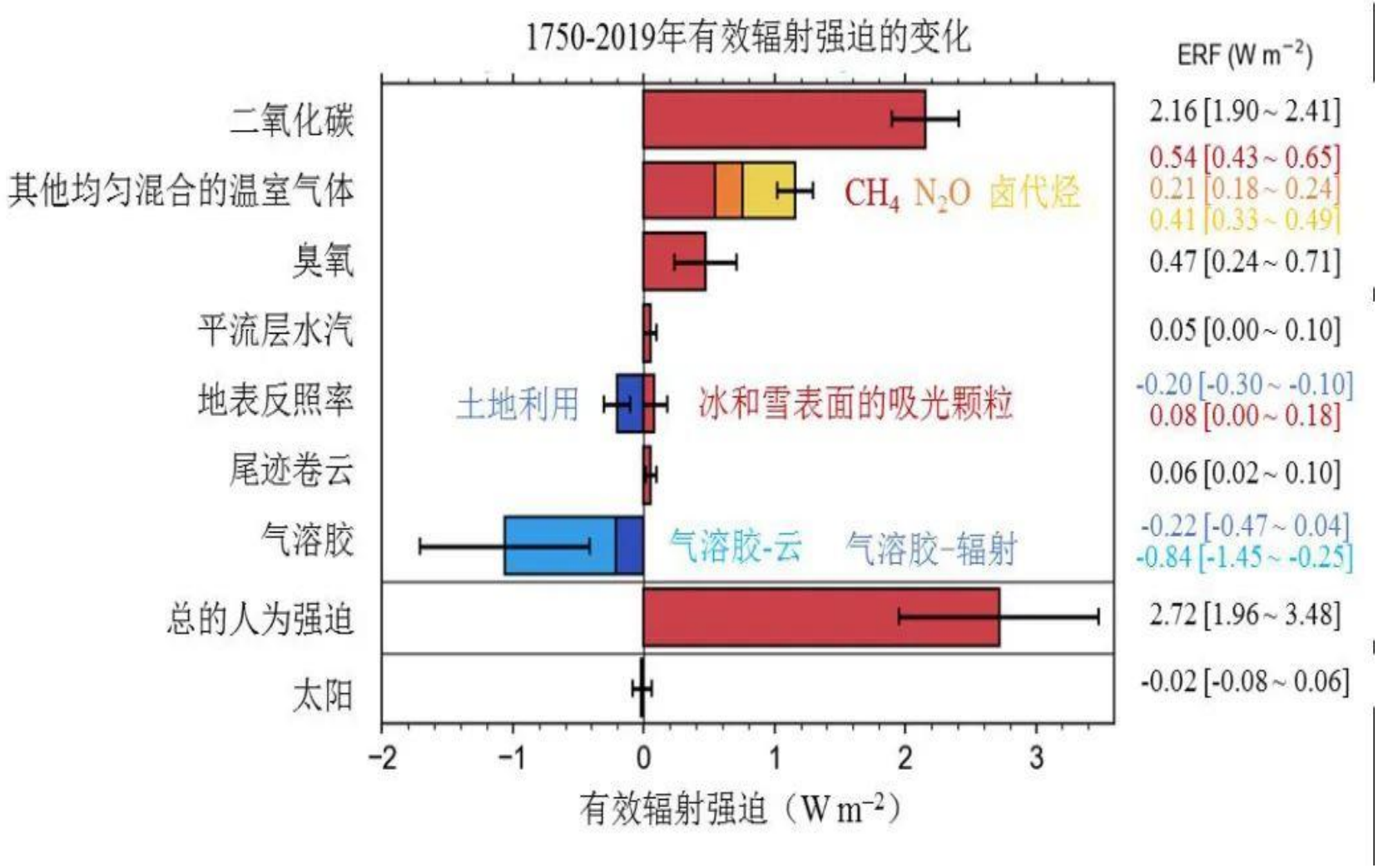

IPCC AR6　　(张华，2021)

1750—2019年间不同强迫因子对全球近地面气温变化的贡献以及不确定性（置信区间为5%~95%）

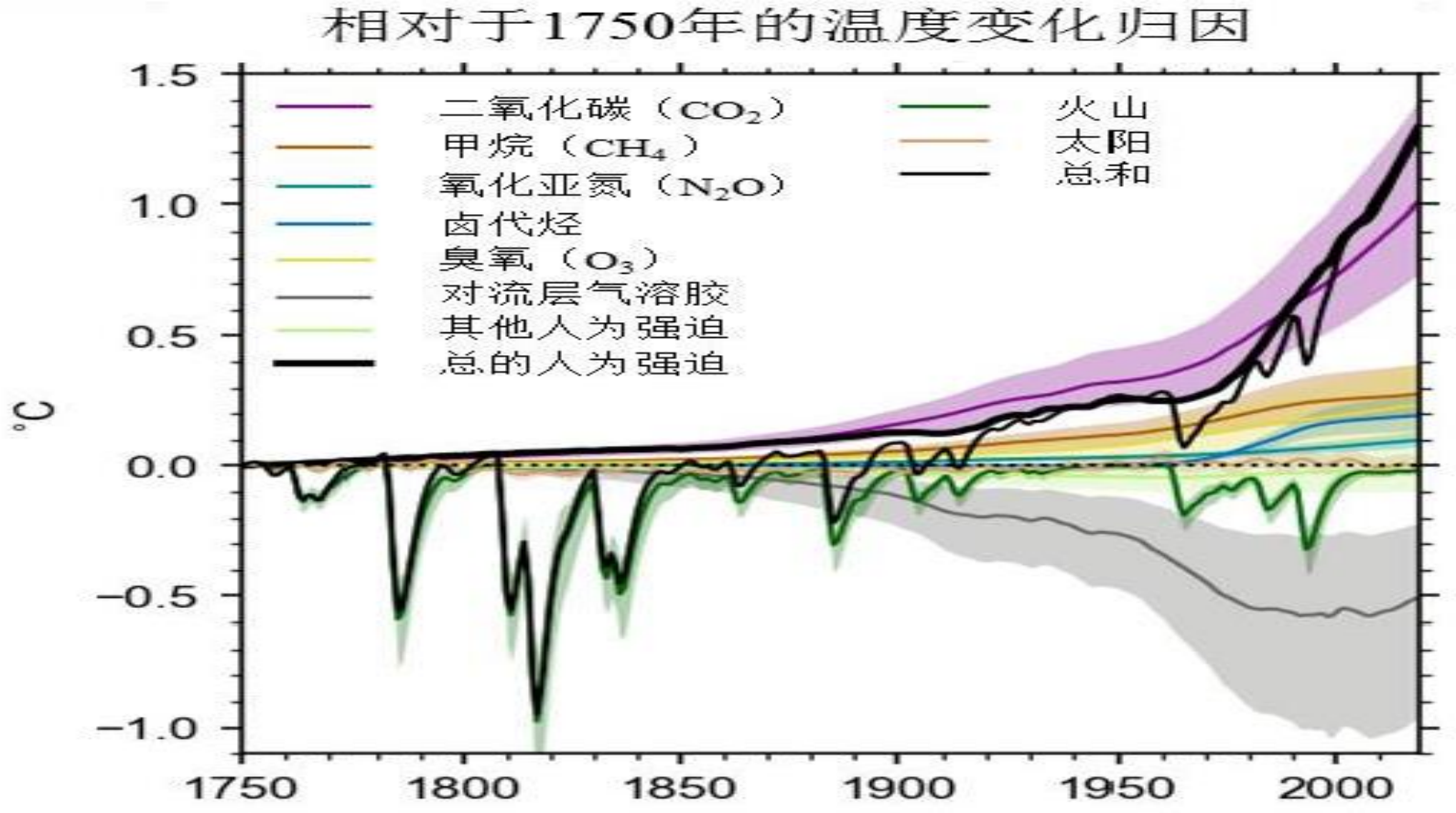

非CO_2温室气体强迫（其它均匀混合的温室气体和O_3）导致的GSAT在全球平均上已经被气溶胶导致的GSAT冷却趋势大致抵消。

IPCC AR6　　(张华，2021)

Air Pollution

Climate Change

Aerosol ($PM_{2.5}$)

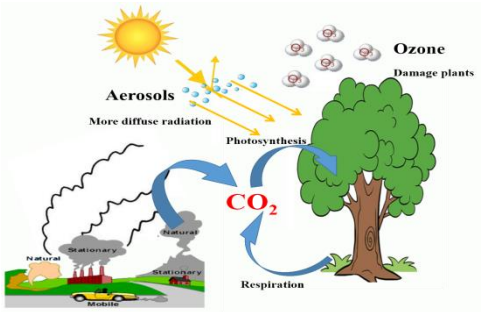

O_3

CO_2

O_3 and particle interaction

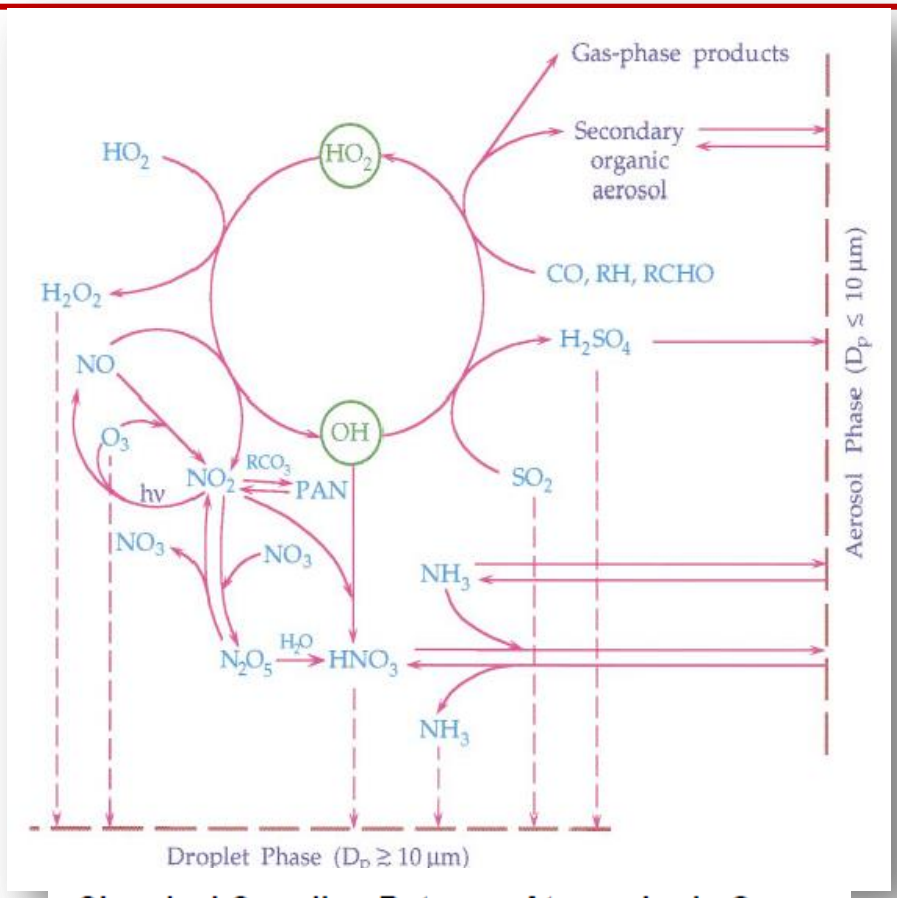

Chemical Coupling Between Atmospheric Ozone and Particulate Matter
Z. Meng, *et al.*
Science **277**, 116 (1997);
DOI: 10.1126/science.277.5322.116

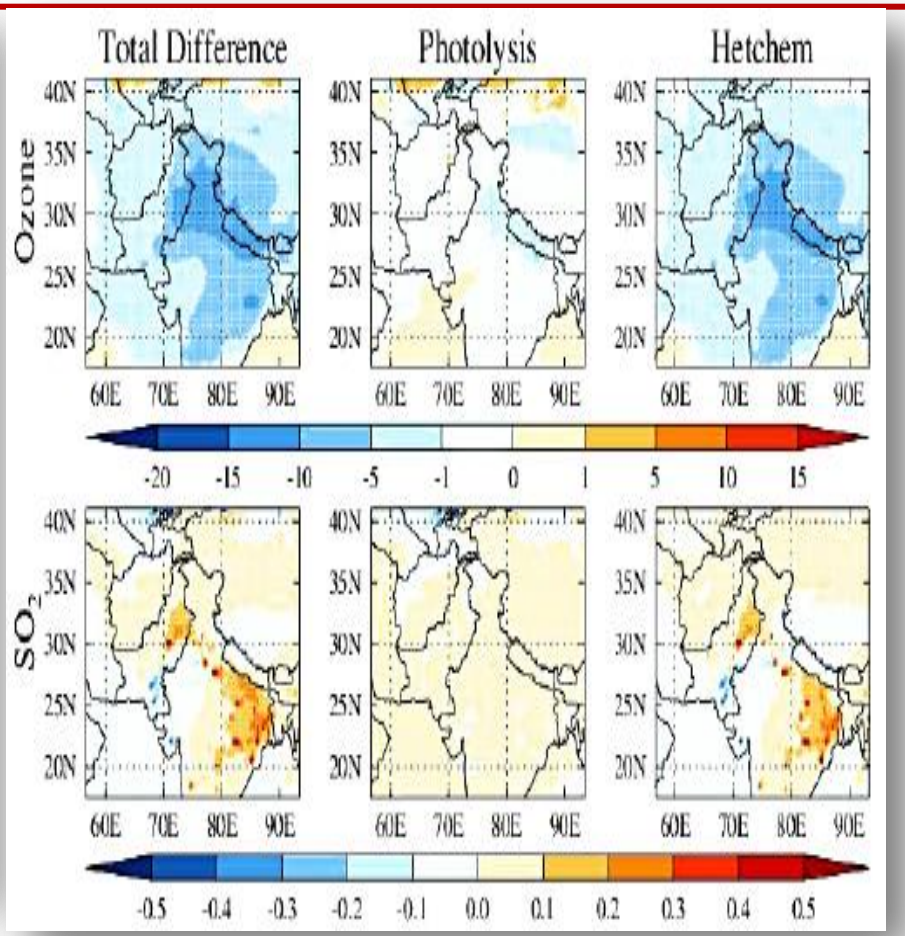

(Kumar et al. 2014)

O_3 and CO_2 interaction

Felzer(2004) found NPP was reduced 2.6%-6.8% by O_3, thus reduction of CO_2 absorption 18–38 Tg C yr^{-1}

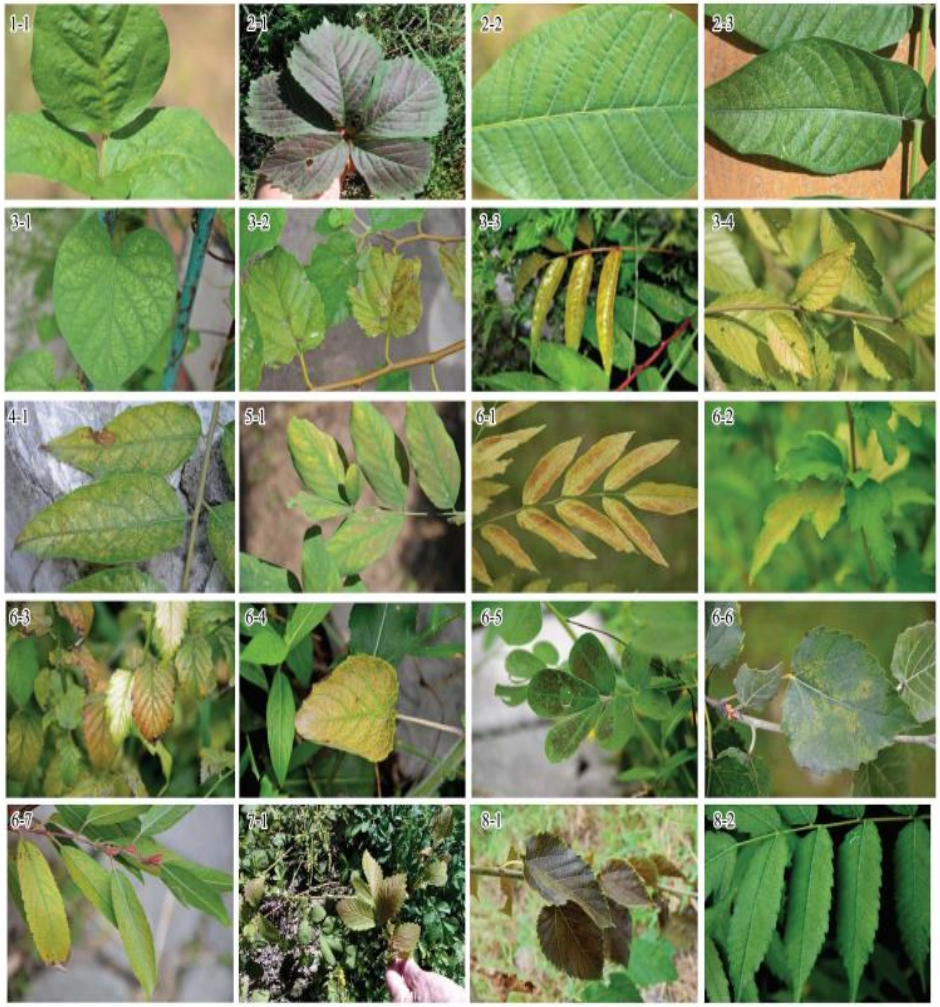

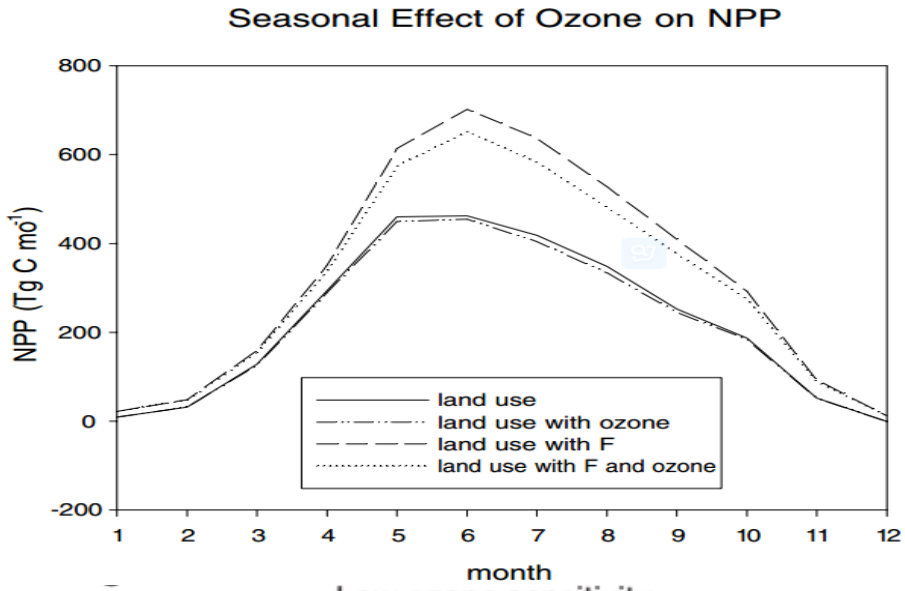

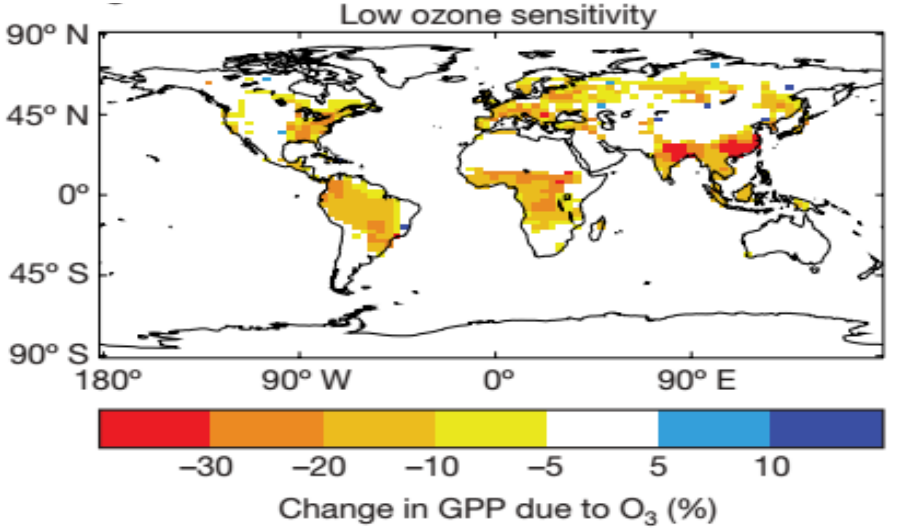

（source: Stich et al.，2007）

- **Excessive O_3 exposure can damage plant cell, reduce photosynthetic rates . Global GPP is estimated to reduce 14% to 23% .**

Particle and CO_2 interaction

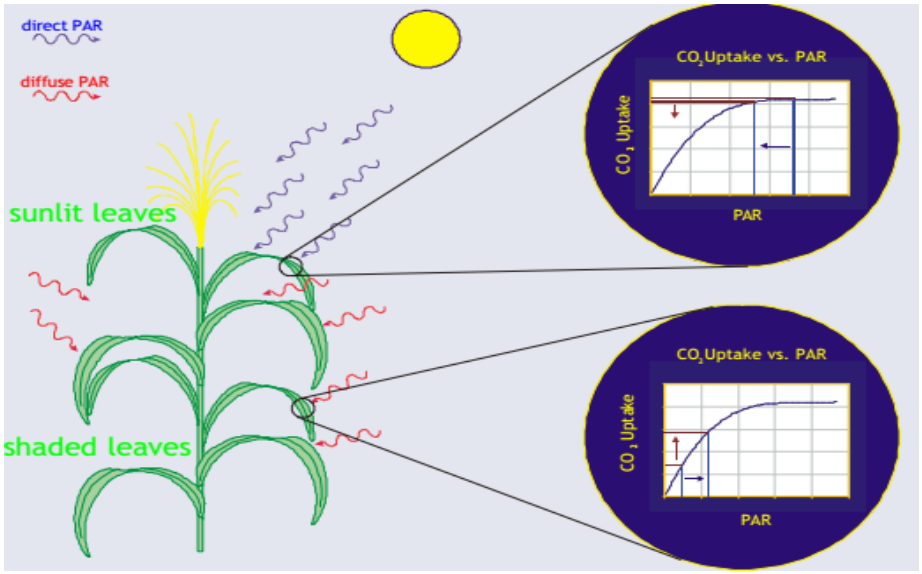

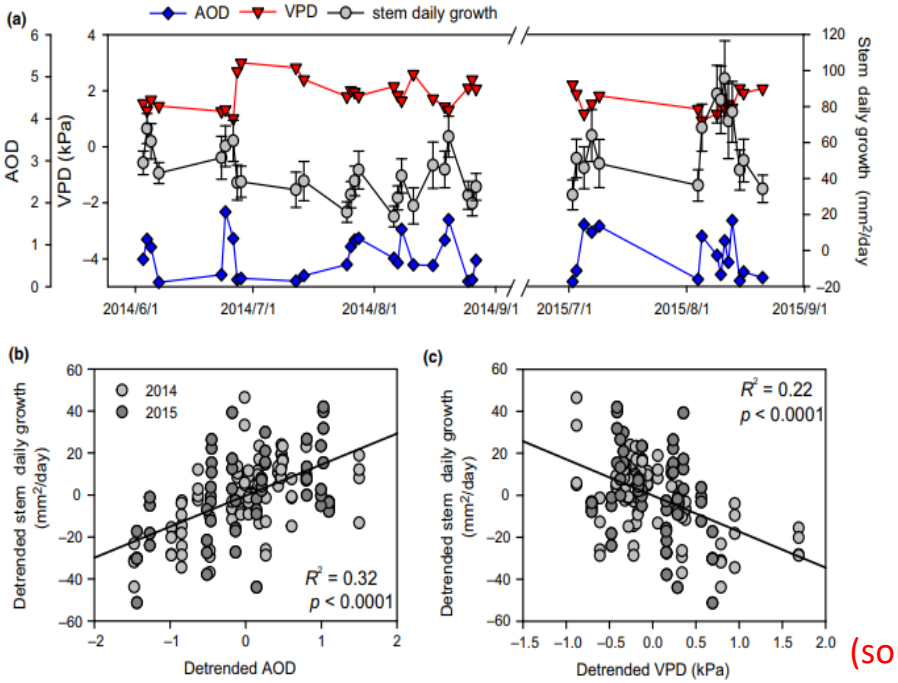

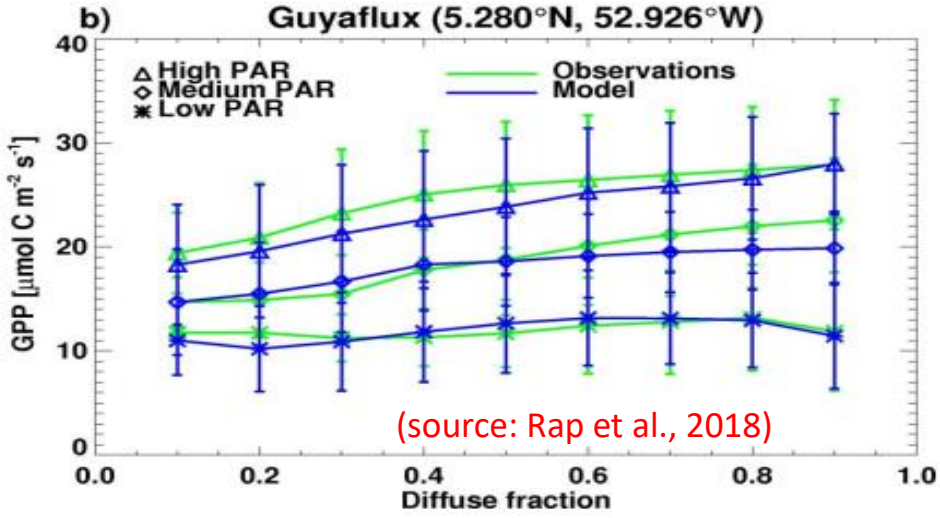

(source: Rap et al., 2018)

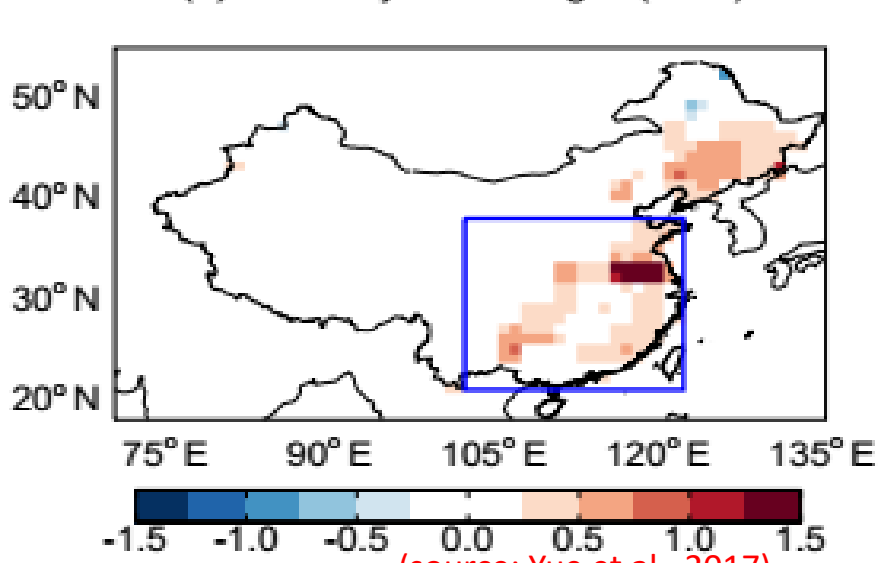

(source: Yue et al., 2017)

- **Aerosol can alter plant production through changing the diffuse radiation, surface temperature and hydrologic cycle.**

(source: Wang et al., 2018)

$PM_{2.5}$ and O_3 level in China during 2015-2019

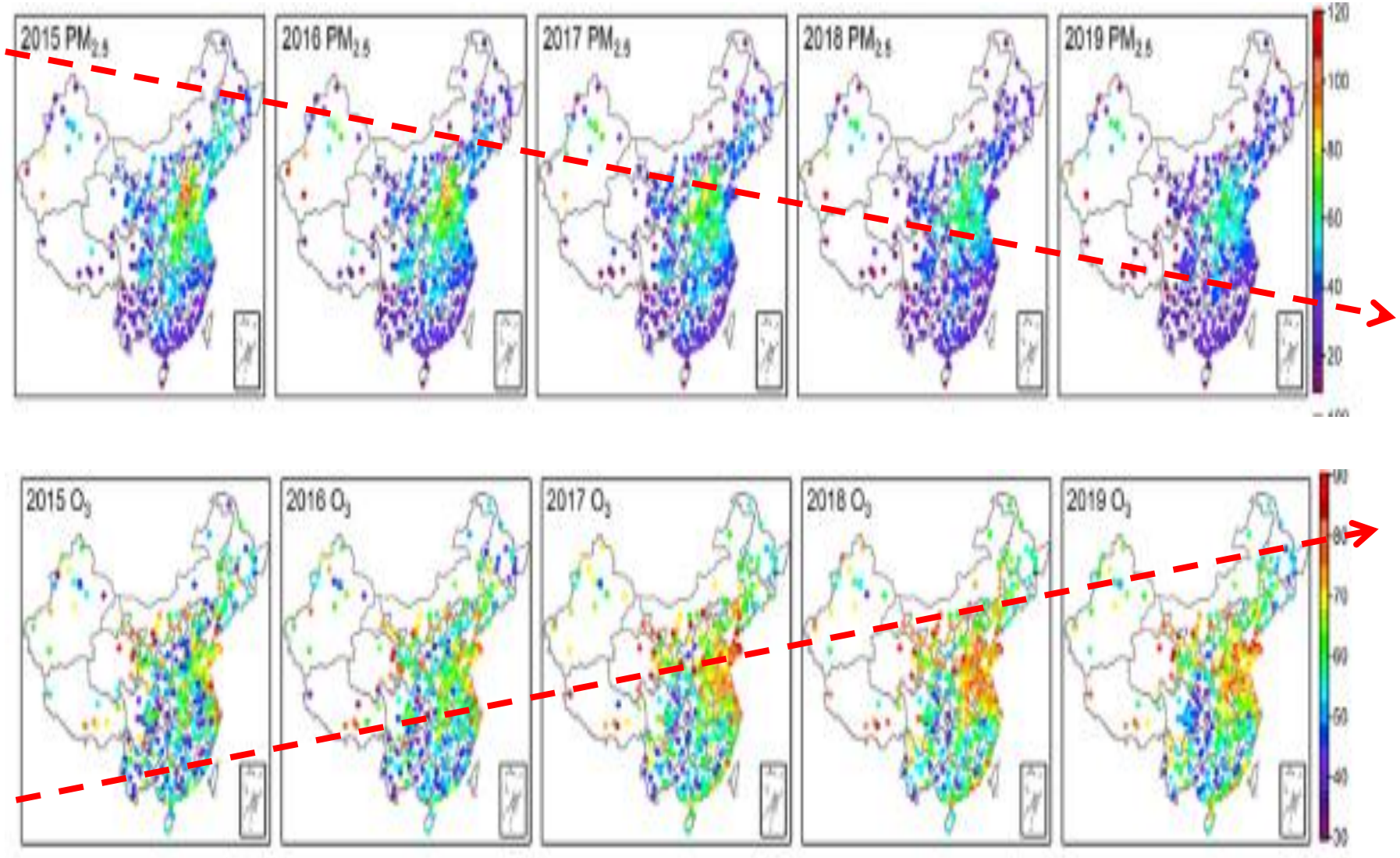

Zhou et al.（2021）

CO_2 level in China

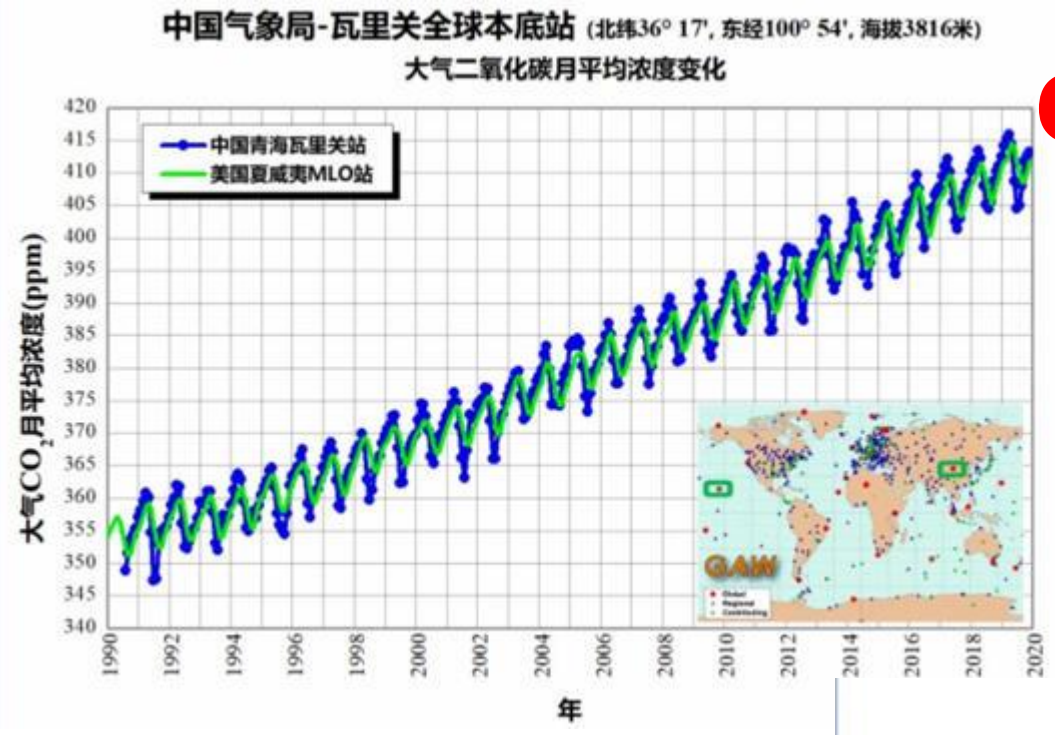

(a)中国瓦里关背景站观测的CO_2 浓度

(中国气象局，2020)

(b)卫星监测的CO_2浓度分布

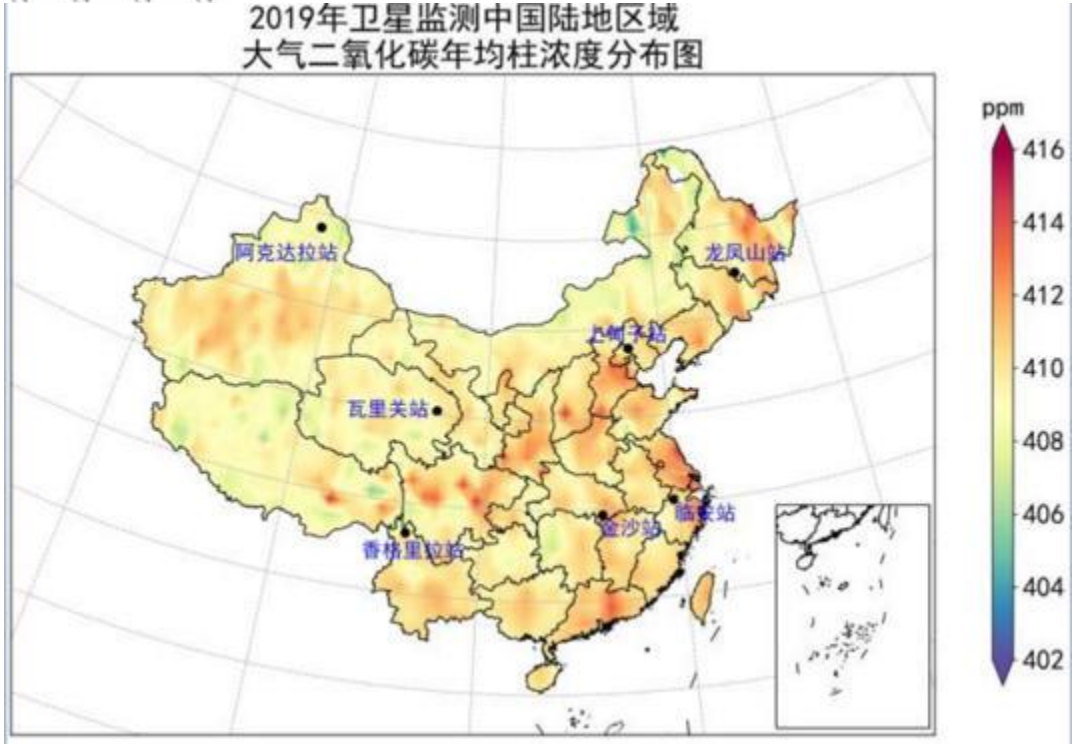

2019年青海瓦里关站观测的CO_2浓度分别上升至411.4±0.2 ppm，与北半球中纬度地区平均浓度大体相当，略高于2019年全球平均值。

中国气候变化蓝皮书（2022）

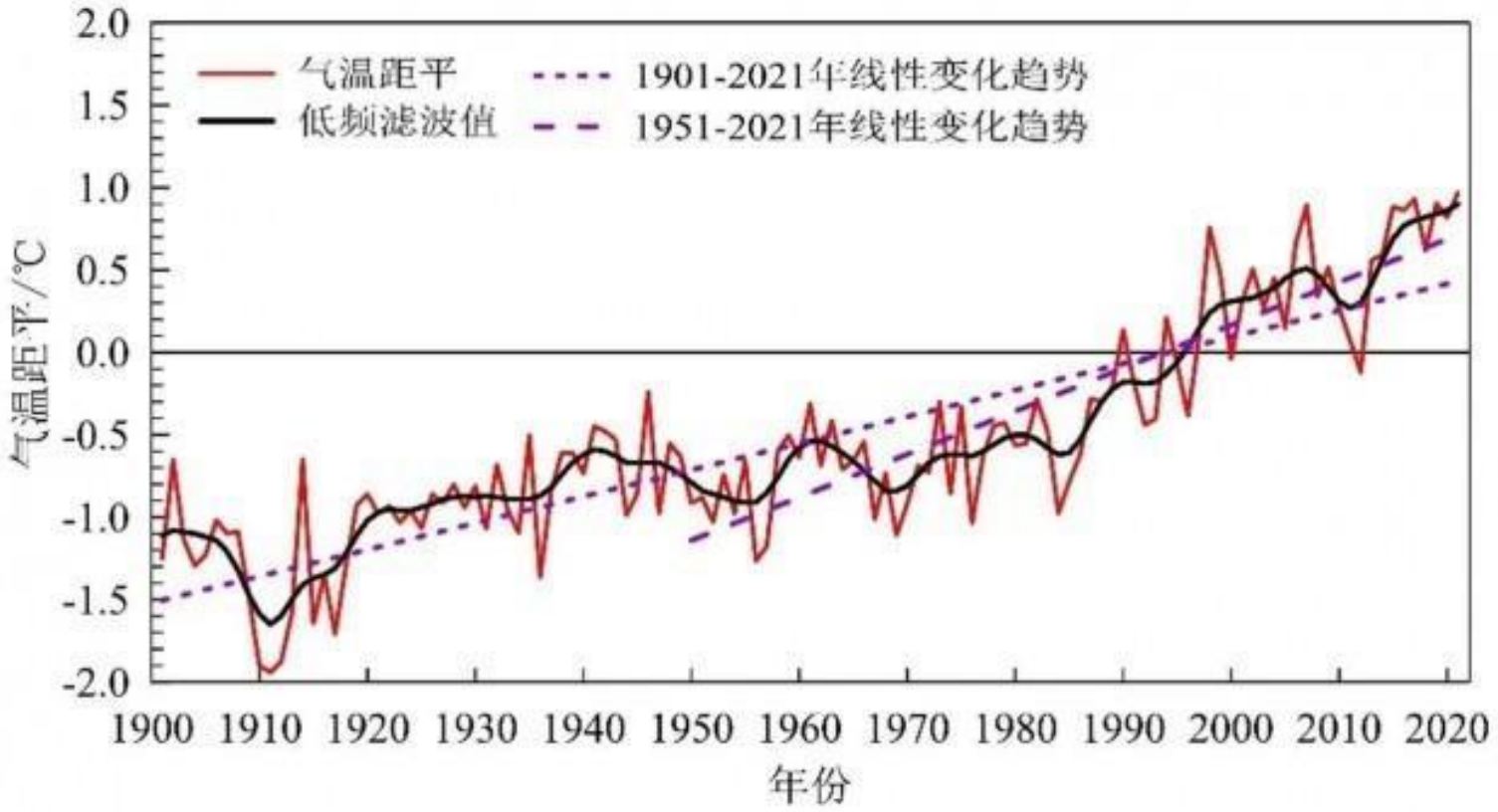

中国升温速率高于同期全球平均水平，是全球气候变化的敏感区。1951—2021年，中国地表年平均气温呈显著上升趋势，升温速率为0.26℃/10年，高于同期全球平均升温水平（0.15℃/10年）。近20年是20世纪初以来中国的最暖时期；2021年，中国地表平均气温较常年值偏高0.97℃，为1901年以来的最高值。

1980年以后东亚夏季风持续偏弱

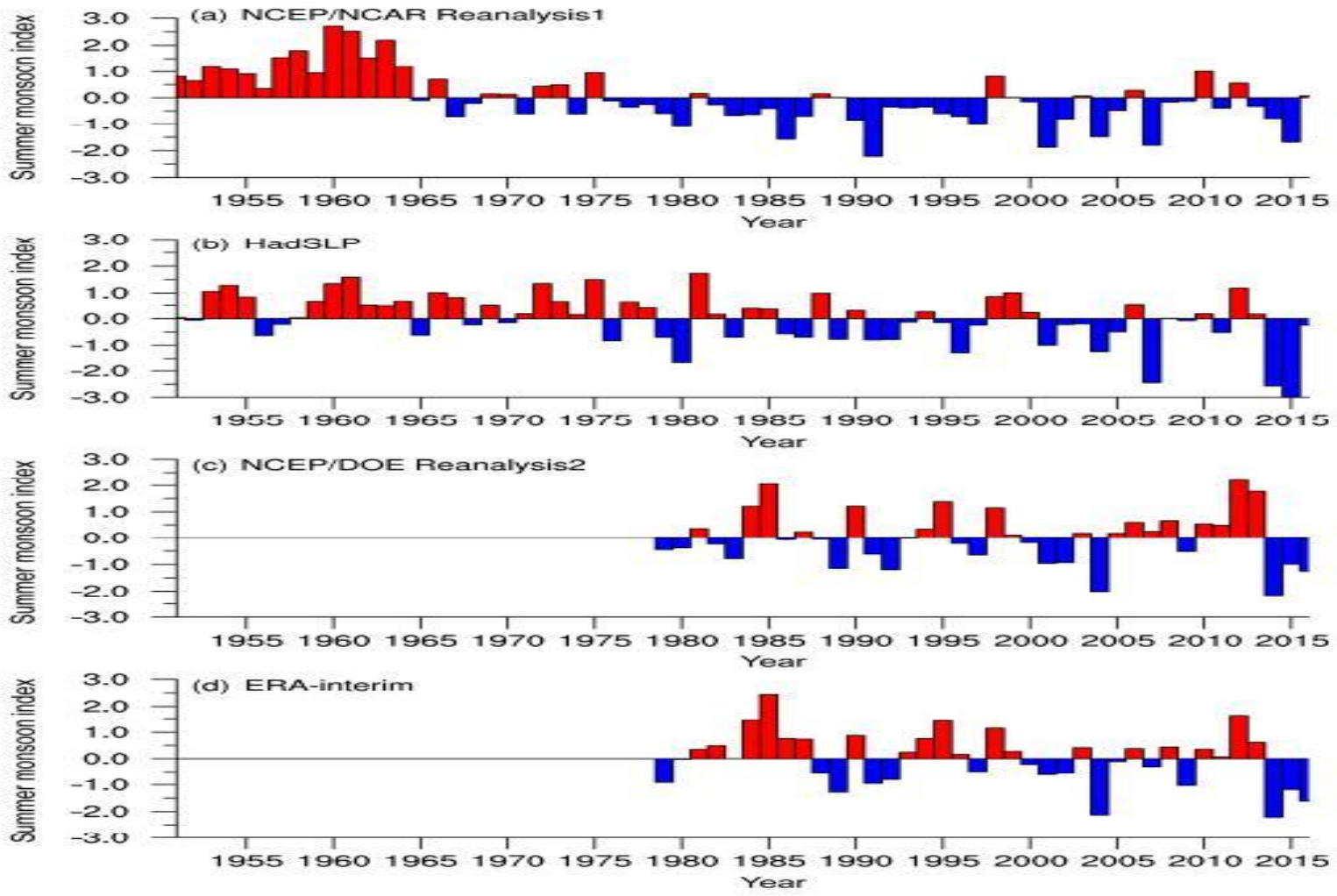

丁一汇(2018)

1980年以后东亚冬季风总体偏强

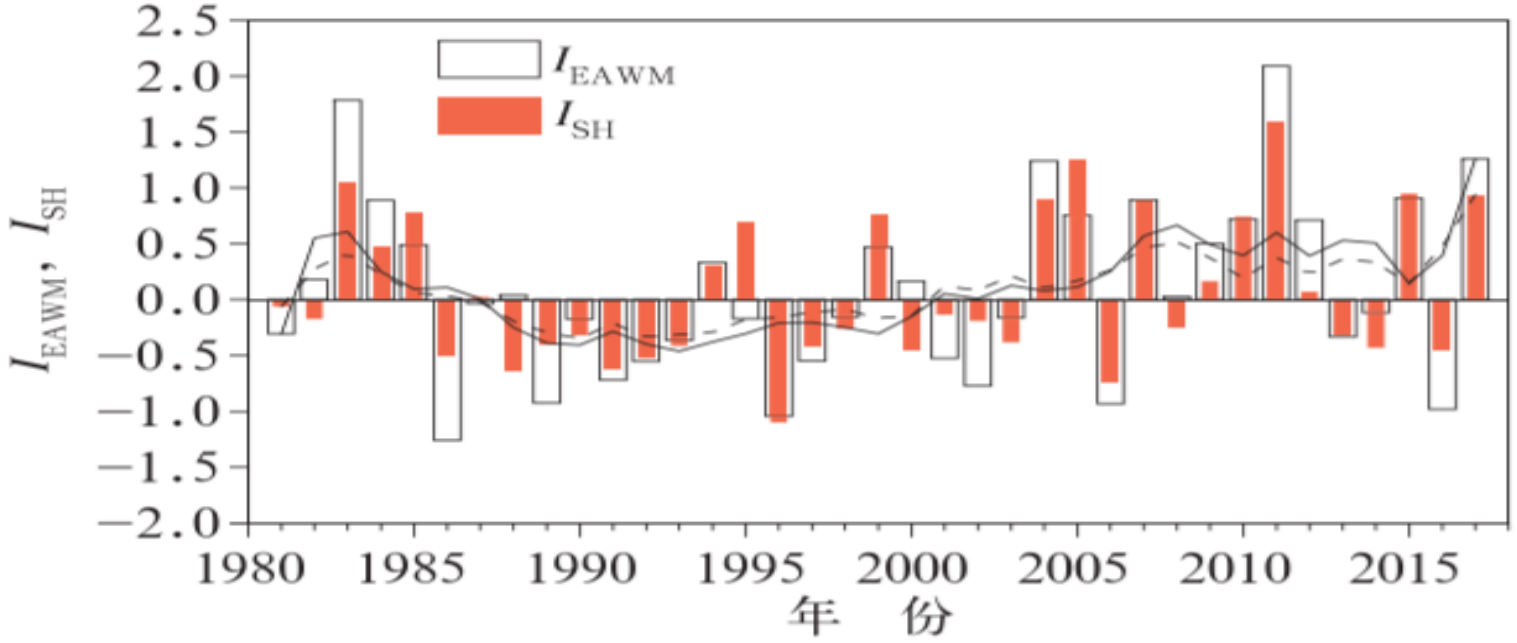

图 6　1981/1982 至 2017/2018 年冬季标准化 I_{EAWM} 和 I_{SH} 的逐年变化

（图中黑色实线和虚线分别为 I_{EAWM} 和 I_{SH} 的 9 年滑动平均）

章大全(2018)

报告提纲

- 研究背景
- 模式发展
- 应用研究
- 总结展望

RegCM-Chem

区域气候模式RegCM

- RegCM 模式最初开发于美国国家大气研究中心(NCAR)，后来由国际理论物理中心(ICTP)负责维护和更进一步的模式发展工作

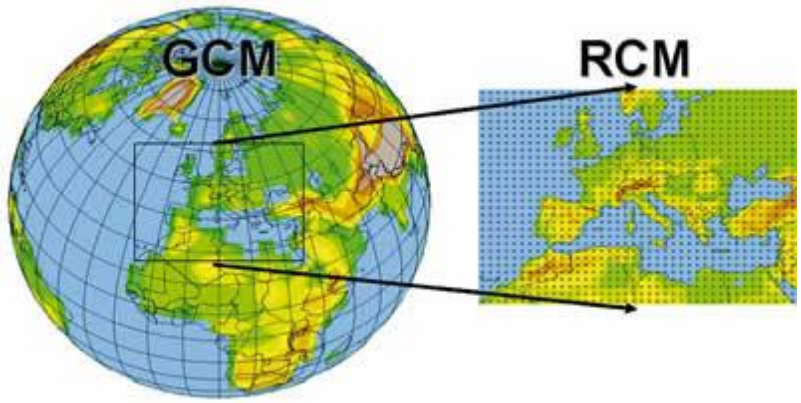

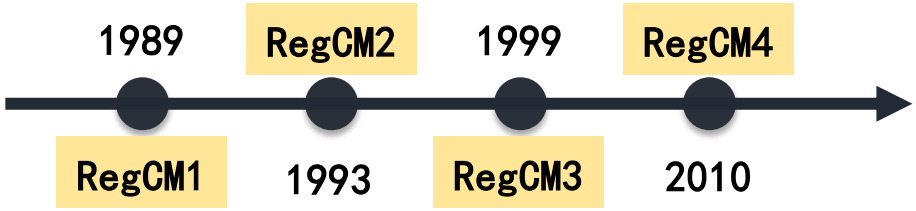

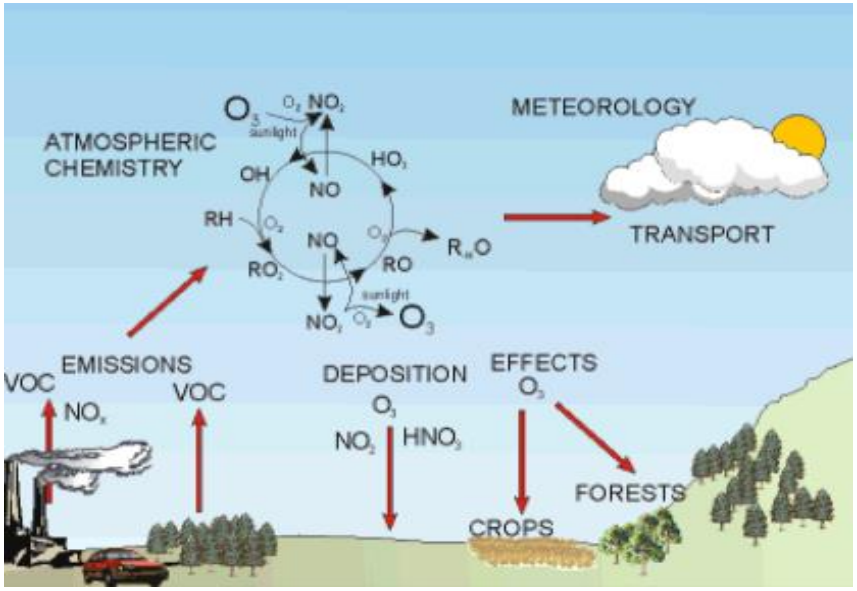

耦合化学模块RegCM-Chem

$$\frac{\partial \chi_i}{\partial t} = -\bar{V}\cdot\nabla\chi_i + F_H + F_V + T_{CUM} + S_{\chi_i} - R_{w,ls} - R_{w,cum} - D_{dep} + \sum Q_{p_i} - Q_{l_i}$$

Transport | Primary Emissions | Removal terms | Physico – chemical transformations

- 沙尘(Solmon et al., 2006).
- CBMZ气相化学机制(Shalaby等,2012)
- 硫酸盐（Zhou, 2013）
- SOA-VBS 方案（Yin, 2015）
- ISORROPIA II(二次无机盐)(Li等,2016)
- 花粉（Liu,2016）

Development 1:
SIA scheme(*ISORROPIA*)

Thermodynamic equilibrium model *ISORROPIA* *(Nenes,1998)*

- **Calculate the concentration under the state of equilibrium from the viewpoint of chemical thermodynamics**

- **15 equilibrium reactions，include species：**

  Gas phase： NH_3，HNO_3，H_2O

  Liquid phase： NH_4^+，H^+，NO_3^-，SO_4^{2-}，HSO_4^-，OH^-，H_2O

  Solid phase： $(NH_4)_2SO_4$，NH_4HSO_4，$(NH_4)_3H(SO_4)_2$，NH_4NO_3，H_2SO_4

Reaction	Constant expression	K° (298.15K)	$\frac{\Delta H^o(T_o)}{RT_o}$	$\frac{\Delta C_p^o}{R}$	Units
$HSO_{4(aq)}^- \xleftrightarrow{K_1} H_{(aq)}^+ + SO_{4(aq)}^{2-}$	$\frac{[H^+][SO_4^{2-}]}{[HSO_4^-]}\frac{\gamma_{H^+}\gamma_{SO_4^{2-}}}{\gamma_{HSO_4^-}}$	1.015×10^{-2}	8.85	25.14	mol kg^{-1}
$NH_{3(g)} \xleftrightarrow{K_{21}} NH_{3(aq)}$	$\frac{[NH_{3(aq)}]}{[P_{NH_3}]}\gamma_{NH_3}$	5.764×10^{1}	13.79	-5.39	mol kg^{-1} atm^{-1}
$NH_{3(aq)} + H_2O_{(aq)} \xleftrightarrow{K_{22}} NH_{4(aq)}^+ + OH_{(aq)}^-$	$\frac{[NH_4^+][OH^-]}{[NH_{3(aq)}]a_w}\frac{\gamma_{NH_4^+}\gamma_{OH^-}}{\gamma_{NH_3}}$	1.805×10^{-5}	-1.50	26.92	mol kg^{-1}
$HNO_{3(g)} \xleftrightarrow{K_4} H_{(aq)}^+ + NO_{3(aq)}^-$	$\frac{[H^+][NO_3^-]}{P_{HNO_3}}\gamma_{H^+}\gamma_{NO_3^-}$	2.511×10^{6}	29.17	16.83	mol^2 kg^{-2} atm^{-1}
$HCl_{(g)} \xleftrightarrow{K_3} H_{(aq)}^+ + Cl_{(aq)}^-$	$\frac{[H^+][Cl^-]}{P_{HCl}}\gamma_{H^+}\gamma_{Cl^-}$	1.971×10^{6}	30.20	19.91	mol^2 kg^{-2} atm^{-1}
$H_2O_{(aq)} \xleftrightarrow{K_w} H_{(aq)}^+ + OH_{(aq)}^-$	$\frac{[H^+][OH^-]}{a_w}\gamma_{H^+}\gamma_{OH^-}$	1.010×10^{-14}	-22.52	26.92	mol^2 kg^{-2}
$Na_2SO_{4(s)} \xleftrightarrow{K_5} 2Na_{(aq)}^+ + SO_{4(aq)}^{2-}$	$[Na^+]^2[SO_4^{2-}]\gamma_{Na^+}^2\gamma_{SO_4^{2-}}$	4.799×10^{-1}	0.98	39.75	mol^3 kg^{-3}
$(NH_4)_2SO_{4(s)} \xleftrightarrow{K_7} 2NH_{4(aq)}^+ + SO_{4(aq)}^{2-}$	$[NH_4^+]^2[SO_4^{2-}]\gamma_{NH_4^+}^2\gamma_{SO_4^{2-}}$	1.817×10^{0}	-2.65	38.57	mol^3 kg^{-3}
$NH_4Cl_{(s)} \xleftrightarrow{K_6} NH_{3(g)} + HCl_{(g)}$	$P_{NH_3}P_{HCl}$	1.086×10^{-16}	-71.00	2.40	atm^2
$NaNO_{3(s)} \xleftrightarrow{K_9} Na_{(aq)}^+ + NO_{3(aq)}^-$	$[Na^+][NO_3^-]\gamma_{Na^+}\gamma_{NO_3^-}$	1.197×10^{1}	-8.22	16.01	mol^2 kg^{-2}
$NaCl_{(s)} \xleftrightarrow{K_8} Na_{(aq)}^+ + Cl_{(aq)}^-$	$[Na^+][Cl^-]\gamma_{Na^+}\gamma_{Cl^-}$	3.766×10^{1}	-1.56	16.90	mol^2 kg^{-2}
$NaHSO_{4(s)} \xleftrightarrow{K_{11}} Na_{(aq)}^+ + HSO_{4(aq)}^-$	$[Na^+][HSO_4^-]\gamma_{Na^+}\gamma_{HSO_4^-}$	2.413×10^{4}	0.79	14.75	mol^2 kg^{-2}
$NH_4NO_{3(s)} \xleftrightarrow{K_{10}} NH_{3(g)} + HNO_{3(g)}$	$P_{NH_3}P_{HNO_3}$	5.746×10^{-17}	-74.38	6.12	atm^2
$NH_4HSO_{4(s)} \xleftrightarrow{K_{12}} NH_{4(aq)}^+ + HSO_{4(aq)}^-$	$[NH_4^+][HSO_4^-]\gamma_{NH_4^+}\gamma_{HSO_4^-}$	1.383×10^{0}	-2.87	15.83	mol^2 kg^{-2}
$(NH_4)_3H(SO_4)_{2(s)} \xleftrightarrow{K_{13}} 3NH_{4(aq)}^+ + HSO_{4(aq)}^- + SO_{4(aq)}^{2-}$	$[NH_4^+]^3[SO_4^{2-}][HSO_4^-]\times\gamma_{NH_4^+}^3\gamma_{SO_4^{2-}}\gamma_{HSO_4^-}$	2.972×10^{1}	-5.19	54.40	mol^5 kg^{-5}

New Equilibrium Reactions Considered in ISORROPIA II

Equilibrium Reaction
$Ca(NO_3)_{2(s)} \leftrightarrow Ca_{(aq)}^{2+} + 2NO_{3(aq)}^-$
$CaCl_{2(s)} \leftrightarrow Ca_{(aq)}^{2+} + 2Cl_{(aq)}^-$
$K_2SO_{4(s)} \leftrightarrow 2K_{(aq)}^+ + SO_{4(aq)}^{2-}$
$KHSO_{4(s)} \leftrightarrow K_{(aq)}^+ + HSO_{4(aq)}^-$
$KNO_{3(s)} \leftrightarrow K_{(aq)}^+ + NO_{3(aq)}^-$
$KCl_{(s)} \leftrightarrow K_{(aq)}^+ + Cl_{(aq)}^-$
$MgSO_{4(s)} \leftrightarrow Mg_{(aq)}^{2+} + SO_{4(aq)}^{2-}$
$Mg(NO_3)_{2(s)} \leftrightarrow Mg_{(aq)}^{2+} + 2NO_{3(aq)}^-$
$MgCl_{2(s)} \leftrightarrow Mg_{(aq)}^{2+} + 2Cl_{(aq)}^-$

Binary activity coefficients in the new code are calculated using the Kusik-Meissner relationships (Kussik and Meissner, 1978), while the ***multicomponent activity coefficients*** are calculated using Bromley's formula (Bromley, 1973). Water uptake is calculated using the ZSR relationship (Robinson and Stokes, 1965).

$$\log\gamma_{12} = -A_\gamma\frac{z_1z_2I^{1/2}}{1+I^{1/2}} + \frac{z_1z_2}{z_1+z_2}\left(\frac{F_1}{z_1}+\frac{F_2}{z_2}\right)$$

$$F_1 = Y_{21}\log\gamma_{12}^0 + Y_{41}\log\gamma_{14}^0 + Y_{61}\log\gamma_{16}^0 + \ldots + \frac{A_\gamma I^{1/2}}{1+I^{1/2}}\times\left(z_1z_2Y_{21} + z_1z_4Y_{41} + z_1z_6Y_{61} + \ldots\right)$$

$$F_2 = X_{12}\log\gamma_{12}^0 + X_{32}\log\gamma_{32}^0 + X_{52}\log\gamma_{52}^0 + \ldots + \frac{A_\gamma I^{1/2}}{1+I^{1/2}}\times\left(z_1z_2X_{12} + z_3z_2X_{32} + z_5z_2X_{52} + \ldots\right)$$

Aerosol Equilibrium Calculations

$$\sum_i \nu_{ij}\mu_i = 0 \qquad K_j(T) = \exp\left[-\frac{\sum_i \nu_{ij}\mu_i^0(T)}{RT}\right]$$

$$K(T) = K_0\exp\left[-\frac{\Delta H^0(T_0)}{RT_0}\left(\frac{T_0}{T}-1\right) - \frac{\Delta c_p^0}{R}\left(1+\ln\left(\frac{T_0}{T}\right)-\frac{T_0}{T}\right)\right]$$

Development 2:
SOA scheme 1 (SORGAM)

The concept of two-product module:
The products are lumped into two main categories: 1. high volatility; 2. low volatility.

SOA parameterization (reversible gas-particle partition)

$VOC_i + OXIDANT_j \rightarrow \alpha_{i,j}P1_{i,j} + \alpha_{i,j}P2_{i,j}$

$P_{i,j}$ → $G_{i,j}$ ⇄ $A_{i,j}$

Equilibrium ($Kom_{i,j}$) → f(POA)

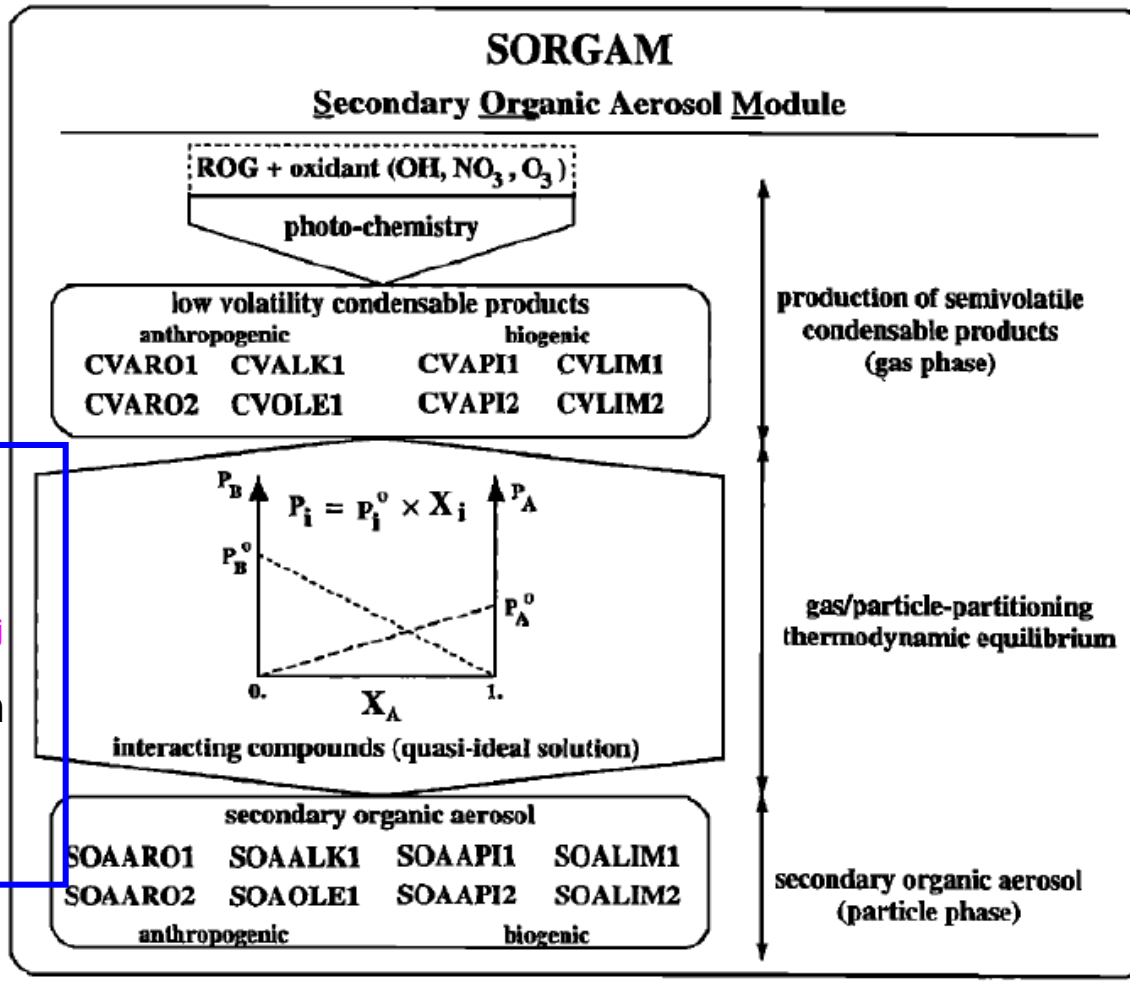

Development 2:
SOA scheme1 (SORGAM)

Species in SORGAM and the parameters

Precursor Classes	SOA Model Classes		MW g/mol	P^{o}_{298k}, pa	ΔH_{vap} kj/mol	Remarks
	Gas Phase	Particle Phase				
TOL, XYL, CSL	CVARO1	SOAARO1	150	5.7E-5	156	Reaction products of aromatic precursors
	CVARO2	SOAARO2	150	1.6E-3	156	
HC	CVALK1	SOAALK1	140	5.0E-6	156	Reaction products of higher alkanes
OLT, OLI	CVOLE1	SOAOLE1	140	5.0E-6	156	Reaction products of higher alkenes
API	CVAPI1	SOAAPI1	184	4.0E-6	156	Reaction products of α-pinene
	CVAPI2	SOAAPI2	184	1.7E-4	156	
LIM	CVLIM1	SOALIM1	200	2.5E-5	156	Reaction products of limonene
	CVLIM2	SOALIM2	200	1.2E-4	156	

Reactions taken into account

TOL	+	OH	—>	0.039 CVARO1 + 0.108CVARO2
XYL	+	OH	—>	0.039 CVARO1 + 0.108CVARO2
CSL	+	OH	—>	0.039 CVARO1 + 0.108CVARO2
CSL	+	NO_3	—>	0.039 CVARO1 + 0.108CVARO2
HC	+	OH	—>	0.048 CVALK1
OLT	+	OH	—>	0.008 CVOLE1
OLT	+	NO_3	—>	0.008 CVOLE1
OLT	+	O_3	—>	0.008 CVOLE1
OLI	+	OH	—>	0.008 CVOLE1
OLI	+	NO_3	—>	0.008 CVOLE1
OLI	+	O_3	—>	0.008 CVOLE1
API	+	OH	—>	fOH (0.028 CVAPI1 + 0.241 CVAPI2)
API	+	NO_3	—>	fNO_3 (0.028 CVAPI1+ 0.241CVAPI2)
API	+	O_3	—>	fO_3 (0.028 CVAPI1 + 0.241CVAPI2)
LIM	+	OH	—>	fOH (0.163 CVLIM1 + 0.247 CVLIM2)
LIM	+	NO_3	—>	fNO_3 (0.163 CVLIM1+ 0.247 CVLIM2)
LIM	+	O_3	—>	fO_3 (0.163 CVLIM1 + 0.247 CVLIM2)

Development 2: SOA scheme2 (VBS)

The concept of VBS:
The reaction products are expanded to more categories, and the aging processes of these products are considered.

[Manish K. Shrivastava, et al., 2008]

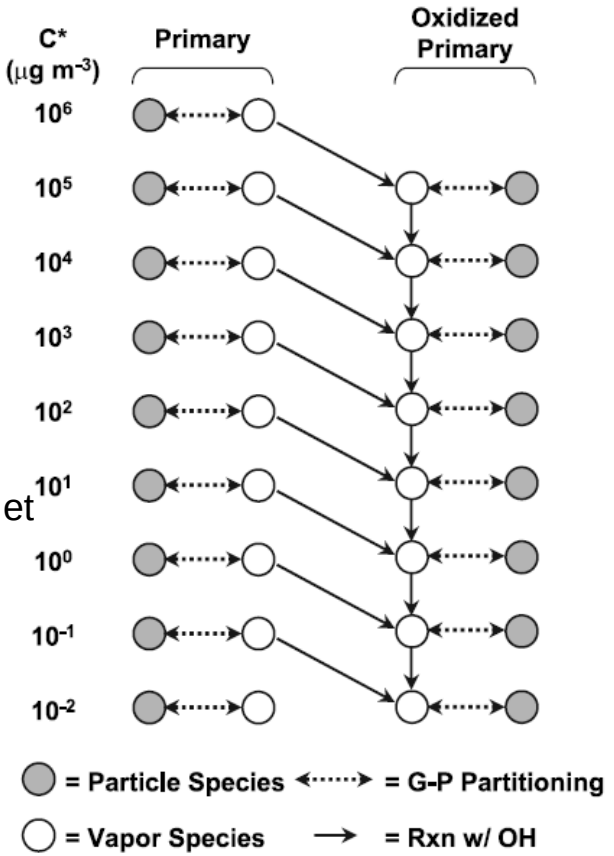

[R. Ahmadov et al., 2012]

Table 4. SOA Mass Yields [*Murphy and Pandis*, 2009] for the VOC Precursors and Volatility Bins Used in WRF-CHEM[a]

	High NO_x Conditions				Low NO_x Conditions			
VOC	1	10	100	1000	1	10	100	1000
HC5	0.0000	0.0375	0.0000	0.0000	0.0000	0.0750	0.0000	0.0000
HC8	0.0000	0.1500	0.0000	0.0000	0.0000	0.3000	0.0000	0.0000
OLT	0.0008	0.0450	0.0375	0.1500	0.0045	0.0090	0.0600	0.2250
OLI	0.0030	0.0255	0.0825	0.2700	0.0225	0.0435	0.1290	0.3750
TOL	0.0030	0.1650	0.3000	0.4350	0.0750	0.2250	0.3750	0.5250
XYL, CSL	0.0015	0.1950	0.3000	0.4350	0.0750	0.3000	0.3750	0.5250
ISO	0.0003	0.0225	0.0150	0.0000	0.0090	0.0300	0.0150	0.0000
SESQ	0.0750	0.1500	0.7500	0.9000	0.0750	0.1500	0.7500	0.9000
API, LIM	0.0120	0.1215	0.2010	0.5070	0.1073	0.0918	0.3587	0.6075

[a]Yields are for four volatility bins with saturation concentrations of 1, 10, 100, and 1000 $\mu g/m^3$ at 300 K and depend on RO_2/NO_x conditions as described in the text.

Development 3:
Schemes for direct and indirect effects

Direct effects

Carbonaceous aerosols

$$\tau_i(\lambda) = M_i \beta_{i\lambda} (1 - RH)^{-k}$$

***Kasten(* 1969)**

Other-aerosols

$$\tau_i(\lambda) = M_i \beta_{i\lambda,0} e^{(\beta_{i\lambda,1} + \frac{\beta_{i\lambda,2}}{RH + \beta_{i\lambda,3}} + \frac{\beta_{i\lambda,4}}{RH + \beta_{i\lambda,5}})}$$

***Kiehl and Briegleb* (1993) and *Kiehl et al.* (2000)**

M: Conc of aerosols; β: Specific extinction

λ: Wave length; i: Species (N, S, BC, OC)

First indirect effect

$$Nc = \begin{cases} 162 \times \log_{10}(Na) - 273 & (\text{Ocean}) \\ 298 \times \log_{10}(Na) - 595 & (\text{Land}) \end{cases}$$

S: Solution fraction

N: Number conc of aerosols

$$Na = \sum_i S_i N_i$$

***Gultope and Isaac* (1999)**

Second indirect effect

$$P = C_{l,aut} q_l^2 \rho / \rho_w (q_l \rho / \rho_w N_c)^{1/3} H(r_e - r_{ec})$$

$$C_{l,aut} = 0.55 \pi^{1/3} k_1 (3/4)^{4/3} (1.1)^4, \quad k_1 = 1.18 \times 10^6 / \text{cm/s}$$

（***Chen and Cotton*. 1987; *Liou and Ou*. 1989; *Boucher and Lohmann*. 1995**）

Development 4:
CO_2 source, sink and transport

- ICBC (initial condition and boundary condition):
  carbontracker global simulation
  - horizontal resolution: 3° *2°
  - vertical resolution: 34 layers
  - time step: 3 hourly (6 hourly for use)

- Emission: carbontracker global flux
  - horizontal resolution: 1° *1°
  - time step: 3 hourly
  - 4 type:
    fossil fuel,terrestrial biosphere,ocean,fire

引入CO_2物种模拟

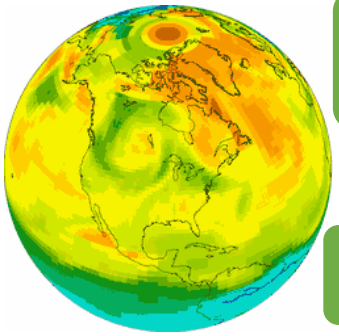

CarbonTracker
CO_2浓度数据

初始边界条件

RegCM-CHEM

输送扩散过程

CO_2源汇过程

$[CO_2]$

■ 4种CO_2源汇过程：

1. 化石燃料CO_2排放

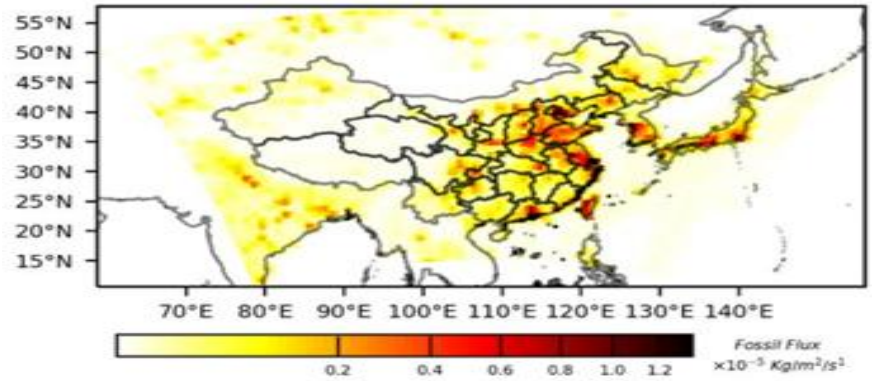

2. 生物质燃烧CO_2排放

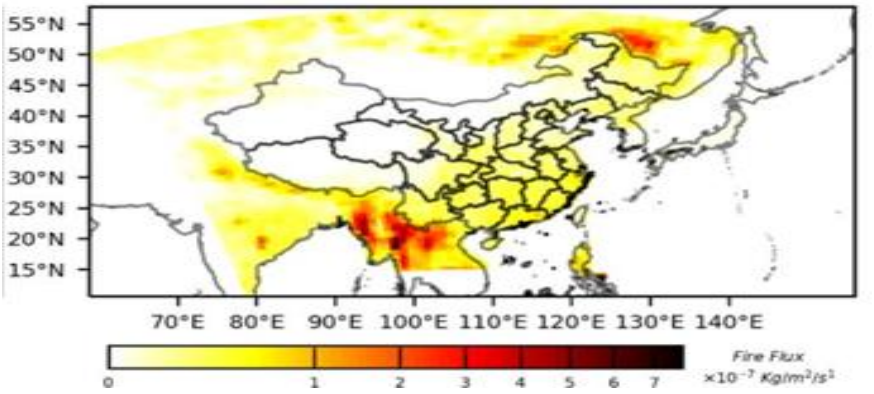

3. 海洋CO_2通量

4. 陆地生态系统CO_2通量

Development 5: Coupling with YIBs

- **The Yale Interactive terrestrial Biosphere model (YIBs)**，which is a process-based vegetation model developed by Yale University.

（**Yue et al., 2015**）

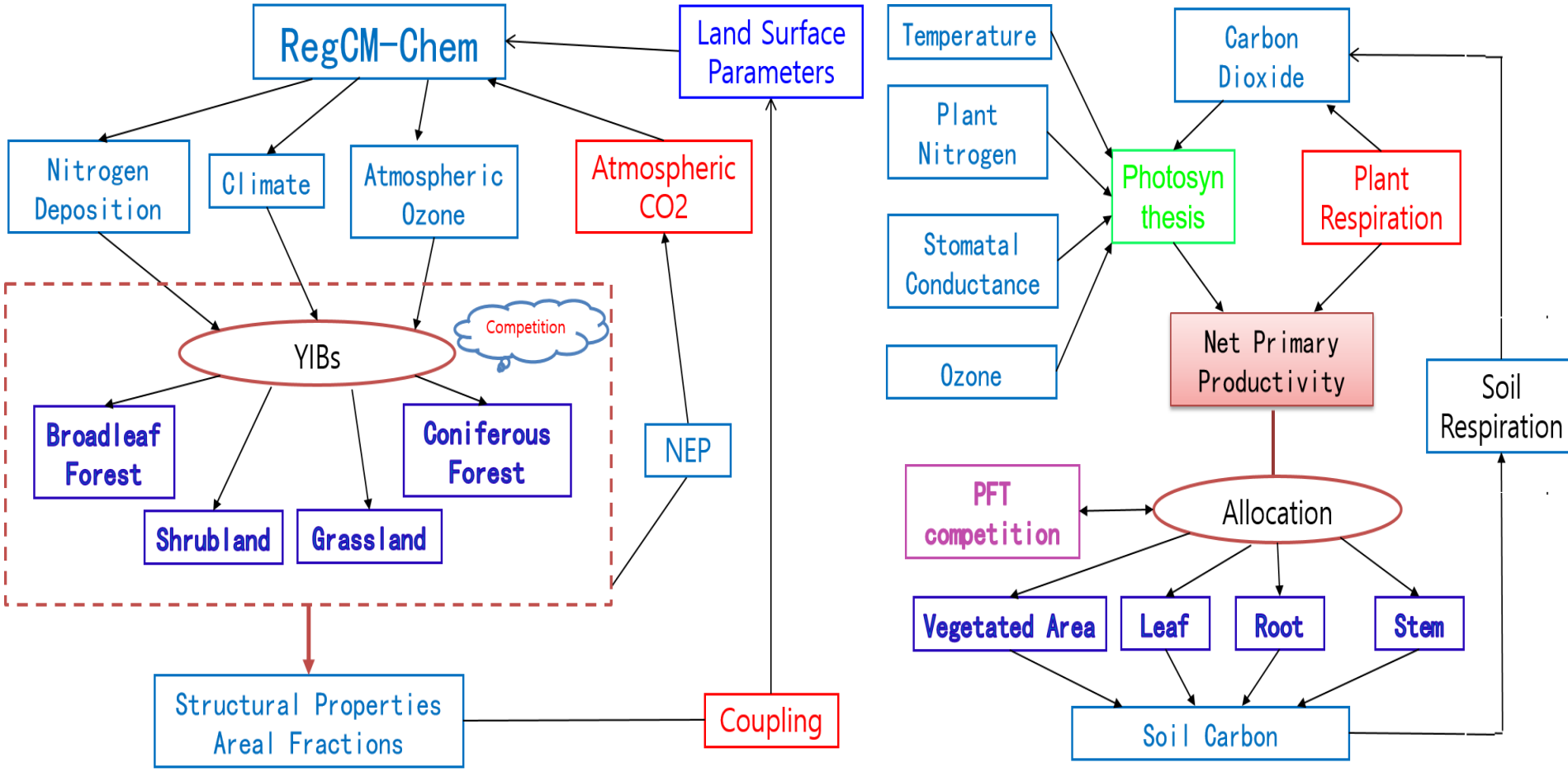

耦合陆地生态系统模型YIBs

- YIBs模式是Yue and Unger (2015)开发的、基于植物生理过程的动态植被模型，能够模拟植物的光合作用、呼吸作用、碳再分配、植被物候等生理过程

Geosci. Model Dev., 8, 2399–2417, 2015
www.geosci-model-dev.net/8/2399/2015/
doi:10.5194/gmd-8-2399-2015

Geoscientific Model Development
Open Access

The Yale Interactive terrestrial Biosphere model version 1.0: description, evaluation and implementation into NASA GISS ModelE2

X. Yue and N. Unger
School of Forestry and Environment Studies, Yale University, New Haven, Connecticut 06511, USA

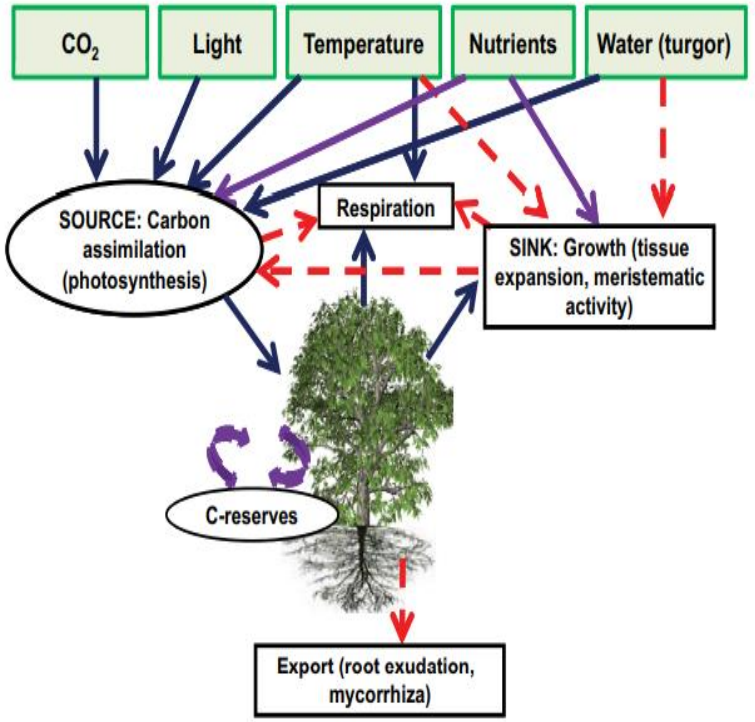

$$A_{tot} = \min(J_c, J_e, J_s) \quad (1)$$

$$J_c = \begin{cases} V_{cmax}\left(\dfrac{c_i - \Gamma_*}{c_i + K_c(1 + O_i/K_o)}\right) & \text{for C3 plant} \\ V_{cmax} & \text{for C4 plant} \end{cases}, \quad (2)$$

$$J_e = \begin{cases} a_{leaf} \times \mathrm{PAR} \times \alpha \times \left(\dfrac{c_i - \Gamma_*}{c_i + 2\Gamma_*}\right) & \text{for C3 plant} \\ a_{leaf} \times \mathrm{PAR} \times \alpha & \text{for C4 plant} \end{cases}, \quad (3)$$

$$J_s = \begin{cases} 0.5V_{cmax} & \text{for C3 plant} \\ K_s \times V_{cmax} \times \dfrac{c_i}{P_s} & \text{for C4 plant'} \end{cases} \quad (4)$$

$$g_s = m\frac{A_{net} \times \mathrm{RH}}{c_s} + b, \quad (6)$$

$$\mathrm{GPP} = \int_0^{\mathrm{LAI}} A_{tot}\,dL. \quad (7)$$

耦合陆地生态系统模型YIBs

- YIBs模式中采用Sitch et al. (2007)提出的参数化方案来描述臭氧对植被的影响：

$$A = A_{tot} \times F$$

$$F = 1 - a \times max\left[F_{O_3} - F_{O_3 crit}, 0.0\right]$$

$$F_{O_3} = \frac{[O_3]}{r_b + k \cdot r_s'}$$

$$r_s' = \frac{1}{g_s'} = \frac{1}{F \cdot g_s}$$

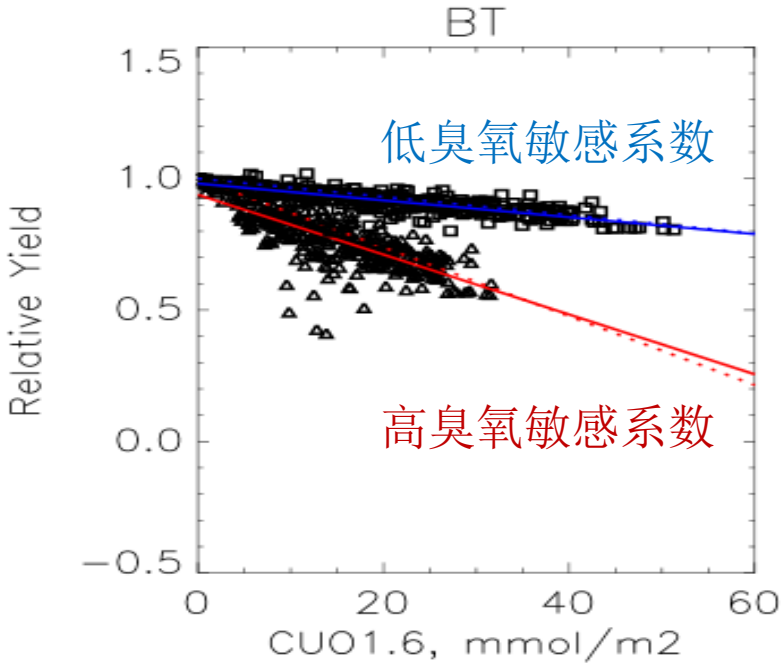

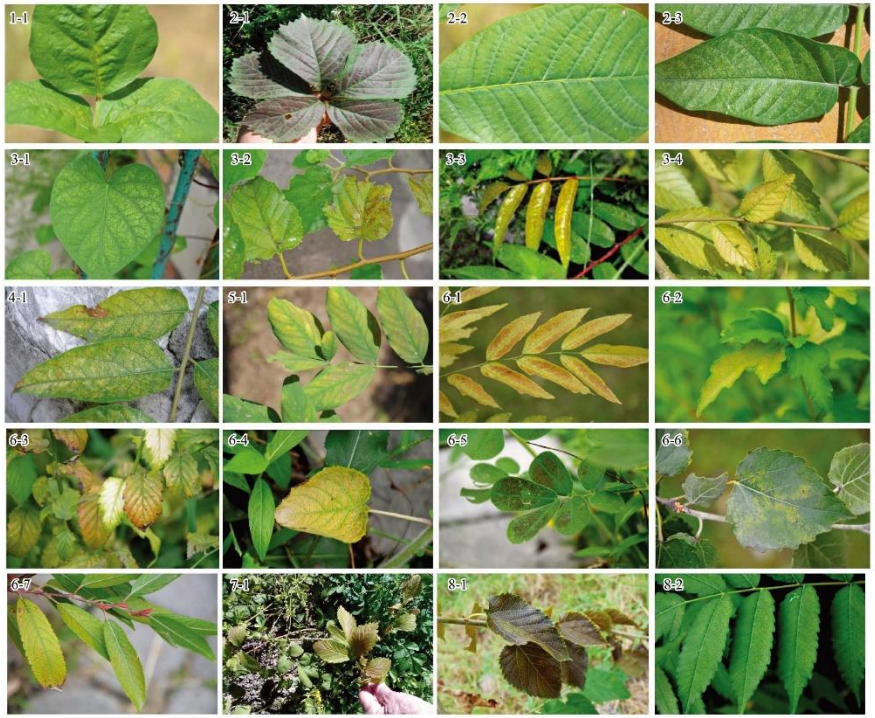

	BT	NT	C3	C4	Shrub
F_{O3crit} (nmol m^{-2} s^{-1})	1.6	1.6	5.0	5.0	1.6
'High' a ($mmol^{-1}$ m^{-2})	0.15	0.075	1.40	0.735	0.10
'Low' a ($mmol^{-1}$ m^{-2})	0.04	0.02	0.25	0.13	0.03

* 阔叶林(BT)、针叶林(NT)、草地(C3, C4) 、灌木(Shrub)

(Sitch et al., 2007)

Development 6: Radiation effect of CO_2 and O_3

- The simulated **CO_2 and O_3** concentrations with a spatiotemporal variation were taken into the radiation module and improved the associated radiation effects.

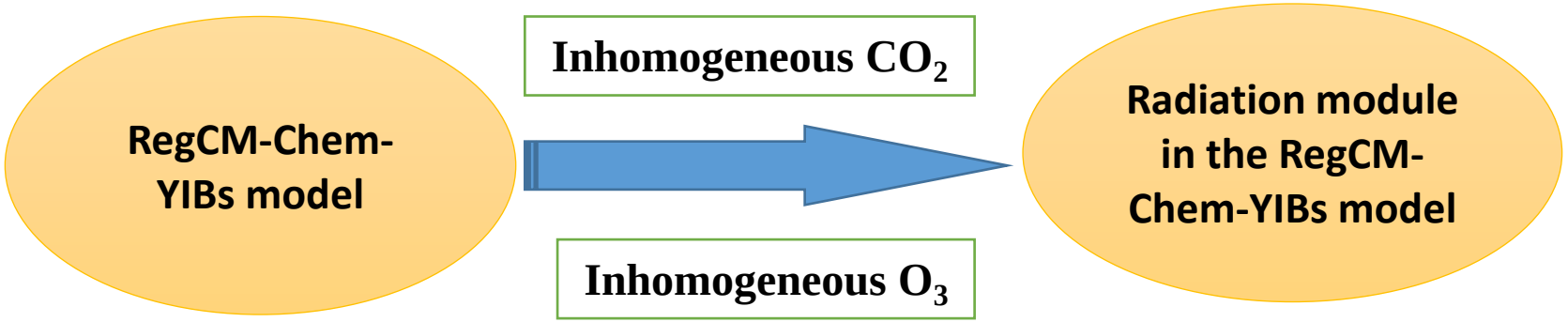

- The previous version RegCM-Chem-YIBs model simulated the radiation effect that considers spatial-temporal variations of aerosol only.
- The air CO_2 and O_3 concentrations in the radiation module were constant in the year to calculate the radiation.

Development 7: Impact of aerosol on photolysis

The photodissociation rate for each chemical species:

$$J = \int f(\lambda)\sigma_0(\lambda)\phi(\lambda)d\lambda = \int f(\lambda)\sigma(\lambda)d\lambda$$

where the actinic flux $f(\lambda)$ depends on local optical conditions, absorption cross section $\sigma_0(\lambda)$, and quantum yield $\phi(\lambda)$ of the molecule of interest. For simplicity, we assign the product of absorption cross section $\sigma_0(\lambda)$ and quantum yield $\phi(\lambda)$ as an effective cross section $\sigma(\lambda)$. The actinic flux varies according to atmospheric absorption and molecular (Rayleigh) and particle (Mie) scattering. Atmospheric absorbers include oxygen (Schumann-Runge and Hertzberg structures) and ozone (Hartley, Huggins, and Chappuis structures). A host of other gaseous absorbers (sulfur and nitrogen dioxides) can attenuate the actinic flux under polluted conditions. The effect of Rayleigh-scattering on actinic flux is relatively well known and is routinely modeled. However, Mie-scattering due to the presence of clouds and aerosols is more complex, depending upon the composition and distribution of the particles. A detailed description of the TUV model is provided by *Madronich* [1987].

[Tie et al., 2003]

Aerosol optical parameter inputs:

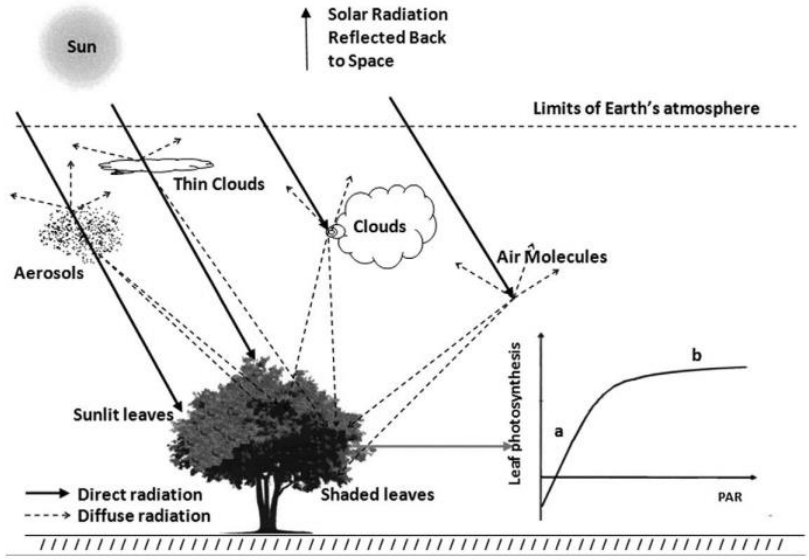

[Kanniah et al., 2012]

Species: AOD,SSA

The extinction effect of the particles can be fed back to the photolysis reaction correctly

Development 8: Heterogeneous reactions

Heterogeneous reaction :
The heterogeneous reactions on black carbon were added to the model

Reaction rate coefficient

$$k_{p,j} = \int_{r_1}^{r_2} k_{d,j}(r) n(r) dr$$

[Heikes and ThompsonTie, 1983]

Gas-to-particle diffusion rate constant

$$k_{d,j} = \frac{4\pi r D_j V}{1 + K_n[\lambda + 4(1-\gamma)/3\gamma]}$$

[Fuks and Sutugin, 1970]

（b）在黑碳气溶胶表面

非均相反应	吸收系数 γ		参考
O_3 (g) → O_3 (ads)	$1.8 \times 10^{-4} \times e^{-\frac{1000}{T}}$		(Tie 2005)
OH (g) → OH (ads)	5.0×10^{-2}		(Slade and Knopf 2013)
HO_2 (g) → HO_2 (ads)	1.0×10^{-2}		(Saathoff et al. 2001)
NO_2(g) → 0.5HONO + 0.5HNO_3	5.0×10^{-4}		(Lei 2004)
NO_3 (g) → HNO_3 (ads)	3.0×10^{-4}	(*RH*<0.5)	(Saathoff et al. 2001)
	1.0×10^{-4}	(*RH*>0.5)	
N_2O_5 (g) → 2HNO_3 (ads)	4.0×10^{-5}	(*RH*<0.5)	(Saathoff et al. 2001)
	2.0×10^{-4}	(*RH*>0.5)	
HNO_3 (g) → HNO_3 (ads)	1.0×10^{-3}		(Rogaski et al. 1997)

Development 9:海气CO_2通量计算

计算公式：

$$F=k\times\alpha_s\times\Delta pCO_2$$

Wanninkhof (1999)

F 为海–气界面 CO2 交换通量，k 为海–气界面气体传输速度(cm/h)；α_s 为 CO2 在海水中的溶解度系数，ΔpCO2 是海水与大气中 pCO2 的差值

(1) 传输速度k

$$k_L = 0.0283\ U_{10}^3 (S_c/660)^{-1/2}$$

Wanninkhof 99 (Wanninkhof and McGills, 1999)

U10：10米风速；Sc：施密特数；k单位：cm/h

施密特数Sc（0~30℃范围内海水中CO2）

$Sc = 2073.1-125.62*SST+3.6276*SST^2-0.43219*SST^3$

（SST in ℃）

《基于走航监测的海-气CO2交换通量评估技术规程（试行）》，国家海洋局生态环境保护司，2015.10

(2) 海洋CO2分压（pCO2）
使用再分析数据中的pCO2

https://www.ncei.noaa.gov/data/oceans/ncei/ocads/data/0160558/MPI_SOM-FFN_v2020/spco2_MPI-SOM_FFN_v2020.nc

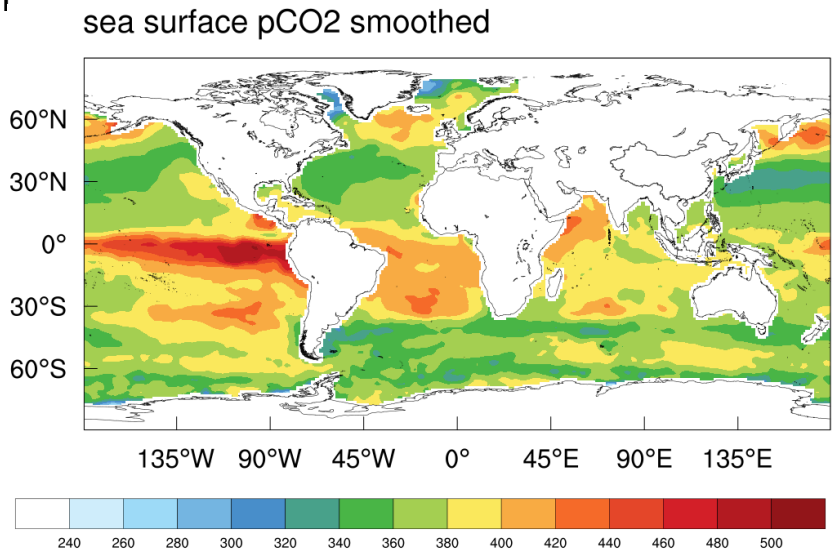

Development 10: 与APSIM连接

农业生产系统模拟器（Agricultural Production Systems Simulator，APSIM）7.10版(Holzworth et al., 2014)由澳大利亚联邦科学和工业研究组织（CSIRO）牵头开发，可以模拟关键的作物生理过程，包括物候学、器官（叶、茎、根和谷物）发育、水和养分吸收、碳同化、生物量和器官间的氮分配，以及对非生物胁迫的反应。

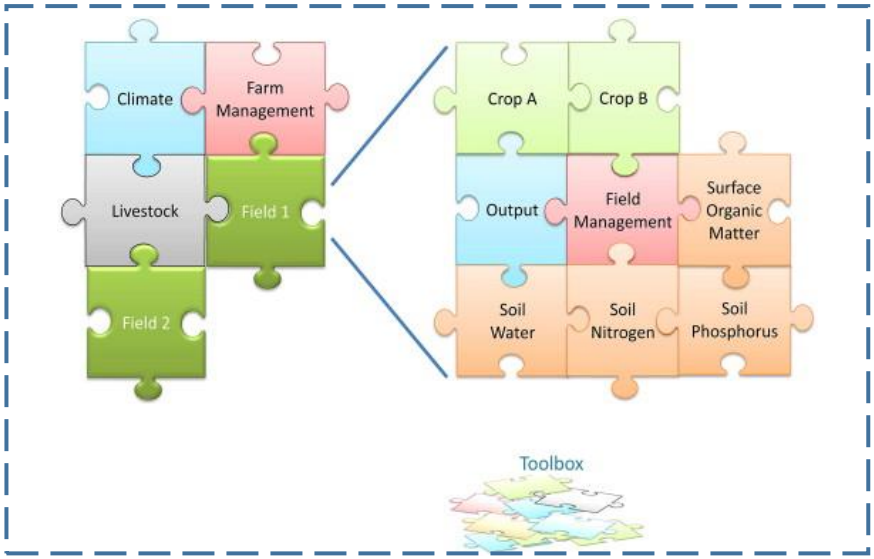

APSIM 模拟概念

APSIM
AGRICULTURAL PRODUCTION SYSTEMS SIMULATOR

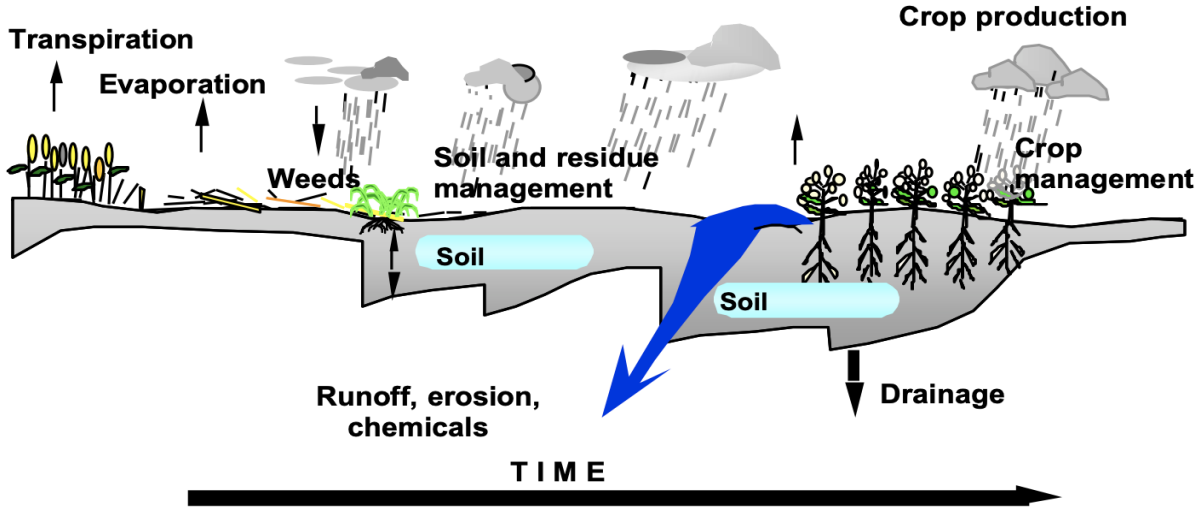

APSIM模拟过程

Ozone impact on crop yield

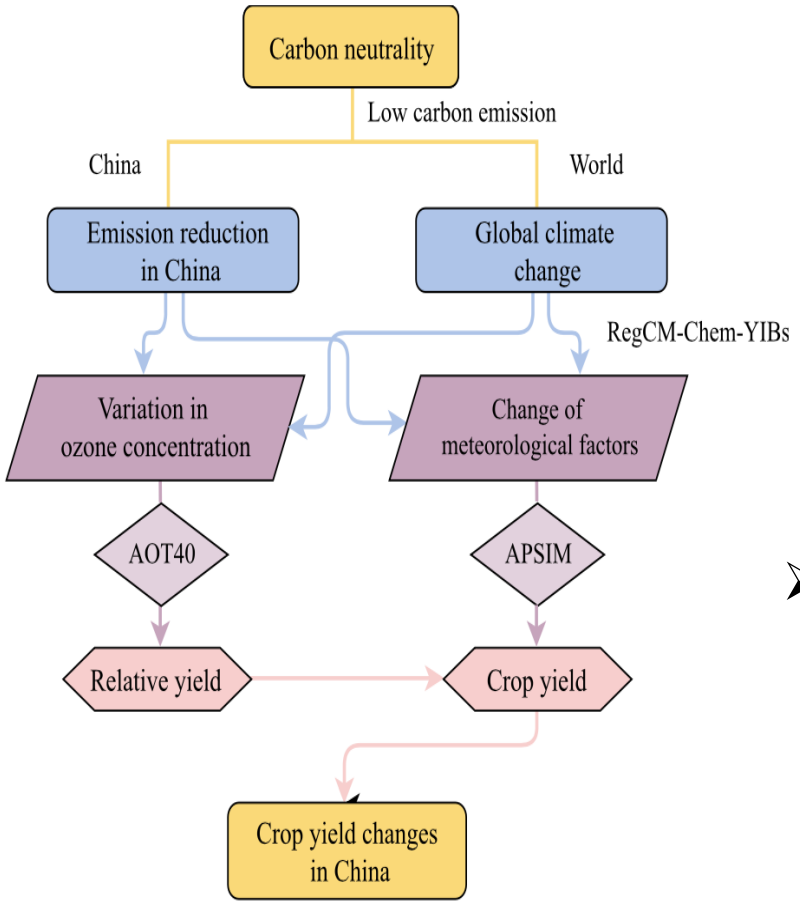

Illustration of the method

- The change in crop yield due to meteorological factors was calculated as follows:

$$f_{met,n} = \frac{Y_{m1,n} - Y_{m2,n}}{Y_{baseline,n}}$$

$$AOT40 = \sum_{i=1}^{n}([O_3]_i - 0.04)$$

$$RY = f(AOT40)$$

- Changes in crop yields under the influence of both O_3 concentration variation and meteorological factors were calculated as follows:

$$f_{both,n} = \frac{Y_{m1,n} \times RY_{m1,n} - Y_{m2,n} \times RY_{m2,n}}{Y_{baseline,n} \times RY_{baseline,n}}$$

RegCM-Chem-YIBs

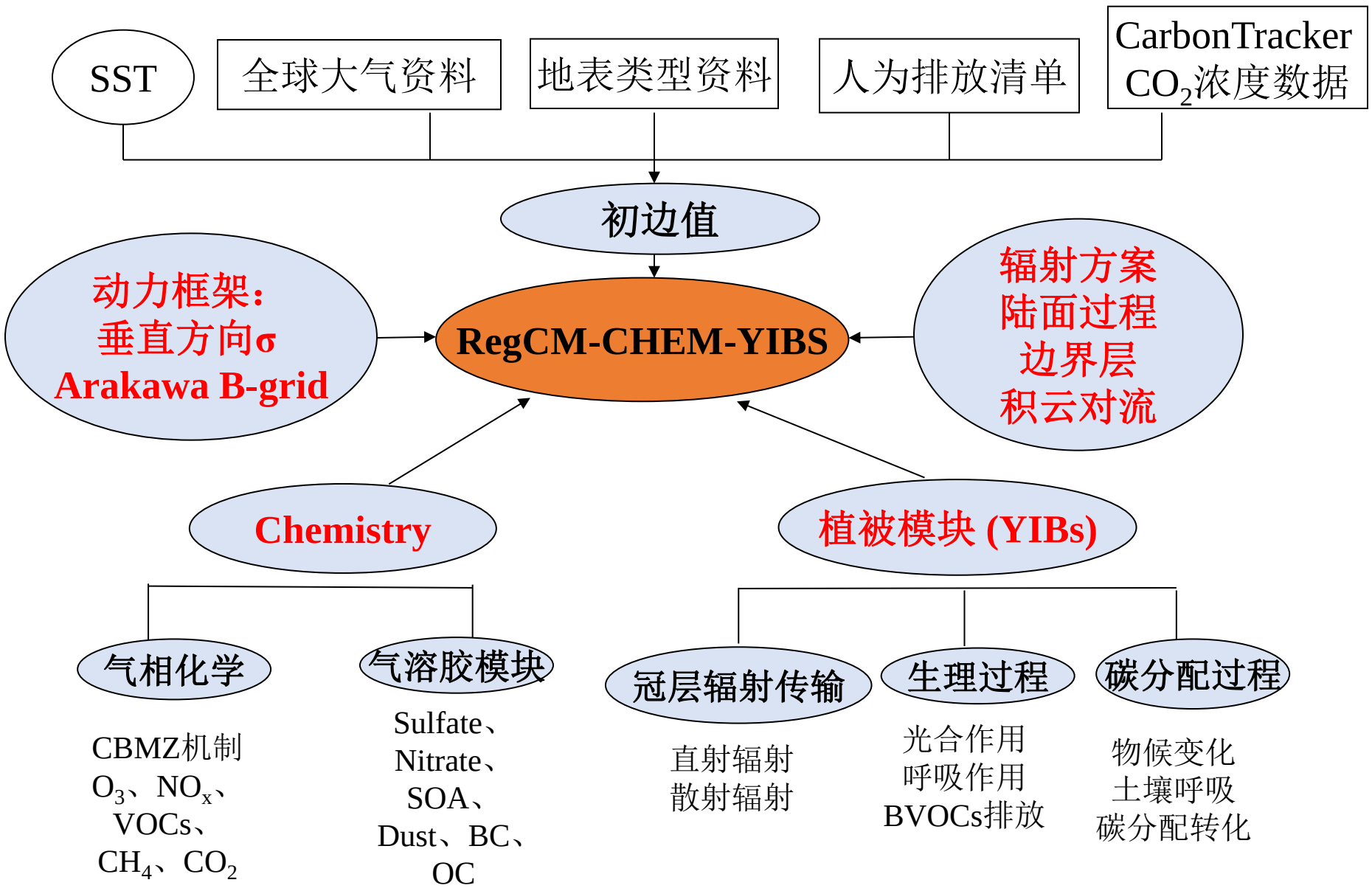

RegCM-Chem-YIBs耦合模式基本框架

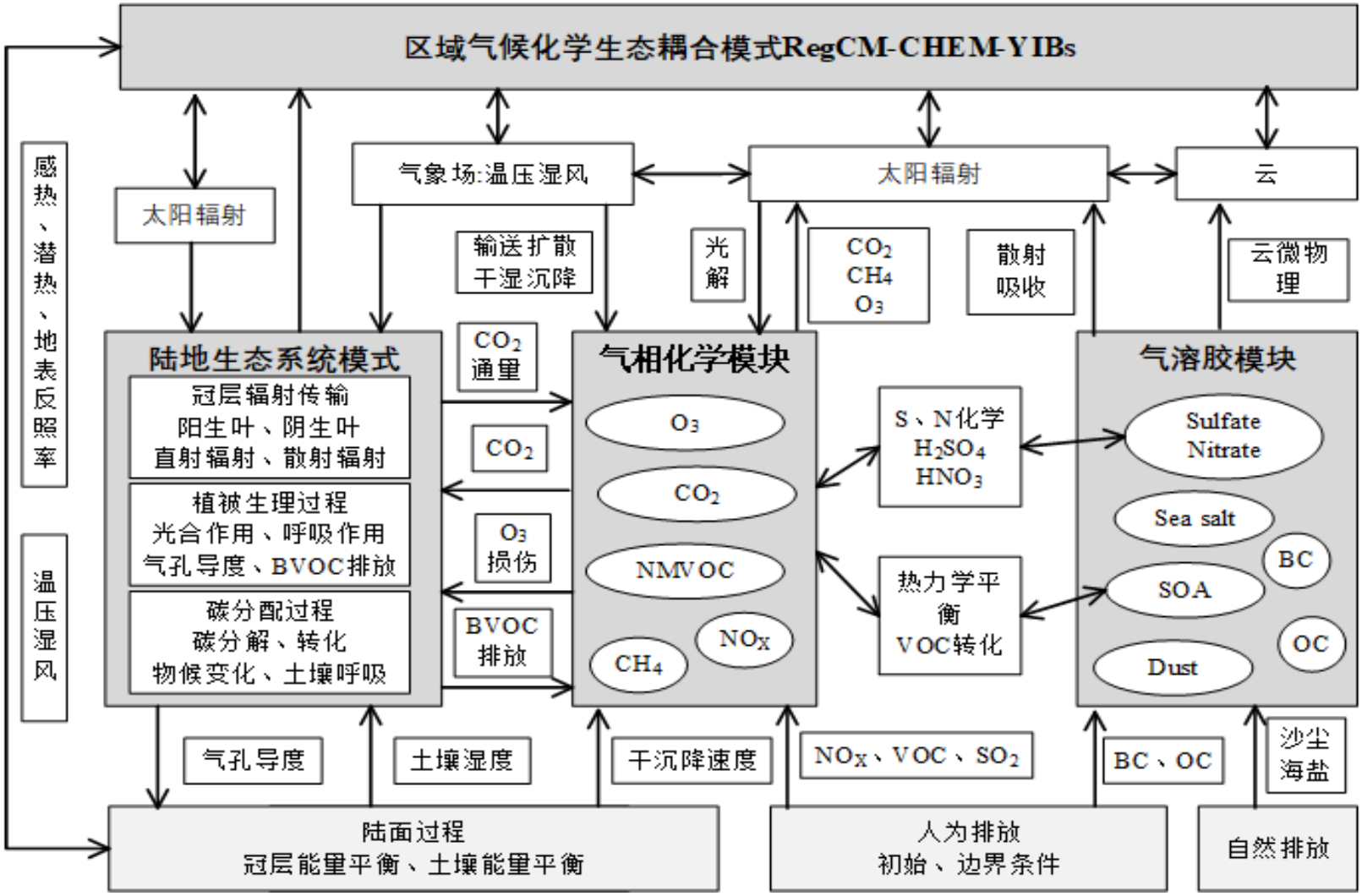

东亚地区模拟模式设置

- 模拟时间：2015年12月1日-2016年12月31日（首个月作为预积分阶段）
- 网格设置：中心经纬度E107°N36°，水平分辨率30km，网格数为256X160，垂直方向分为14层，模式顶层气压为50hpa

模式参数	说明
积云对流方案	Greel方案
侧边界条件方案	松弛边界条件（指数）
辐射方案	CCM3
边界层方案	Holtslag PBL方案
表面层方案	Monin-Obukhov方案
水汽方案	显示水汽方案（SUBEX;Pal et al.2000）
海洋通量方案	Zeng et al(1998)
海平面温度数据	OI_WK
气象初始边界数据	EAR-Interim
排放清单	中国区域:MEIC，中国外区域：MIX
CO2初始边界条件	Carbon Tracker 2019

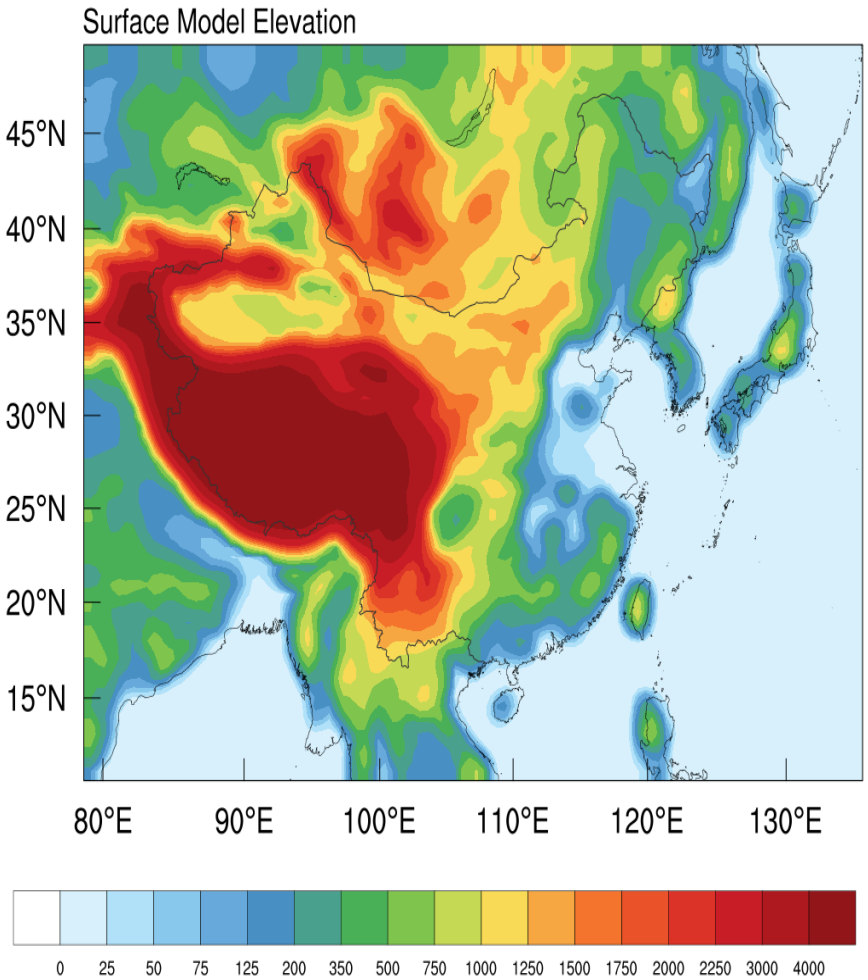

模拟区域

气候模拟与验证

➢将2016年全年不同高度上模拟的温度、比湿和环流特征与ERA-Interim再分析资料对比；温度的相关系数（R）为0.95~0.98，经向风的R为0.71~0.97，纬向风的R为0.81~0.92，比湿的R为0.91~0.92

模拟　　观测

全年

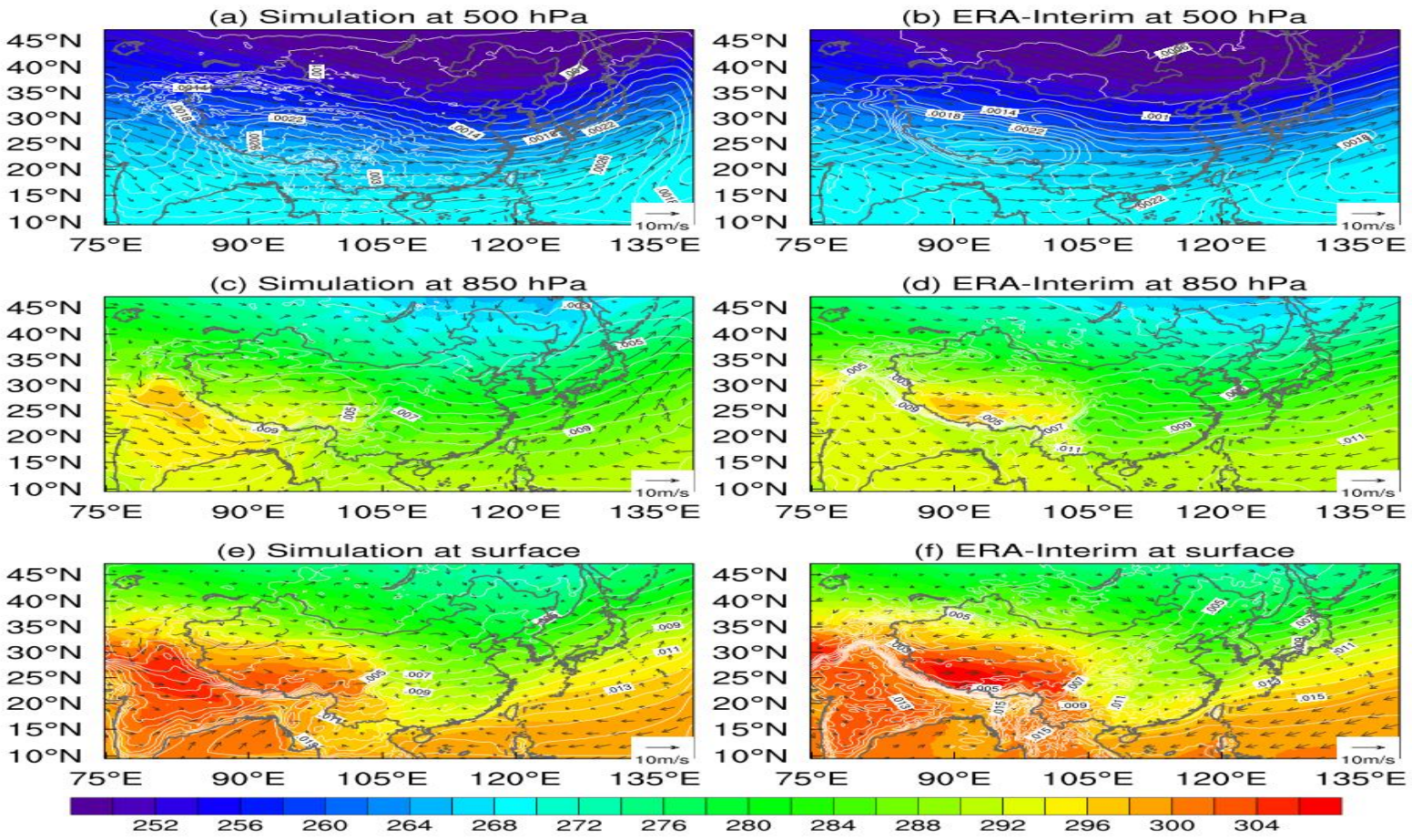

$PM_{2.5}$和O_3模拟与验证

➢将2016年模拟的O_3MDA8和日均$PM_{2.5}$与观测站点对比验证，O_3和$PM_{2.5}$的模拟与观测的相关系数分别为0.74和0.65

➢RegCM-Chem-YIBs模式能够较好地捕捉观测到的近地表臭氧和颗粒物的空间分布，特别是在高污染地区，但在汾渭平原对O_3的模拟有一定的低估

模拟　　观测

O_3MDA8

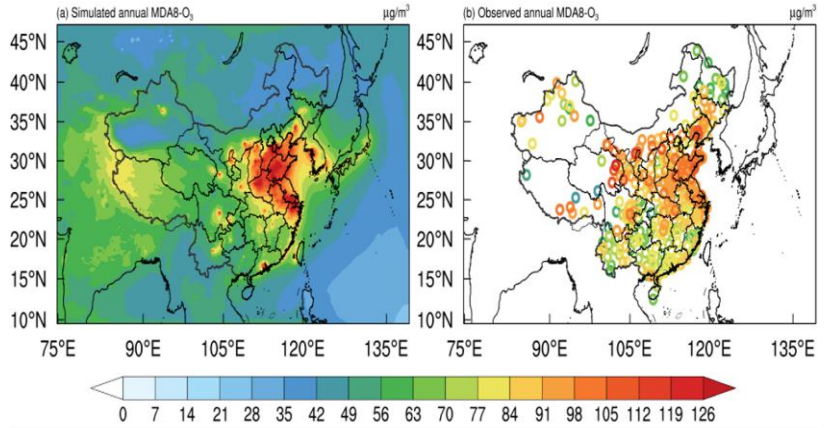

日均$PM_{2.5}$

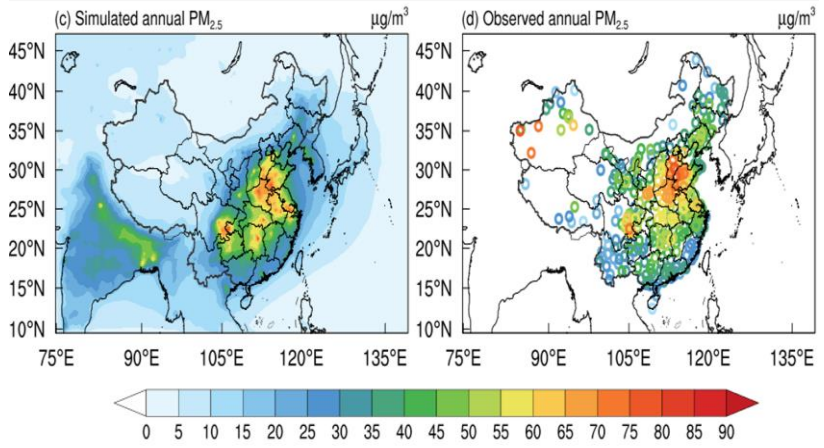

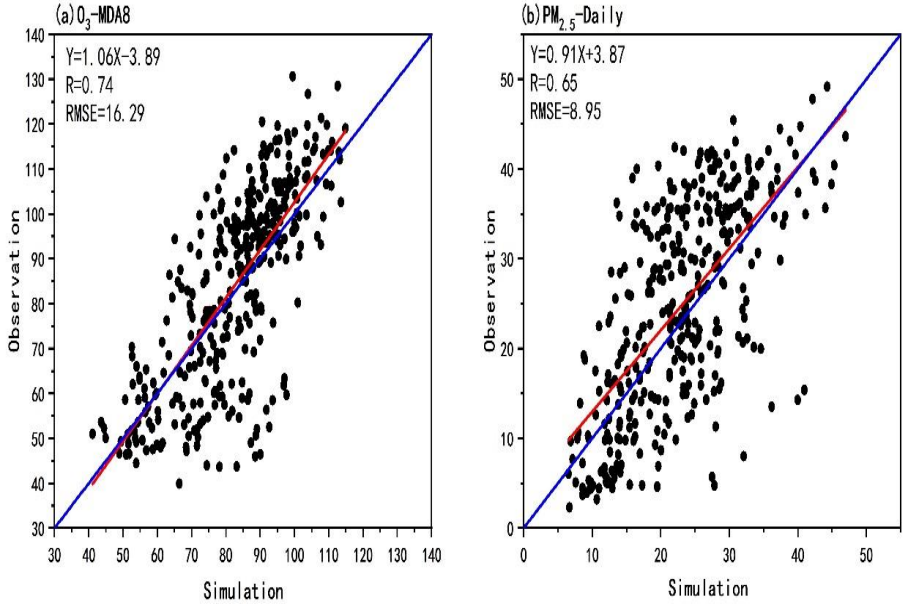

Variables	R	MB	ME	NMB	NME	RMSE
O_3_MDA8	0.74	-1.47	11.61	0.0235	0.1577	16.29
$PM_{2.5}$_Daily	0.65	-1.80	7.21	0.1380	0.4211	8.95

CO_2模拟与验证

- 将2016年模拟的CO_2与东亚观测站点和卫星同化产品对比验证，相关系数为0.89 ~ 0.97
- RegCM-Chem-YIBs模式总体上能较好的模拟了CO_2的时空分布，但不同站点间存在差异（背景站模拟效果好于其它站点）

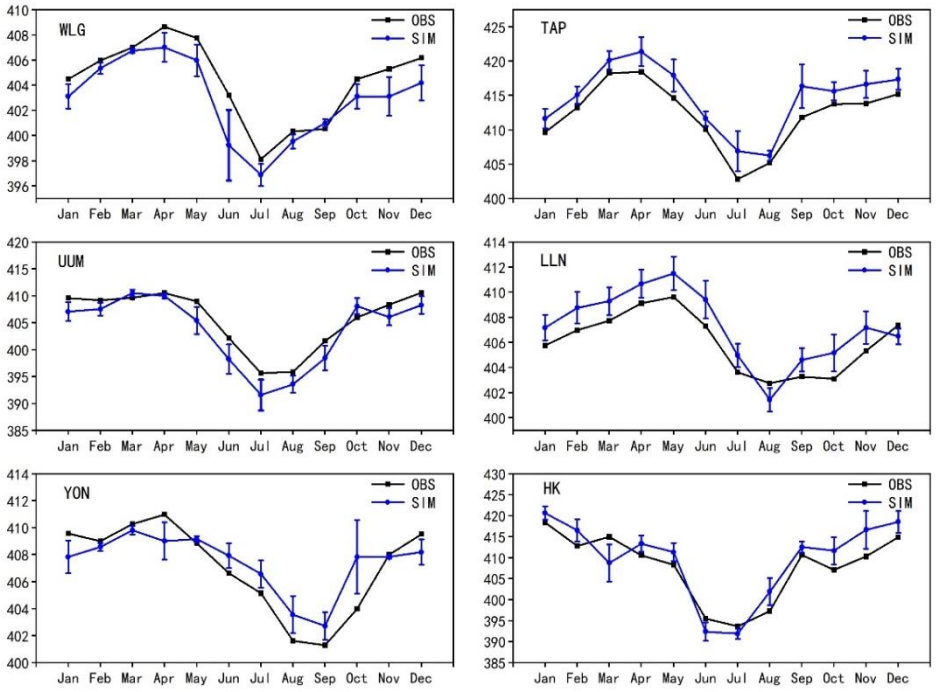

模拟　　观测

全年

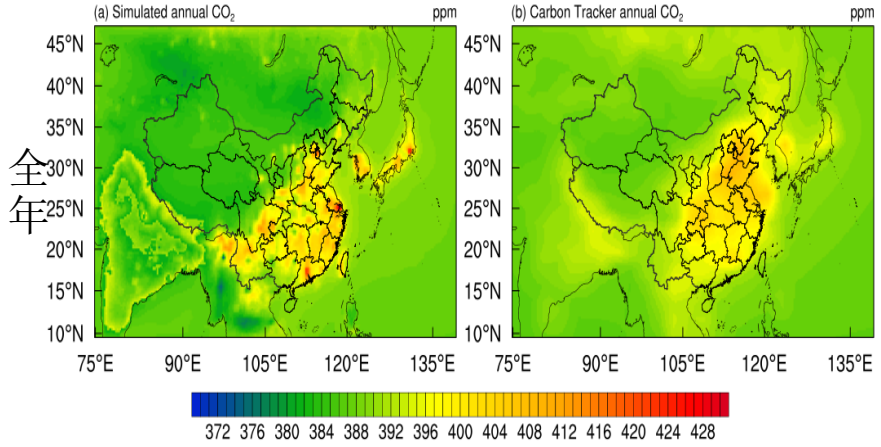

季节变化

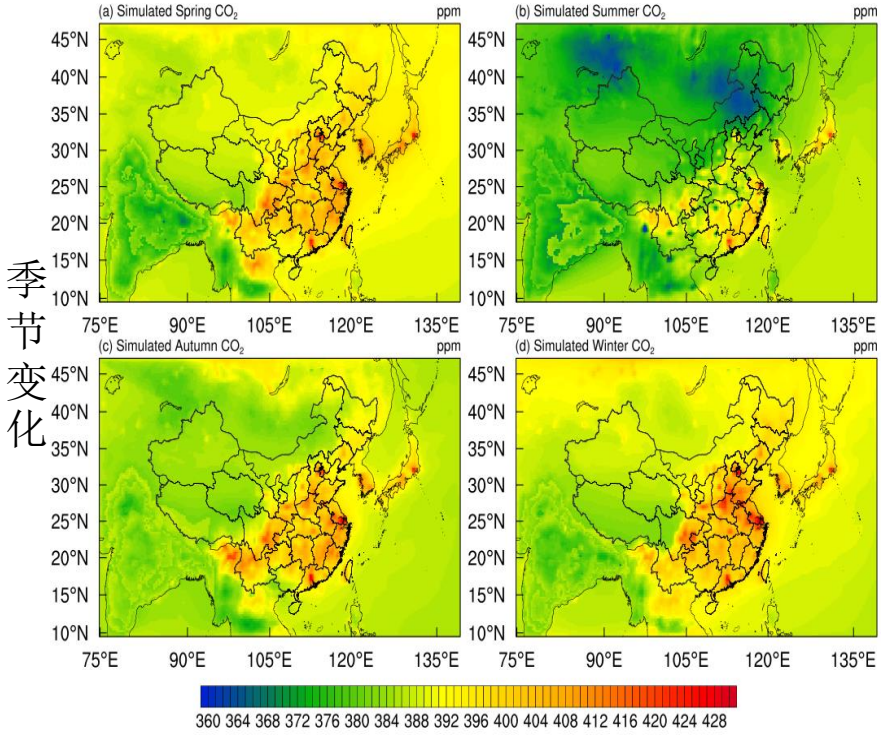

陆地碳通量模拟与验证

- 将2016年模拟的总初级生产力GPP和净初级生产力NPP与MODIS对比验证，相关系数分别为0.91 和0.87，平均偏差分别为0.13 Kg C m^{-2} $year^{-1}$和0.05 Kg C m^{-2} $year^{-1}$
- 中国地区模拟的年平均GPP为6.18 Pg C $^{-1}$，NPP为3.21 Pg C $^{-1}$，模式在西南和华中地区的模拟有一定的高估
- RegCM-Chem-YIBs模式总体上能合理的模拟了陆地碳通量的时空分布

模拟　　观测

GPP

NPP

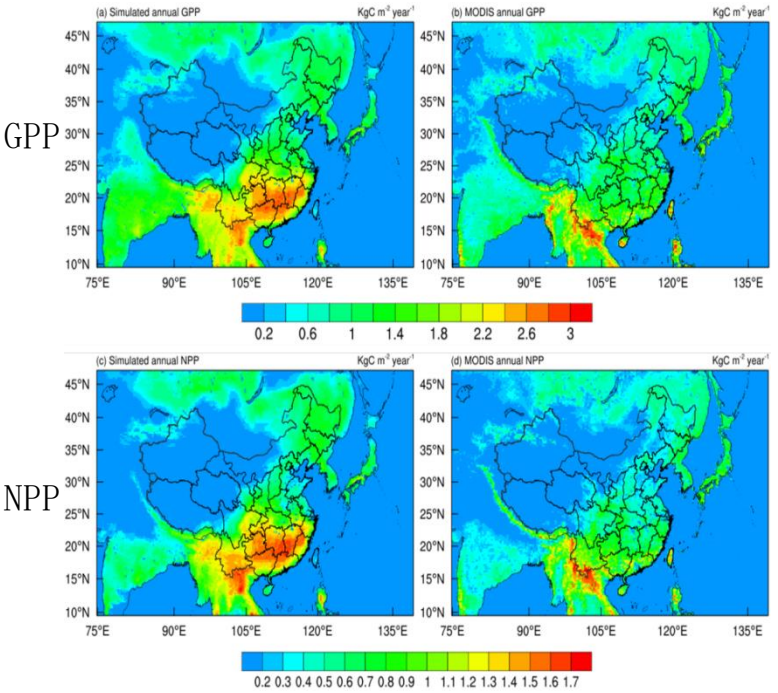

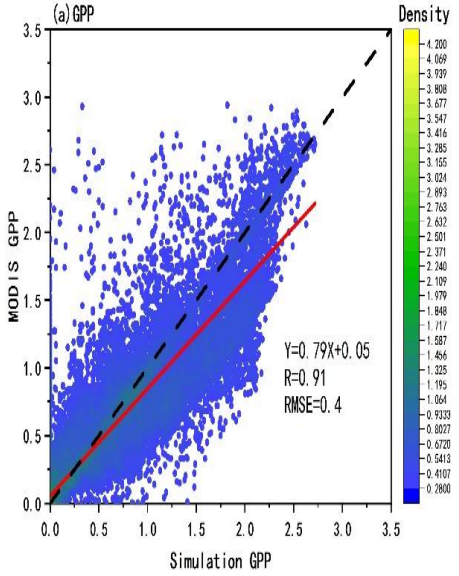

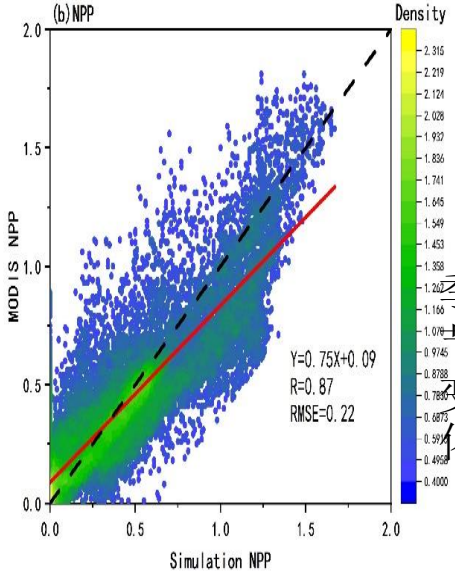

季节变化

GPP　　NPP

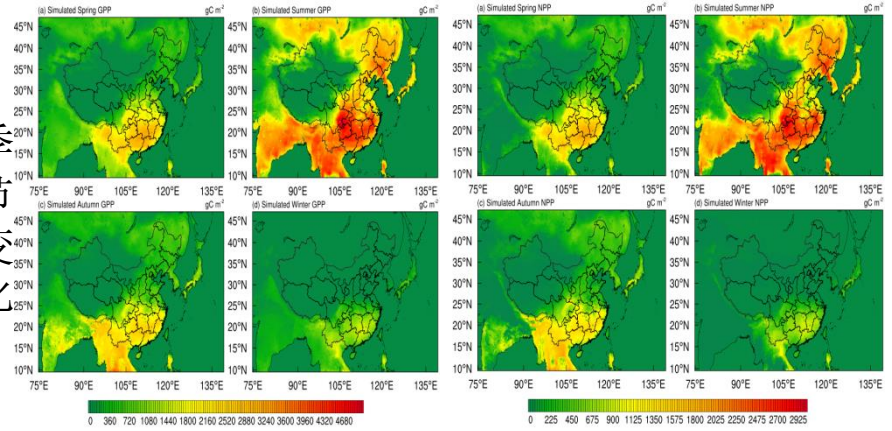

Evaluation of surface CO_2

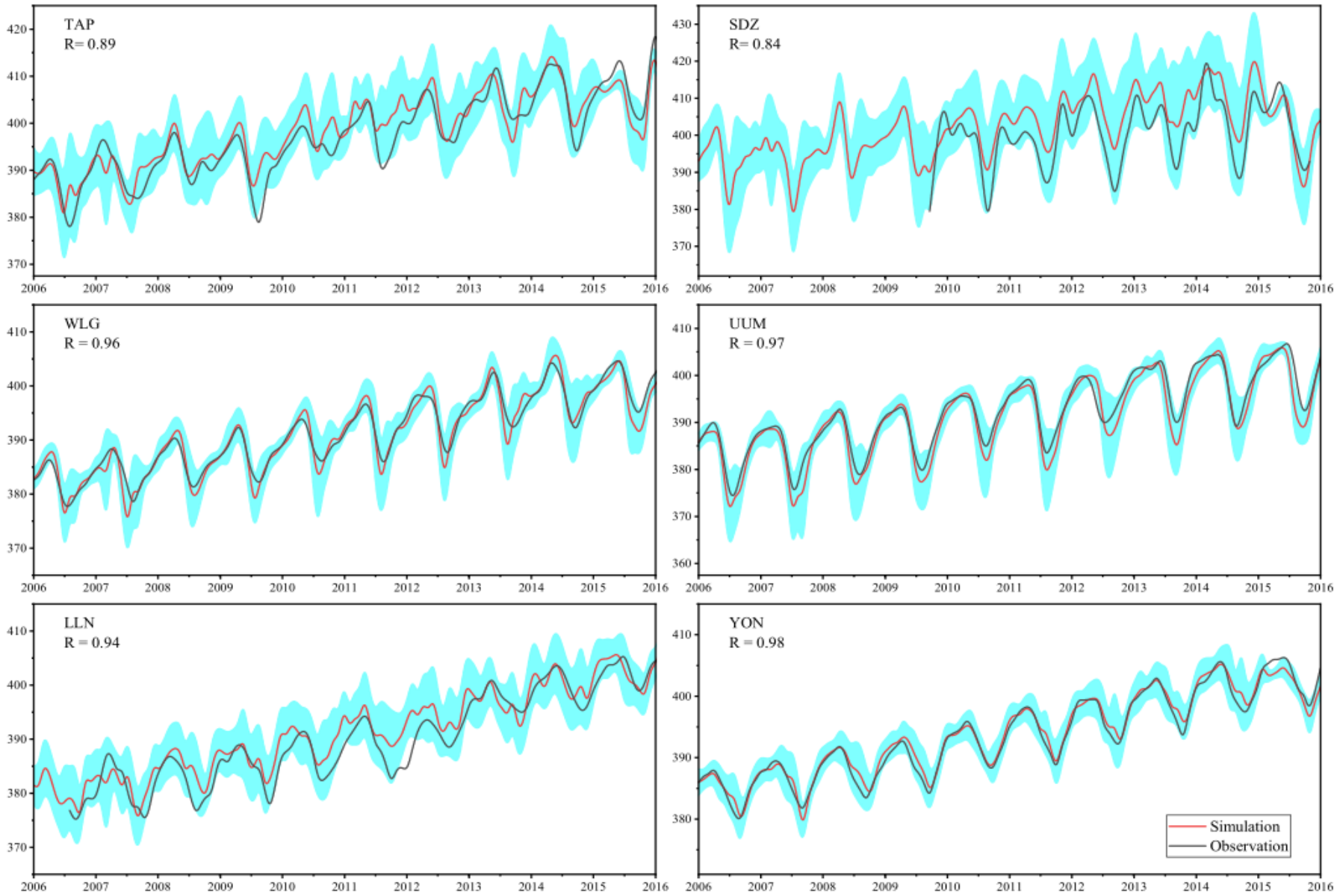

Evaluation of AOD

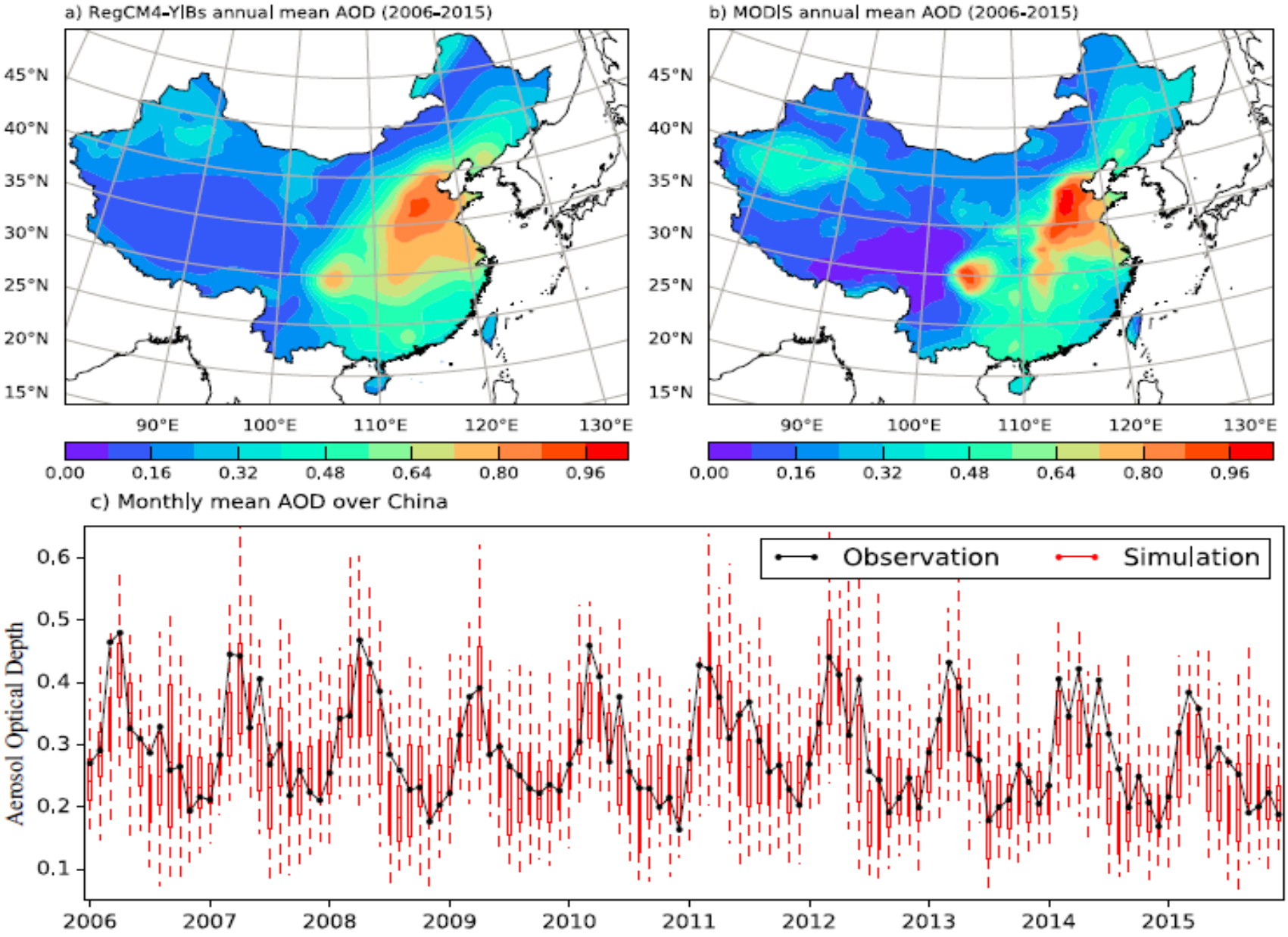

报告提纲

- 研究背景
- 模式发展
- 应用研究
- 总结展望

研究内容

- 大气污染对东亚季风气候的影响
- 极端天气对空气污染的影响
- 未来气候变化对大气污染的影响
- 气象和排放对大气污染的不同影响
- 臭氧-细颗粒物-二氧化碳的的相互作用
- 双碳战略对大气环境和气候的影响
- 空气污染和气候变化对农业和能源的协同影响

Atmospheric Research 279 (2022) 106384

Contents lists available at ScienceDirect

Atmospheric Research

journal homepage: www.elsevier.com/locate/atmosres

Impacts of regional emission reduction and global climate change on air quality and temperature to attain carbon neutrality in China

Beiyao Xu, Tijian Wang *, Danyang Ma, Rong Song, Ming Zhang, Libo Gao, Shu Li, Bingliang Zhuang, Mengmeng Li, Min Xie

School of Atmospheric Sciences, Nanjing University, Nanjing, China

ARTICLE INFO

Keywords:
Air quality
Temperature
China
CO_2
Carbon neutrality
Climate change

ABSTRACT

Future air quality and temperature are major concerns worldwide, especially in East Asia, leading to carbon neutrality targets. China is committed to achieving carbon neutrality by 2060. This study evaluated regional emission reduction targets and global climate change impacts in China. We investigated changes to air quality and temperature in China using the coupled regional climate-ecology model RegCM-Chem-YIBs. The Ambitious-Pollution-Neutral-Goals scenario from the Dynamic Projection model for Emissions in China (DPEC) database was chosen as the future emission reduction pathway in China. Representative concentration pathway (RCP) climate scenarios were used to represent one possibility for future global climate change. The results showed that annual average $PM_{2.5}$ and O_3 concentrations in China could meet World Health Organization (WHO) guidelines if the carbon neutral reduction pathway is followed. Emission reduction is far more effective than climate change in improving air quality. $PM_{2.5}$ and O_3 concentrations in 2060 will decline to 2.6 and 63.0 μg m^{-3}, respectively, under stringent emission reduction policies. Both carbon reduction and photosynthesis of vegetation promoted by global warming will reduce CO_2 concentrations by at least 8 ppm in 2060. Global climate change will heat up the entire country by at least 1 K. Regional emission reduction will diminish the cooling effect of particulate matter, resulting in slight warming, which would slow progress in global warming control. This study shows that regional emission reduction is the main factor affecting future air quality, whereas global climate change is the primary driver of future increases in air temperature. The emission reduction policy, which is designed to achieve carbon neutrality in China, is sufficient to mitigate air pollution, and generate additional health benefits; however, it will contribute to higher air temperature in some areas. Therefore, mitigating rising temperatures requires global efforts and a more rational pathway to reduce emissions.

Environmental Pollution 317 (2023) 120715

Contents lists available at ScienceDirect

Environmental Pollution

journal homepage: www.elsevier.com/locate/envpol

Impacts of meteorological factors and ozone variation on crop yields in China concerning carbon neutrality objectives in 2060

Beiyao Xu [a], Tijian Wang [a,*], Libo Gao [a,c], Danyang Ma [a], Rong Song [a], Jin Zhao [b], Xiaoguang Yang [b], Shu Li [a], Bingliang Zhuang [a], Mengmeng Li [a], Min Xie [a]

[a] School of Atmospheric Sciences, Nanjing University, Nanjing, 210023, China
[b] College of Resources and Environmental Sciences, China Agricultural University, Beijing, 100193, China
[c] Jiangsu Meteorological Observatory, Nanjing, 210041, China

ARTICLE INFO

Keywords:
Carbon neutrality
Ozone
Crop yield
Climate change

ABSTRACT

Carbon neutrality objectives affect meteorology and ozone (O_3) concentration in China, both of which would influence crop yields, thus food security. However, the joint impact of these two factors on crop yields in China is not clear. In this study, we investigated future trends in China's maize, rice, soybean, and wheat yields under a carbon-neutral scenario considering both regional emission reduction and global climate change in 2060. By combining a process-based crop model (Agricultural Production Systems sIMulator, APSIM) with O_3 exposure equations, the impacts of regional emission reduction and global climate change were studied.

The results suggest that regional emission reduction dominated the increase in yield by reducing the O_3 concentration, whereas global climate change led to yield loss mainly through meteorological factors. The national yield decreases for the four crops ranged from 1.0% to 30.0% owing to meteorological factors, while O_3 reduction resulted in additional yield increases ranging from 2.0% to 7.0%. The combined effect of carbon neutrality, which included both meteorological factors and O_3 concentration, resulted in changes to the yields of maize, rice, soybean, and wheat of +4.3%, -7.3%, -24.0%, and -31.7%, respectively.

It seems that crop production loss caused by meteorological factors in 2060 would be mitigated by the O_3 reduction. Given the advantages of declining O_3 concentration, regional emission reduction would likely benefit crop growth. However, global climate change may offset the benefits and threaten food production in China. Therefore, more strict emission reduction policies and global climate change mitigation actions are necessary to ensure food security in China.

Model domain and scheme set

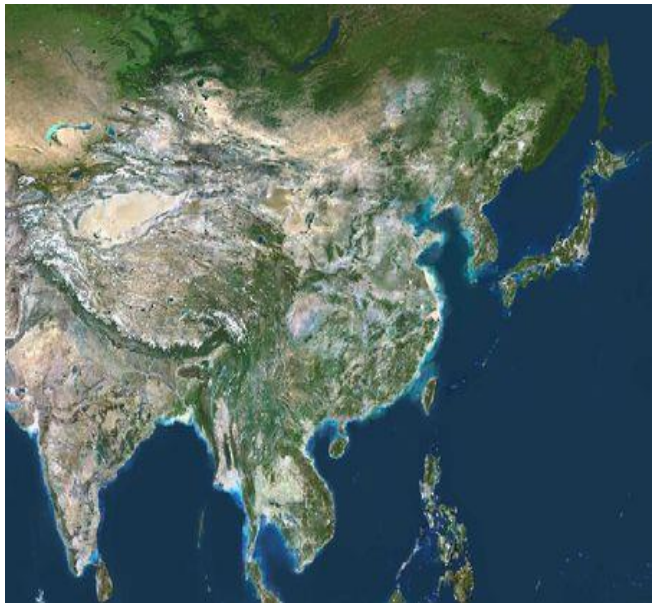

- The vertical resolution is set to 18 levels up to 50 hPa.
- Simulation time： 2015和2060
- Anthropogenic emissions are derived from a mosaic Asian anthropogenic emission inventory MIX with a spatial resolution of 0.25° × 0.25°.
- Initial condition (e.g., tree height and soil carbon pool) for YIBs model comes from a 30-year spin-up procedure.

Scheme	Explanin
Cumulus convection scheme	(Grell, 1993)
Boundary condition scheme	relaxed boundary condition
Boundary layer scheme	(Holtslag et al., 1990)
Radiation scheme	(Kiehl et al., 1996)
Ocean flux	(Zeng et al., 1998)
Meteorological boundary conditions	ERA-Interim
Chemical boundary condition	MOZART
Sea surface temperature	OI_WK

Simulation scenarios and emission data

Simulation scenarios.

Scenarios	Description
Baseline	Global Climate and China's Emissions in 2015.
BE	Global Climate in 2015 with China's emissions in 2060.
CE	Global Climate and China's emissions in 2060.

- The flux of CO_2, SO_2, NOx, NH_3, VOC, CO, OC, and BC in 2060 is based on the source emission inventory **(Ambitious-pollution-Neutral-goals)** generated by Tsinghua University using Dynamic Projection model for Emissions in China (DPEC) .

- The RCP2.6 scenario in the Representative Concentration Pathways (RCPs) proposed by the IPCC was used as input for the 2060 meteorological boundary field.

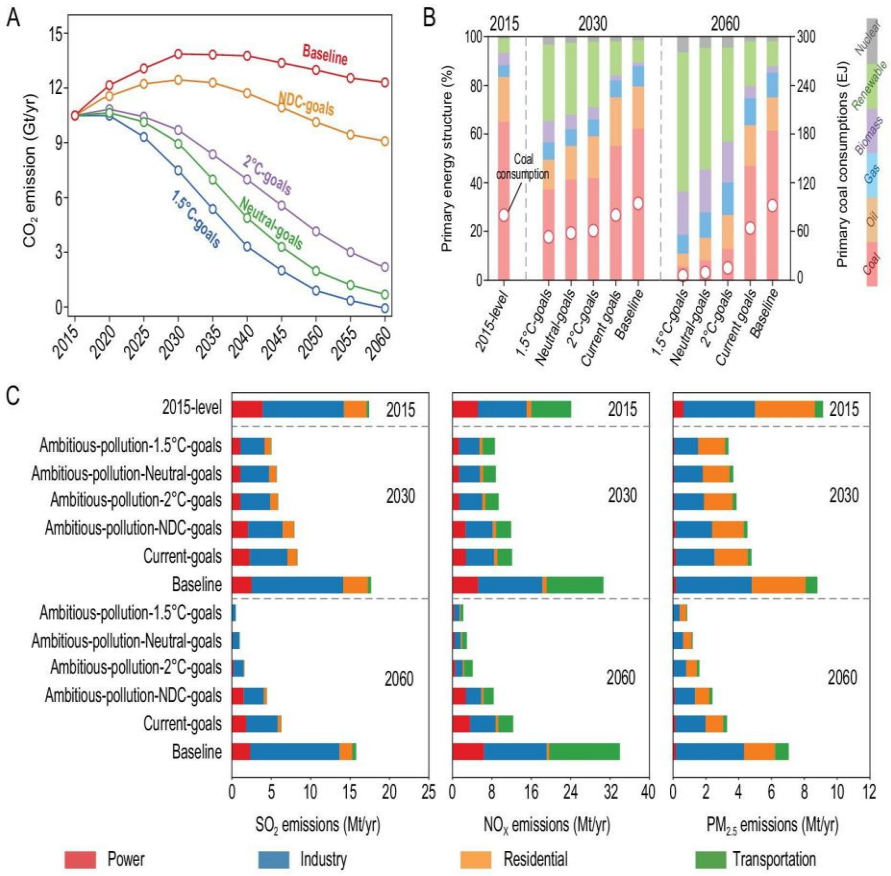

Future anthropogenic emission pathways and energy transitions over China.

(Cheng et al., 2021)

Impact of carbon neutrality on air temperature

Regional emission reduction **Global climate change** **Joint impact**

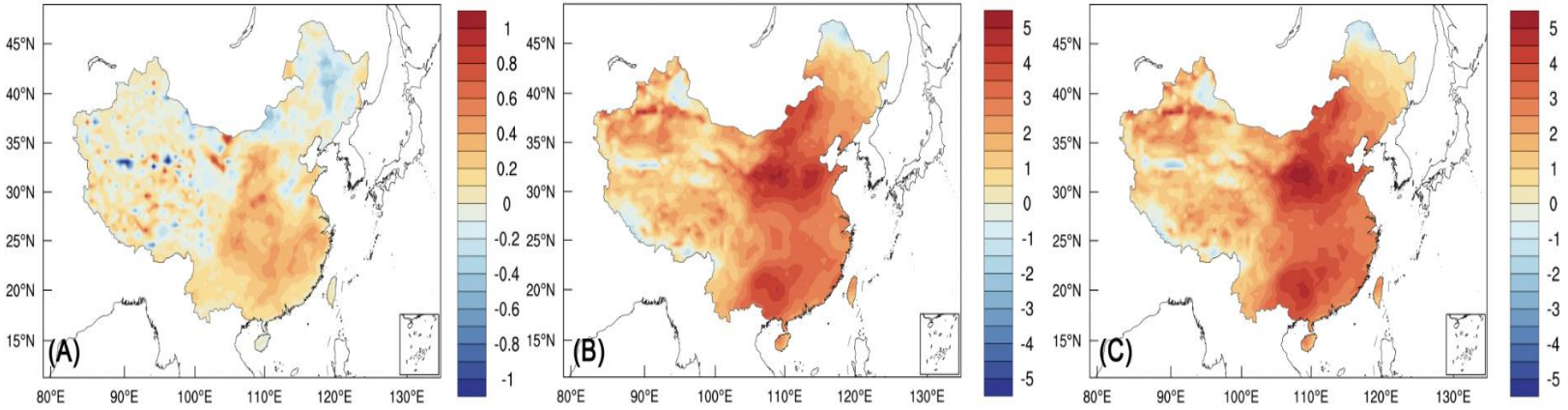

- Global climate change has warmed all of China by at least 1℃,reducing emissions inevitably diminishes the cooling effect of particulate matter.

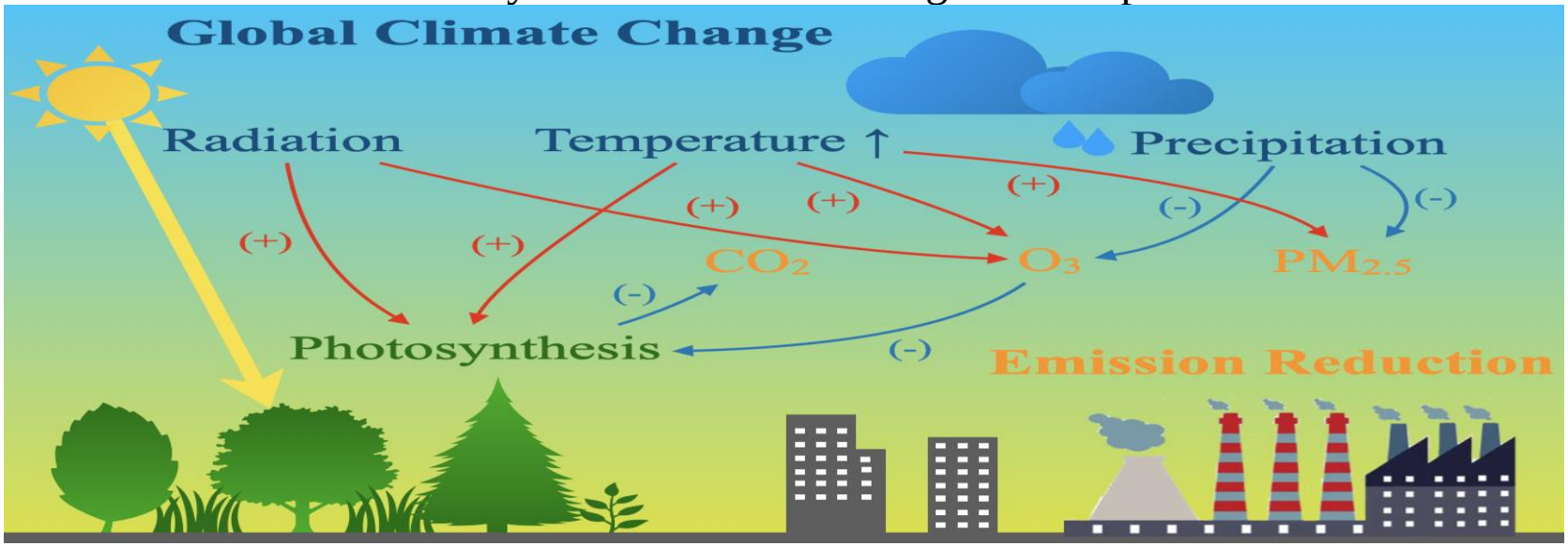

Impact of carbon neutrality on $PM_{2.5}$, O_3 and CO_2

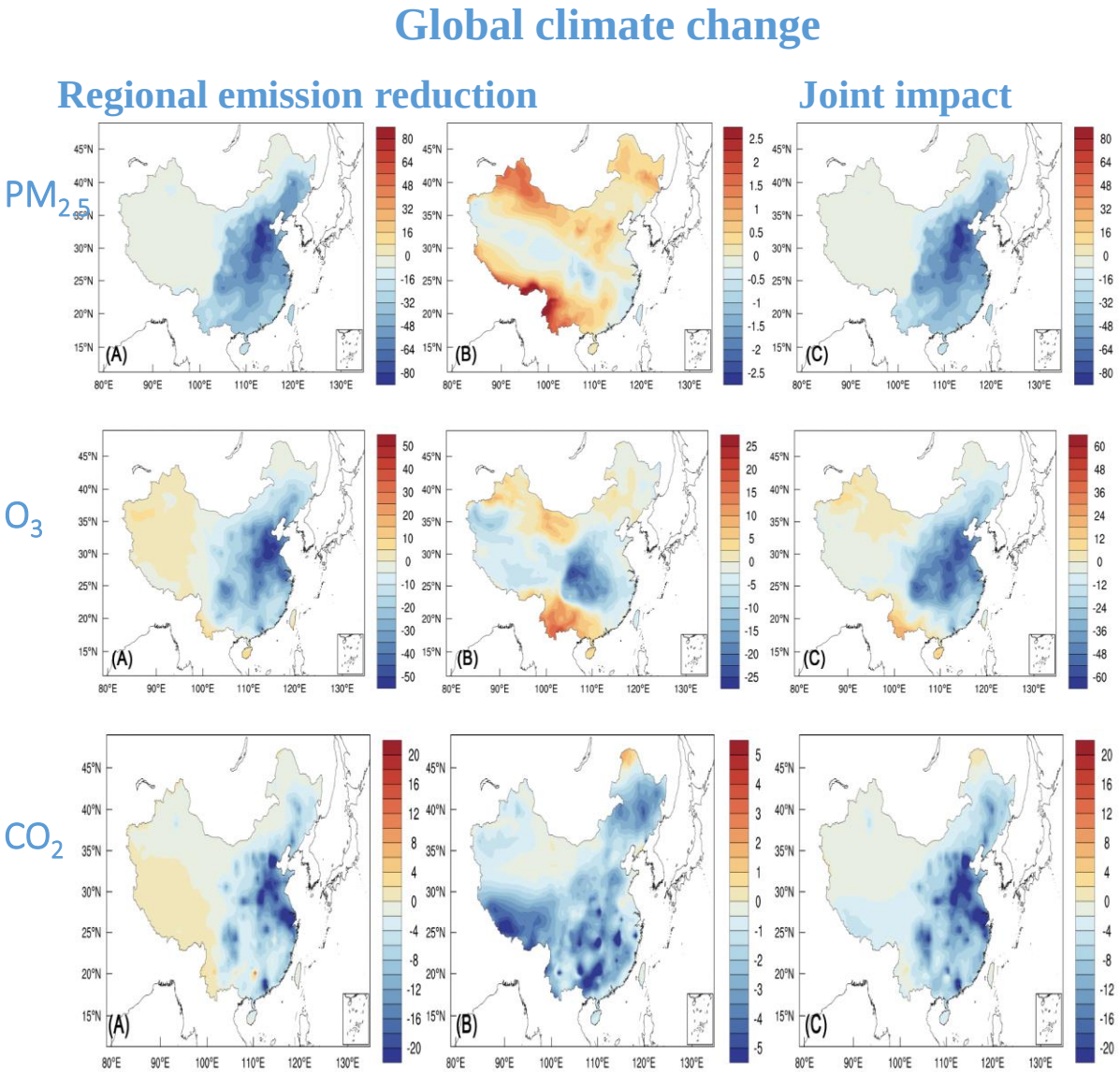

- **A substantial reduction in emissions led to a sharp decline in $PM_{2.5}$, with a maximum reduction of up to 92.2 μg m^{-3} .**
- **Strict carbon neutral emission reduction policies could lead national average annual O_3 concentrations of 63.0 μg m^{-3}, respectively, in 2060.**
- **Both regional emission reduction and global climate change would reduce CO_2 concentration of at least 8 ppm by 2060.**

臭氧

- O_3浓度呈现显著下降趋势，尤其是2015-2035年，O_3浓度以平均每年6.9 μg m^{-3}的速度下降。

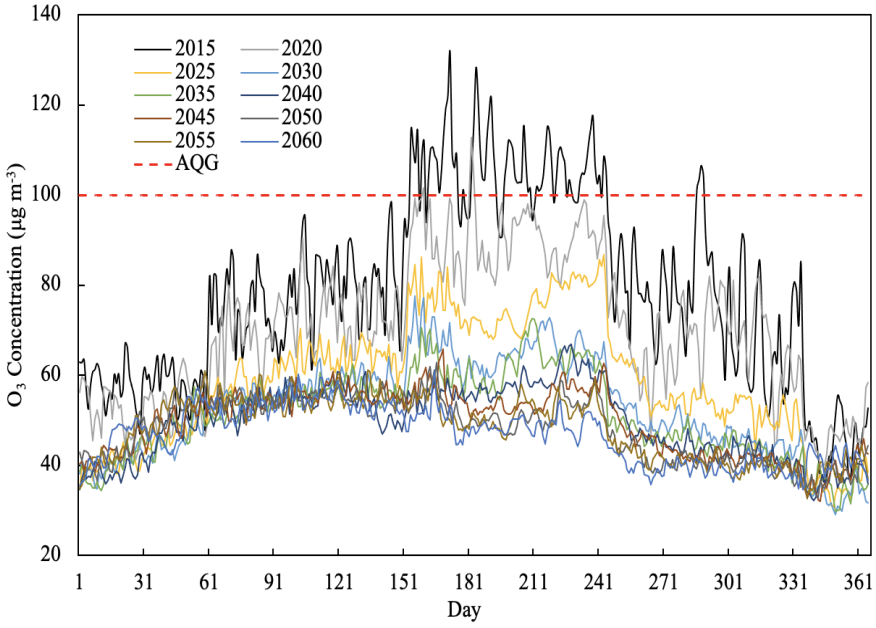

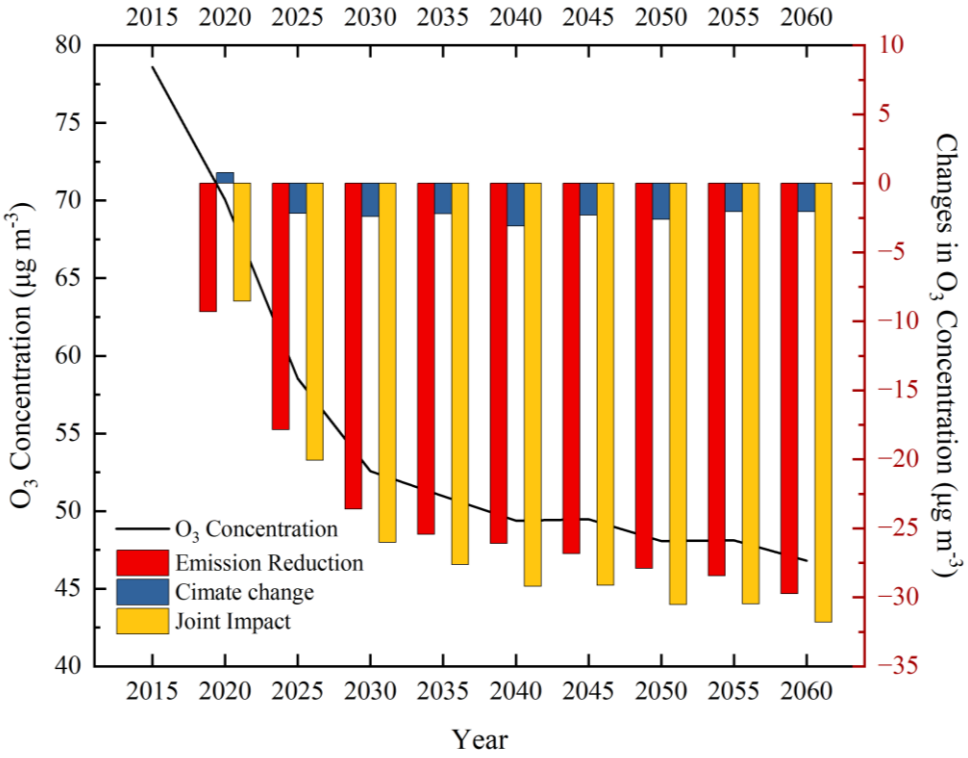

- 在二者的共同影响下，相比于2015年，减排导致2060年的O_3水平降低了31.8 μg m^{-3}。

- 到2060年，O_3浓度将会维持在60 μg m^{-3}以下。

颗粒物

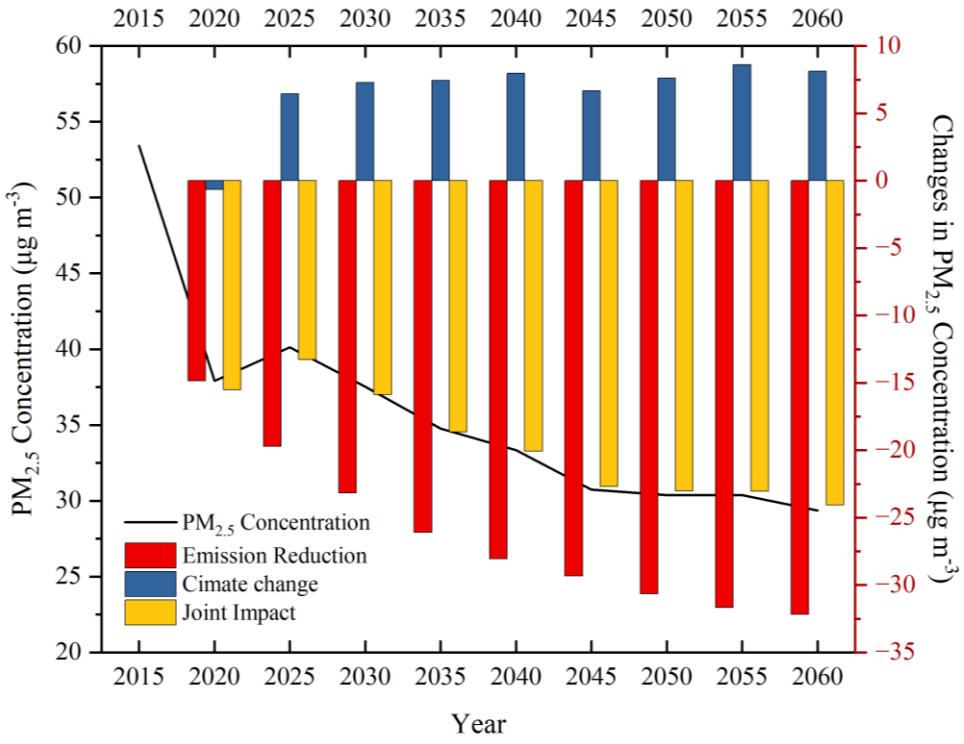

- $PM_{2.5}$浓度曲线呈现显著下降趋势，从2015年的年平均53.4 μg m^{-3}下降至2060年29.4 μg m^{-3}。
- 相比于2015年，减排导致2060年的$PM_{2.5}$水平降低了32.2 μg m^{-3}，全球气候变化反而导致$PM_{2.5}$浓度上升8.1 μg m^{-3}。

- 随着$PM_{2.5}$年均浓度的下降，冬季日均$PM_{2.5}$水平的降低仍不足以达到AQG。

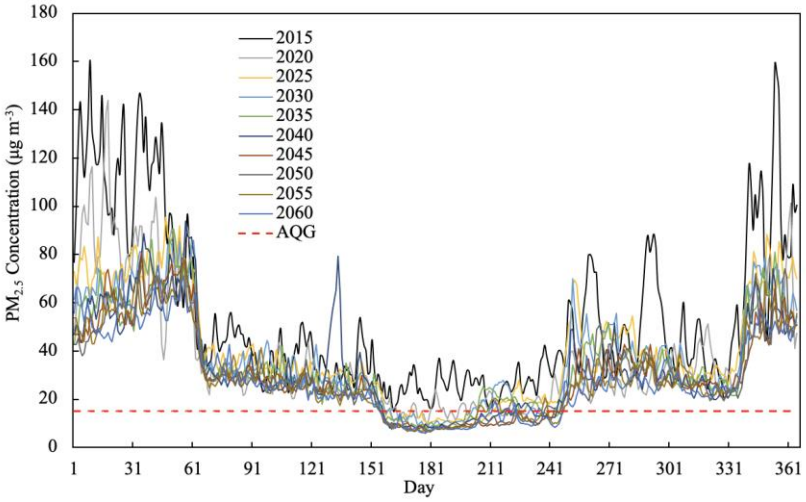

二氧化碳

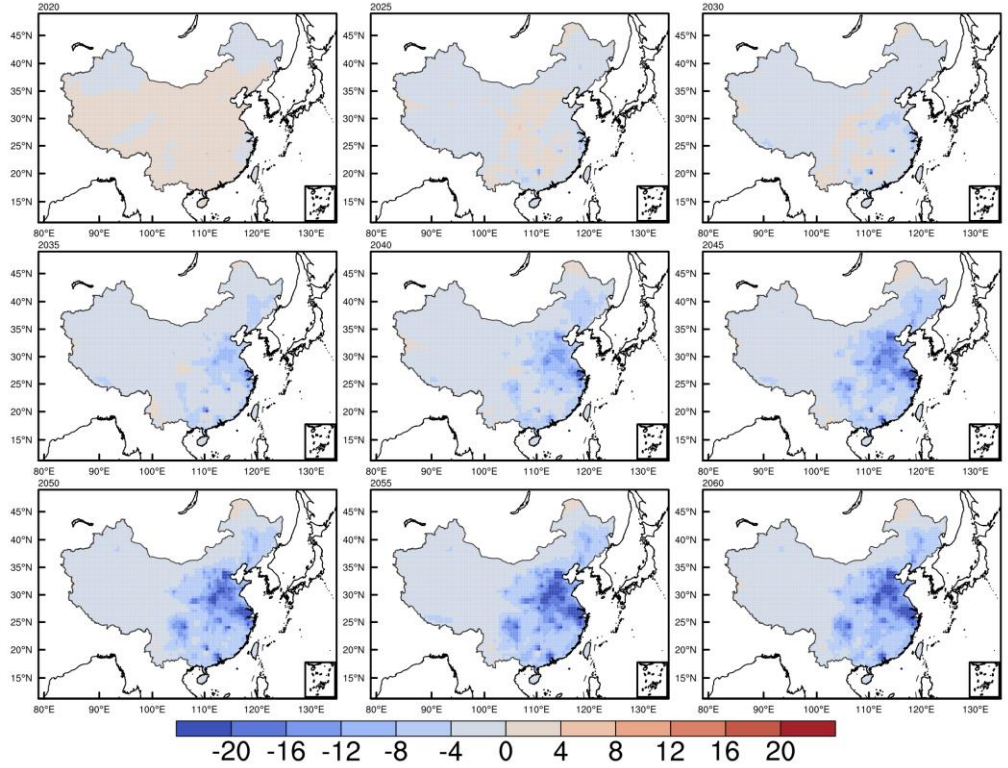

中国双碳政策和全球气候变化对CO_2浓度的共同影响

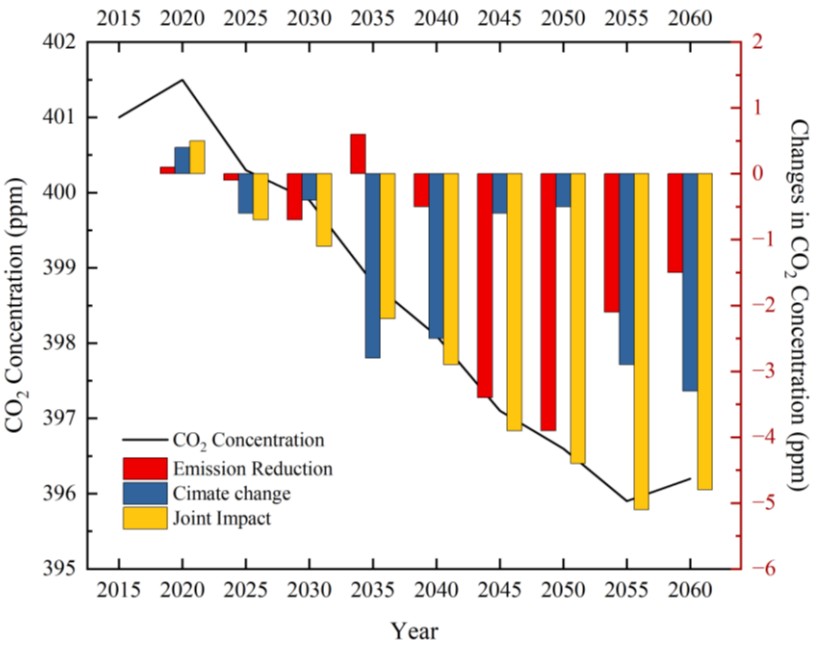

- 2055年CO_2浓度的下降幅度最大，低于2015年平均浓度5.1 ppm，其中57%的减少均是由气候变化带来的。

- 在减排政策和气候变化的协同影响下，CO_2浓度将会提前于2030年达到峰值。

- 升温的刺激下，植被光合作用增强，固碳能力提高，CO_2浓度随之下降。

Impact of carbon neutrality on crops yield

Result 1: Changes in maize yield

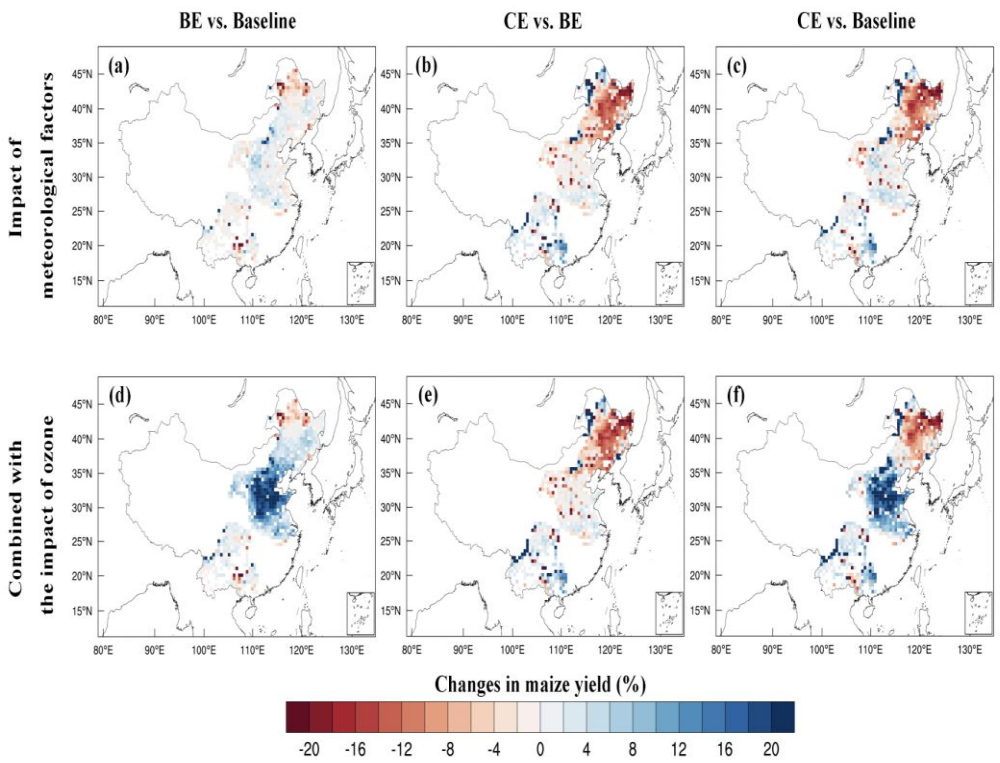

Result 2: Changes in rice yield

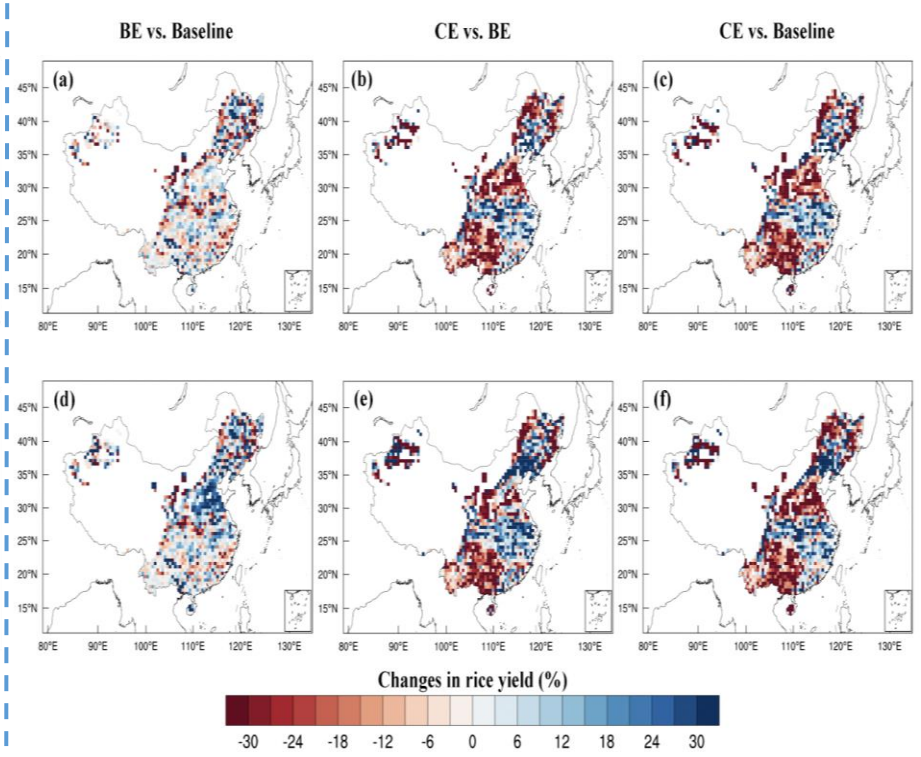

The national yield decreases for the four crops ranged from 1.0% to 38.0% owing to meteorological factors, while O_3 reduction resulted in additional yield increases ranging from 2.8% to 7.0%.

(Xu et al., 2023)

Impact of carbon neutrality on crops yield

Result 3: Changes in soybean yield

Result 4: Changes in wheat yield

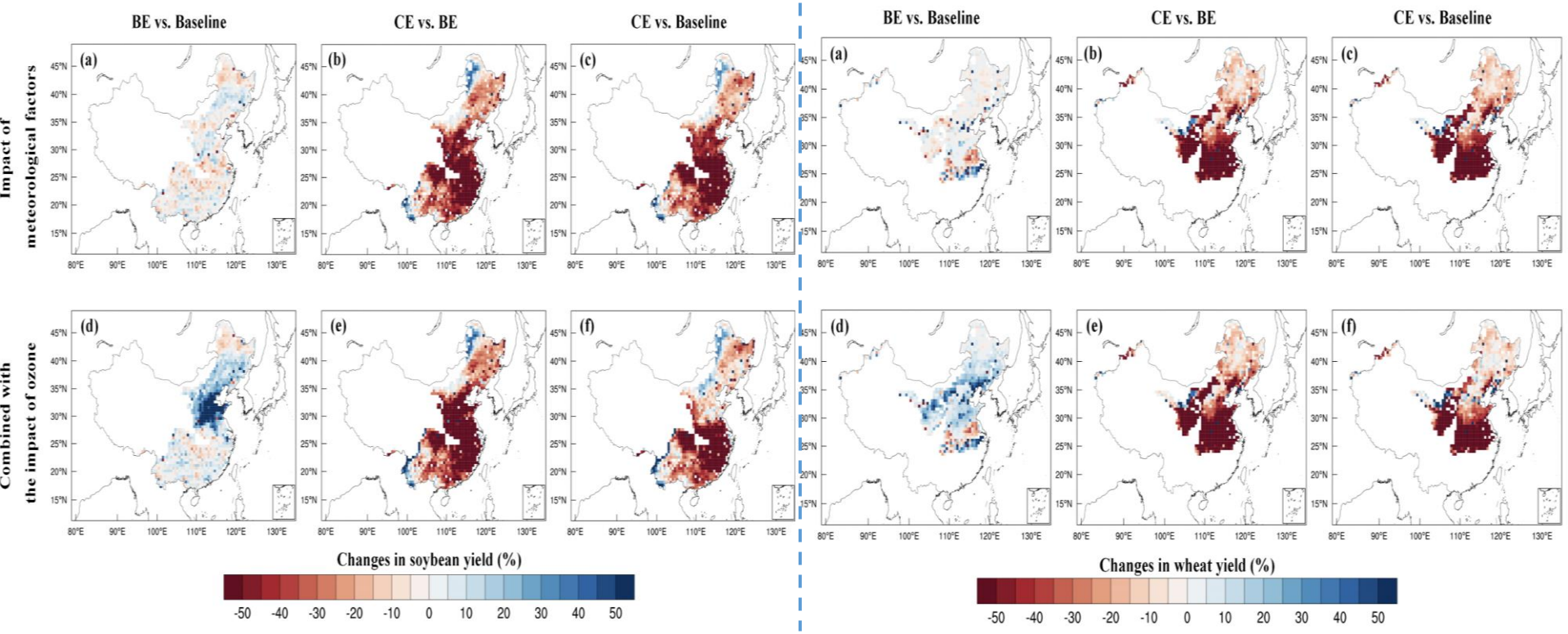

The combined effect of carbon neutrality, which included both meteorological factors and O_3 concentration, resulted in changes to the yields of maize, rice, soybean, and wheat of +4.3%, -7.3%, -24.0%, and -31.7%, respectively.

(Xu et al., 2023)

Atmospheric Environment 299 (2023) 119668

Contents lists available at ScienceDirect

Atmospheric Environment

journal homepage: www.elsevier.com/locate/atmosenv

The mutual interactions among ozone, fine particulate matter, and carbon dioxide on summer monsoon climate in East Asia

Danyang Ma [a], Tijian Wang [a,*], Beiyao Xu [a], Rong Song [a], Libo Gao [a,b], Huimin Chen [a], Xuejuan Ren [a], Shu Li [a], Bingliang Zhuang [a], Mengmeng Li [a], Min Xie [a], Eri Saikawa [c]

[a] School of Atmospheric Sciences, Nanjing University, Nanjing, 210023, China
[b] Jiangsu Meteorological Observatory, Nanjing, 210041, China
[c] Department of Environmental Sciences, Emory University, Atlanta, 30322, USA

HIGHLIGHTS

- Mutual interactions among O_3, $PM_{2.5}$, and CO_2 are considered in RegCM-Chem-YIBs.
- More realistic simulations on meteorolgy and air pollution in East Asia were found when mutual interactions were involved.
- The mutual interactions can significantly modify the summer monsoon climate in East Asia.

ARTICLE INFO

Keywords:
O_3
$PM_{2.5}$
CO_2
Mutual interactions
East Asia summer monsoon climate

ABSTRACT

Ozone (O_3) and fine particulate matter ($PM_{2.5}$) are the major air pollutants, and CO_2 is a critical greenhouse gas in East Asia. They three are active species in terms of radiation. Most importantly, both O_3 and $PM_{2.5}$ can interact with CO_2 through the terrestrial ecosystem, thus having effects on the regional climate. This study investigated the mutual interactions among O_3, $PM_{2.5}$, and CO_2 on the East Asia summer monsoon climate using the coupling regional climate-chemistry-ecology model, RegCM-Chem-YIBs. Two numerical experiments were performed with and without involving the interactions among the three species. The investigations showed that the mutual interactions finally resulted in changes to surface $PM_{2.5}$, O_3, and CO_2 of -6~-2 μg/m^3, 4~6 μg/m^3, and 3~5 ppm, respectively, in northern China. While in southern China, surface $PM_{2.5}$, O_3, and CO_2 varied in the range of 2~4 μg/m^3, 1~2 μg/m^3, and -4~-2 ppm. Surface downward shortwave radiation flux (SWF) and longwave radiation flux (LWF) increased in northern China, whereas showed decreasing in southern China. The lower atmosphere was warmed by 1~2 K in north China, enlarging the air temperature gradient between land and sea, inducing easterly and southerly winds at 850 hpa in the region. On the contrary, surface cooling (-2~-1K) exhibited northerly wind anomalies in southern China. The results indicated that the mutual interactions among the three species could significantly impact regional climate. We argue that future simulations should consider these interactions to better predict air pollution and climate changes in the target region. This work could help to comprehensively understand the climate effects of the mutual interactions among O_3, $PM_{2.5}$, and CO_2. The findings provide a scientific reference for the collaborative governance of regional climate and air pollution in East Asia.

模拟方案

以2018年为例

试验编号	模拟时段	臭氧-颗粒物-二氧化碳之间的相互作用
SIM	2018年4月-2018年8月	考虑
CTRL		不考虑

均对模拟的第一个月不进行分析

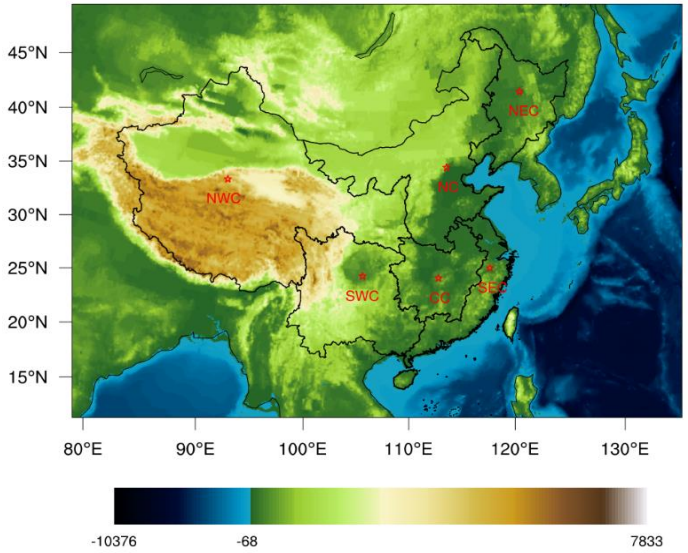

- 模拟时段：2018.4-2018.8，其中4月份为模式预积分阶段
- 两组试验：

✓SIM：模拟真实大气中的三者浓度 ▶▶ 给出O_3、$PM_{2.5}$和CO_2浓度的时空特征

✓CTRL：不包含三者之间的相互作用 ▶▶ 对比SIM，给出相互作用对东亚夏季风气候的影响

模拟方案

■数值模拟

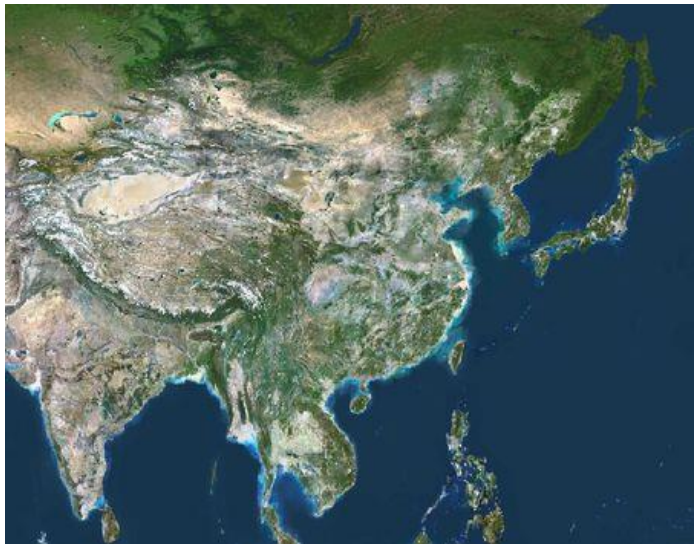

模拟区域

参数化方案

参数	说明
积云对流方案	Grell方案
侧边界条件方案	松弛边界条件(指数)
辐射方案	CCM3
边界层方案	Holtslag PBL方案
表面层方案	Monin-Obukhov方案
水汽方案	显式水汽方案
海洋通量方案	Zeng et al (1998)
海平面温度数据	OI_WK
气象初始边界数据	ERA-Interim

- 分辨率：水平60km、垂直23层
- 排放清单：中国多尺度排放清单MEIC
- 下垫面植被类型数据： MODIS和 AVHRR卫星反演全球土地覆盖类型数据，包含8种植被类型

$PM_{2.5}$-O_3-CO_2相互作用对东亚夏季风气候的影响

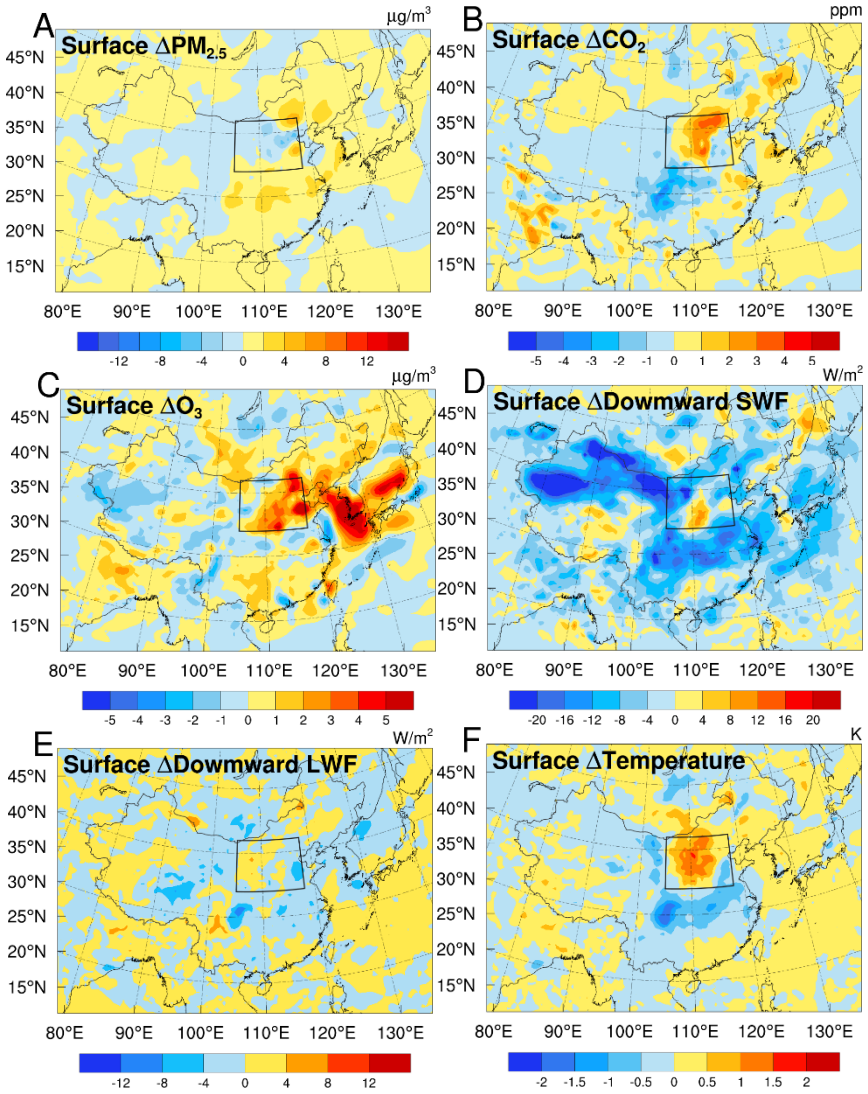

SIM（考虑相互作用）–CTRL（不考虑相互作用）

相互作用对东亚夏季风气候的影响

相互作用

三者浓度

辐射通量

温度

相互作用导致：

- 中国北部增温，海陆温差增大，中国南部海陆温差减小

$PM_{2.5}$-O_3-CO_2 相互作用对东亚夏季风气候的影响

水平风场

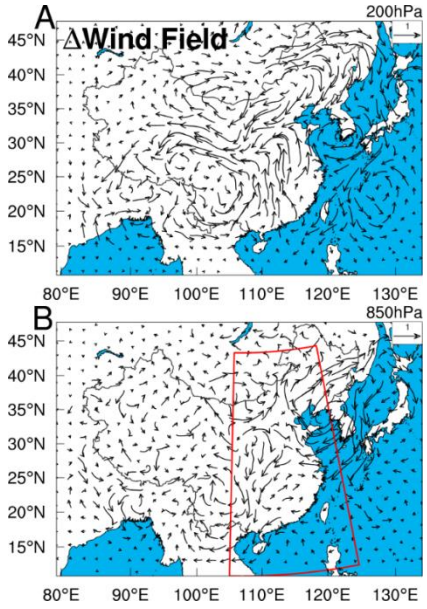

垂直风场

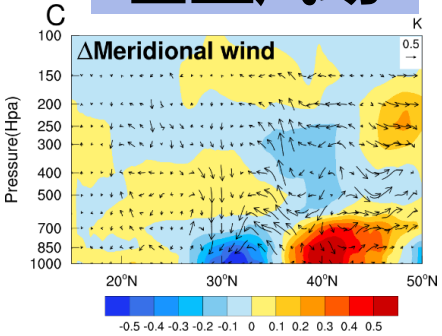

前汛期 **梅雨期** **后汛期**

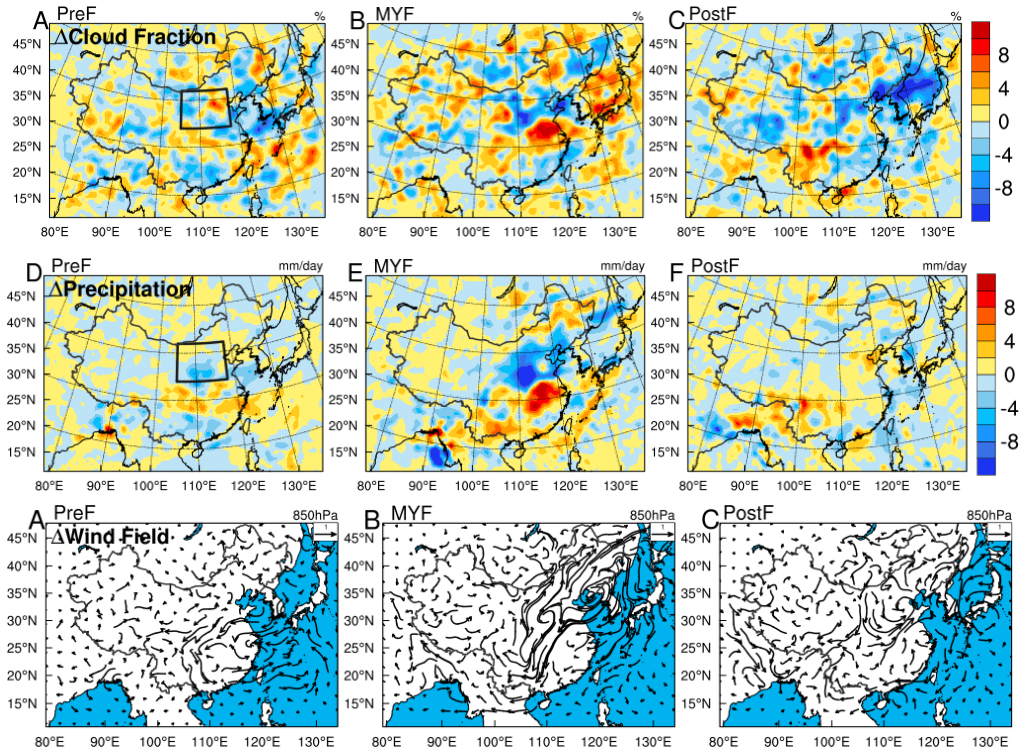

温度变化

↓

风场变化

↓

水汽输送

↓

云和降水

相互作用导致：

- 在近地面，增强了中国北部偏东、偏南风
- 增强了前汛期、梅雨期和后汛中东部的云和降水

$PM_{2.5}$-O_3-CO_2相互作用对东亚夏季风气候的影响

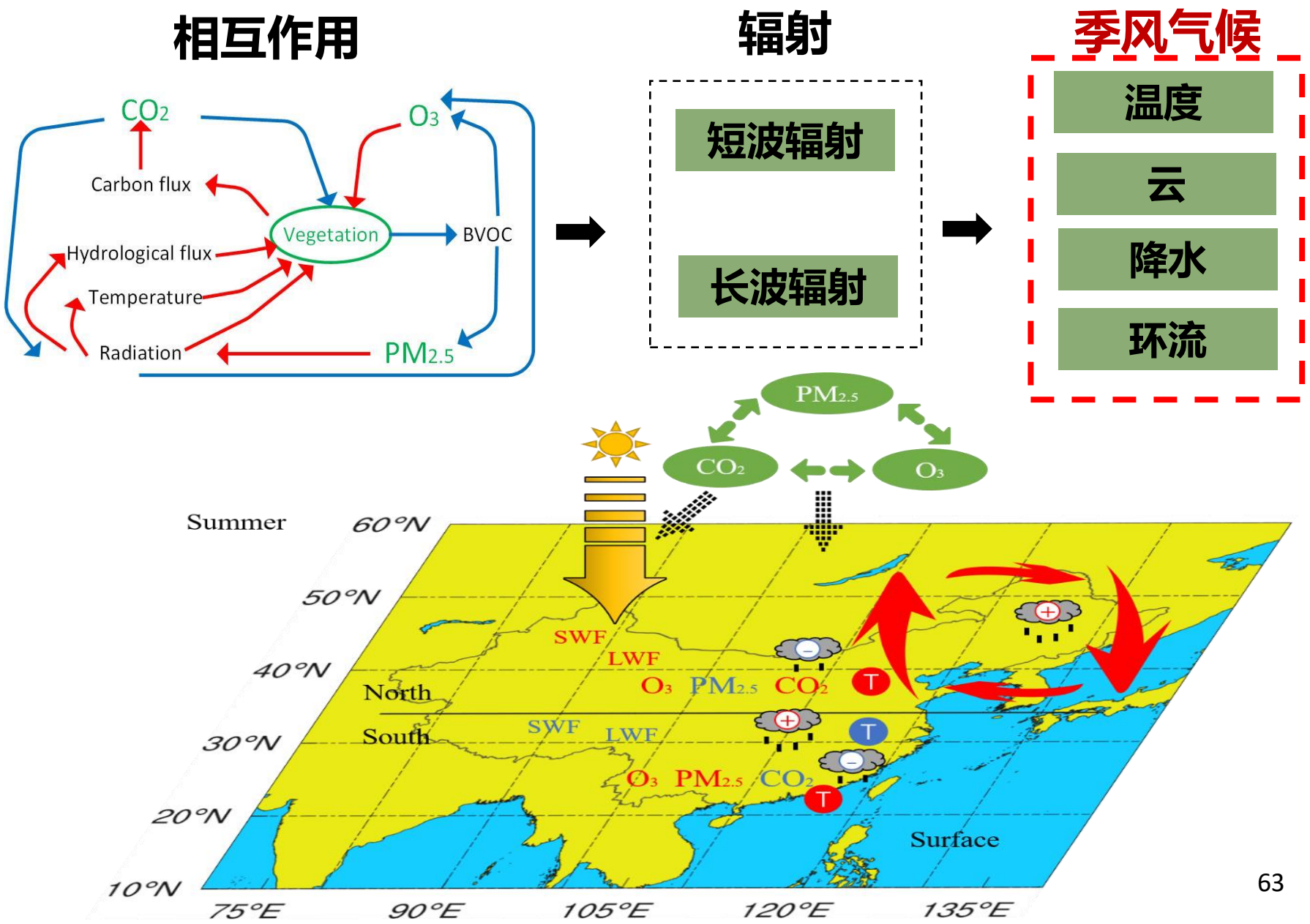

Atmos. Chem. Phys., 23, 6525–6544, 2023
https://doi.org/10.5194/acp-23-6525-2023

Atmospheric Chemistry and Physics
Open Access
EGU

The effect of anthropogenic emission, meteorological factors, and carbon dioxide on the surface ozone increase in China from 2008 to 2018 during the East Asia summer monsoon season

Danyang Ma[1], Tijian Wang[1], Hao Wu[2], Yawei Qu[3], Jian Liu[4], Jane Liu[5], Shu Li[1], Bingliang Zhuang[1], Mengmeng Li[1], and Min Xie[1]

[1]School of Atmospheric Sciences, Nanjing University, Nanjing 210023, China
[2]Key Laboratory of Transportation Meteorology of China Meteorological Administration, Nanjing Joint Institute for Atmospheric Sciences, Nanjing 210000, China
[3]College of Intelligent Science and Control Engineering, Jinling Institute of Technology, Nanjing 211169, China
[4]Key Laboratory for Virtual Geographic Environment of Ministry of Education, Jiangsu Center for Collaborative Innovation in Geographical Information Resource Development and Application, School of Geography Science, Nanjing Normal University, Nanjing 210023, China
[5]Department of Geography and Planning, University of Toronto, Toronto M5S 2E8, Canada

Correspondence: Tijian Wang (tjwang@nju.edu.cn)

Received: 21 December 2022 – Discussion started: 6 February 2023
Revised: 26 April 2023 – Accepted: 5 May 2023 – Published: 14 June 2023

Abstract. Despite the implementation of the Clean Air Action Plan by the Chinese government in 2013, the issue of increasing surface ozone (O_3) concentrations remains a significant environmental concern in China. In this study, we used an improved regional climate–chemistry–ecology model (RegCM-Chem-YIBs) to investigate the impact of anthropogenic emissions, meteorological factors, and CO_2 changes on summer surface O_3 levels in China from 2008 to 2018. Compared to its predecessor, the model has been enhanced concerning the photolysis of O_3 and the radiative impacts of CO_2 and O_3. The investigations showed anthropogenic emissions were the primary contributor to the O_3 increase in China, responsible for 4.08–18.51 ppb in the North China Plain. However, changed meteorological conditions played a crucial role in decreasing O_3 in China and may have a more significant impact than anthropogenic emissions in some regions. Changed CO_2 played a critical role in the variability of O_3 through radiative forcing and isoprene emissions, particularly in southern China, inducing an increase in O_3 on the southeast coast of China (0.28–0.46 ppb) and a decrease in southwest and central China (−0.51 to −0.11 ppb). Our study comprehensively analyzed O_3 variation across China from various perspectives and highlighted the importance of considering CO_2 variations when designing long-term O_3 control policies, especially in high-vegetation-coverage areas.

模拟方案

■数值模拟

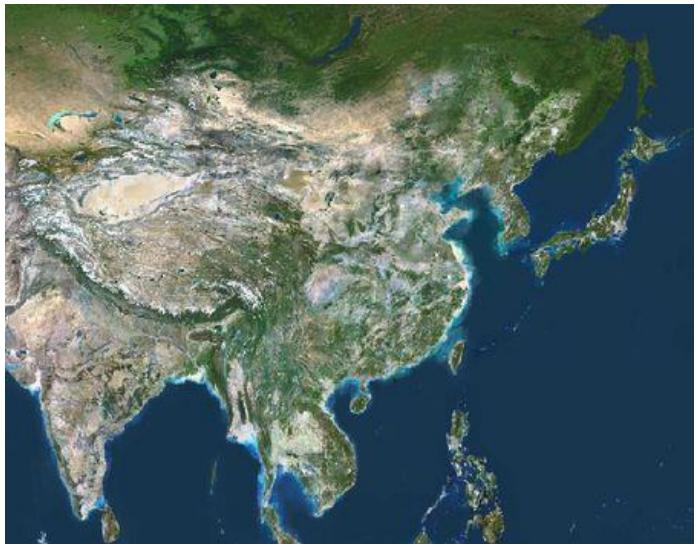

模拟区域

参数化方案

参数	说明
积云对流方案	Grell方案
侧边界条件方案	松弛边界条件(指数)
辐射方案	CCM3
边界层方案	Holtslag PBL方案
表面层方案	Monin-Obukhov方案
水汽方案	显式水汽方案
海洋通量方案	Zeng et al (1998)
海平面温度数据	OI_WK
气象初始边界数据	ERA-Interim

- 分辨率：水平60km、垂直23层
- 排放清单：中国多尺度排放清单MEIC
- 下垫面植被类型数据： MODIS和 AVHRR卫星反演全球土地覆盖类型数据，包含8种植被类型

模拟方案

试验设计

试验编号	模拟时间	气象场	CO_2 排放	人为排放
Base	2008-2018	变化	变化	变化
$SIM_{MET=2008}$	2009-2018	2008	变化	变化
$SIM_{CO2=2008}$		变化	2008	变化

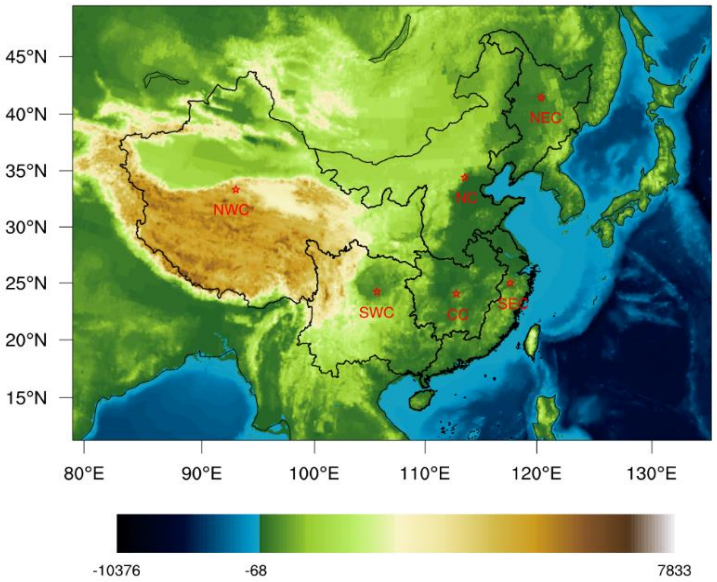

均对模拟的第一个月不进行分析

- 模拟时段：4~8月，其中4月为模式预积分阶段

✓**Base**：模拟真实大气中的O_3浓度 ▶▶ 给出O_3的年际变化特征

✓$SIM_{MET=2008}$：气象场保持在2008年 ▶▶ 对比Base，得到气象条件变化对O_3浓度变化的影响

✓$SIM_{CO2=2008}$：CO_2排放保持在2008年 ▶▶ 对比Base，得到CO_2排放变化对O_3浓度变化的影响

✓人为排放对O_3浓度变化的影响 ▶▶ O_3浓度变化-气象条件的贡献-CO_2排放的贡献

研究数据

■研究资料

1. 地面常规观测

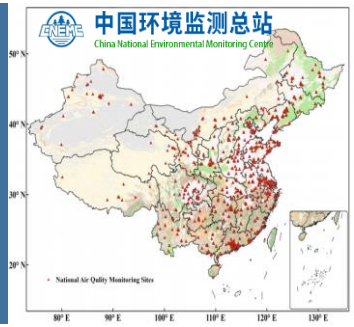

➢ 地面常规观测数据：

✓ 世界温室气体数据中心(WDCGG)，CO_2，月平均

✓ 国家环境空气质量监测网，O_3，$PM_{2.5}$，逐小时

✓ 全球气溶胶监测网(AERONET)，AOD，月平均

2. 卫星遥感监测

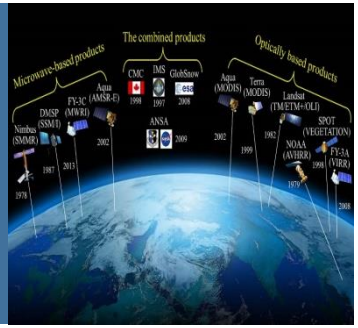

➢ 卫星遥感监测数据：

✓ MODIS-Aqua，云量，1°×1°，日平均

➢ 其他数据：

✓ 欧洲中心再分析资料(ERA-Interim)，温度、相对湿度和风场

✓ MERRA辐射数据，0.5°×0.625°，月平均

✓ GPCP，降水，0.5°×0.5°，月平均

东亚地区O_3和CO_2基本特征

模拟(填色)和观测(圆圈)的空间分布对比

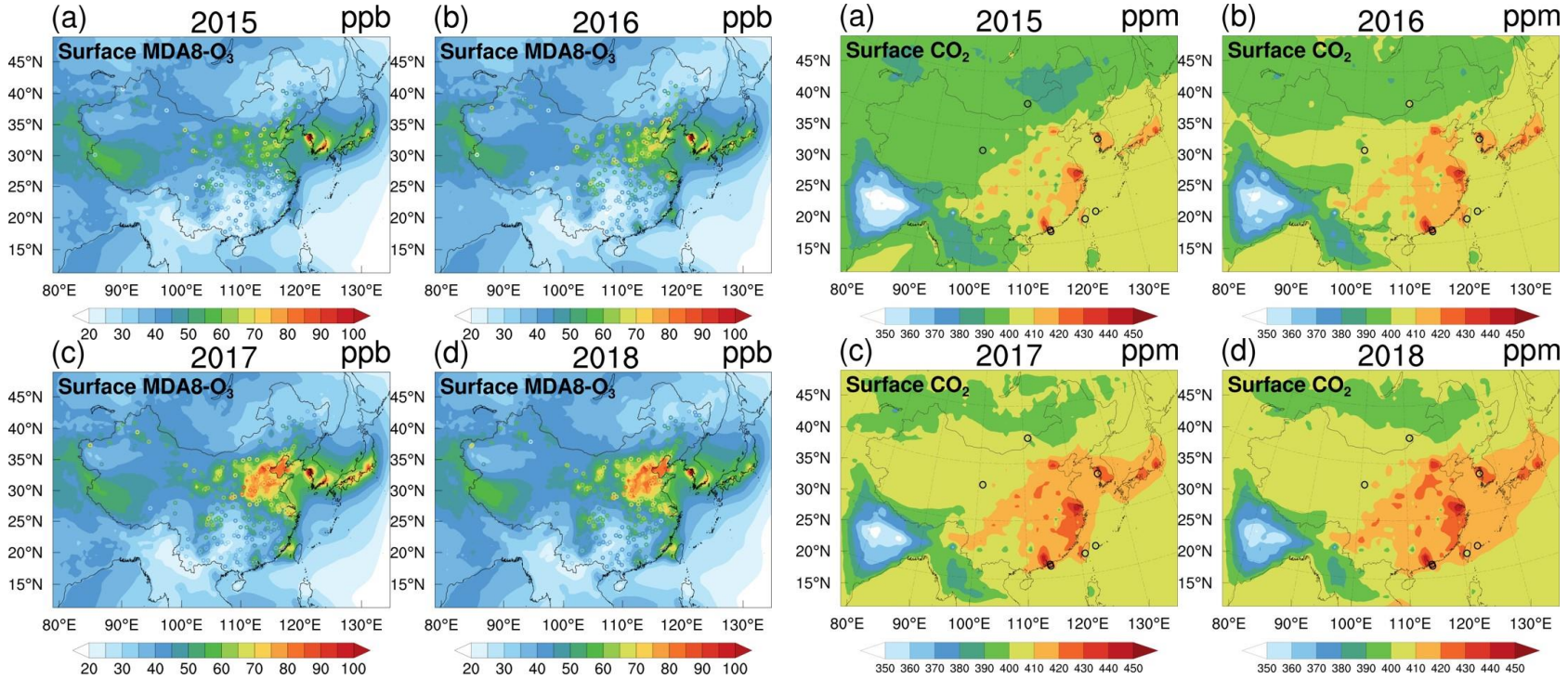

Species	Year	OBS	SIM	MB	RMSE	R
CO_2（ppm）	2015	402.82	406.98	4.16	9.37	0.44
	2016	407.12	410.44	3.32	8.22	0.69
	2017	408.35	413.62	5.27	11	0.39
	2018	409.61	416.68	7.07	11.32	0.41
MDA8 O_3（ppb）	2015	48.77	44.75	-4.02	29.39	0.57
	2016	50.16	46.95	-3.21	27.56	0.60
	2017	55.43	51.87	-3.56	21.55	0.74
	2018	55.53	52.08	-3.42	24.78	0.73

模式验证(Base)

- RegCM-Chem-YIBs模式能够较好地模拟东亚地区O_3和CO_2的浓度水平和空间分布

2008~2018年O_3浓度变化

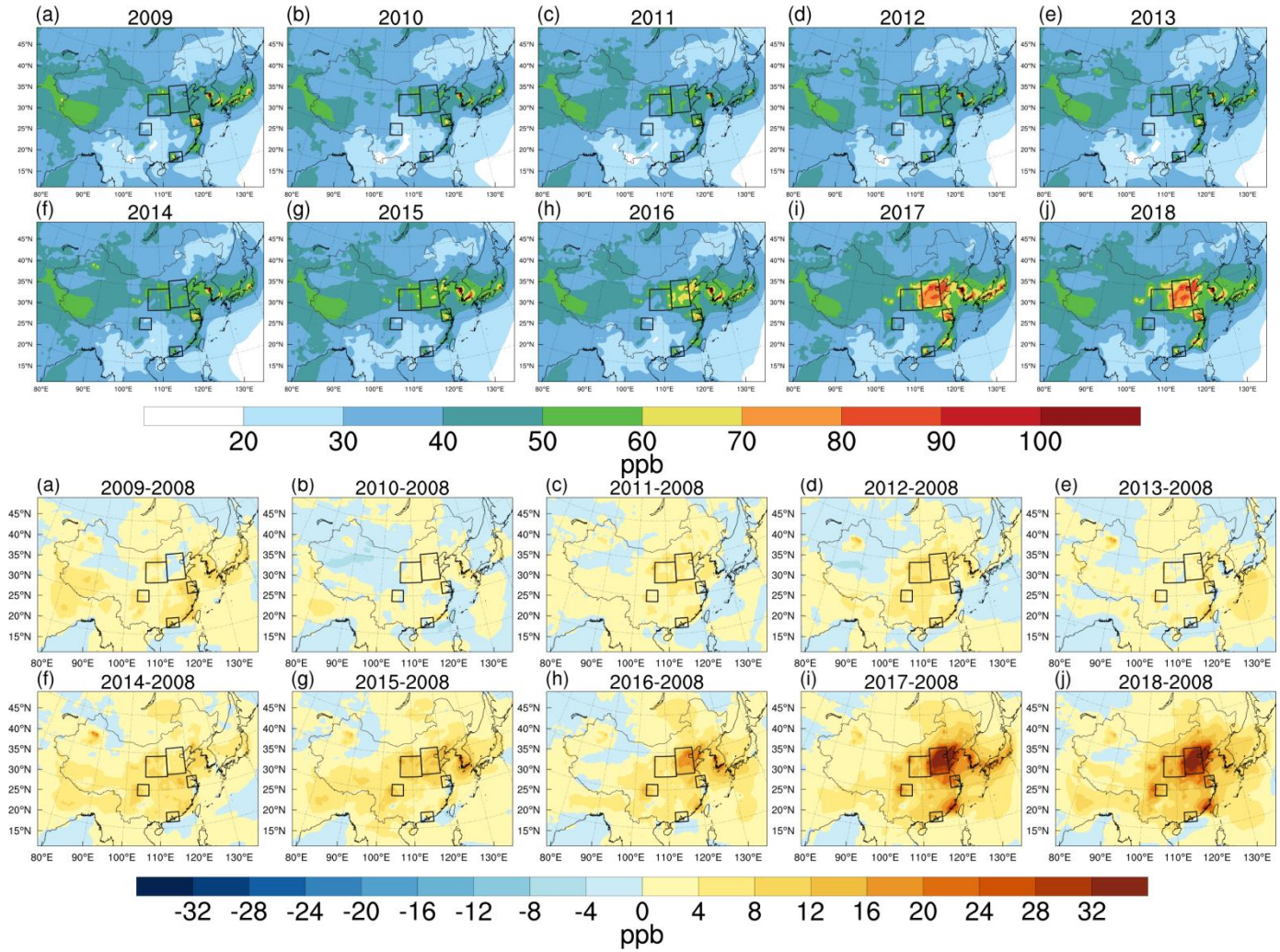

- 2008至2018年间，中国大部分地区的近地面O_3浓度逐年增加，在主要城市群的增加更为显著

气象条件变化对O_3浓度的影响

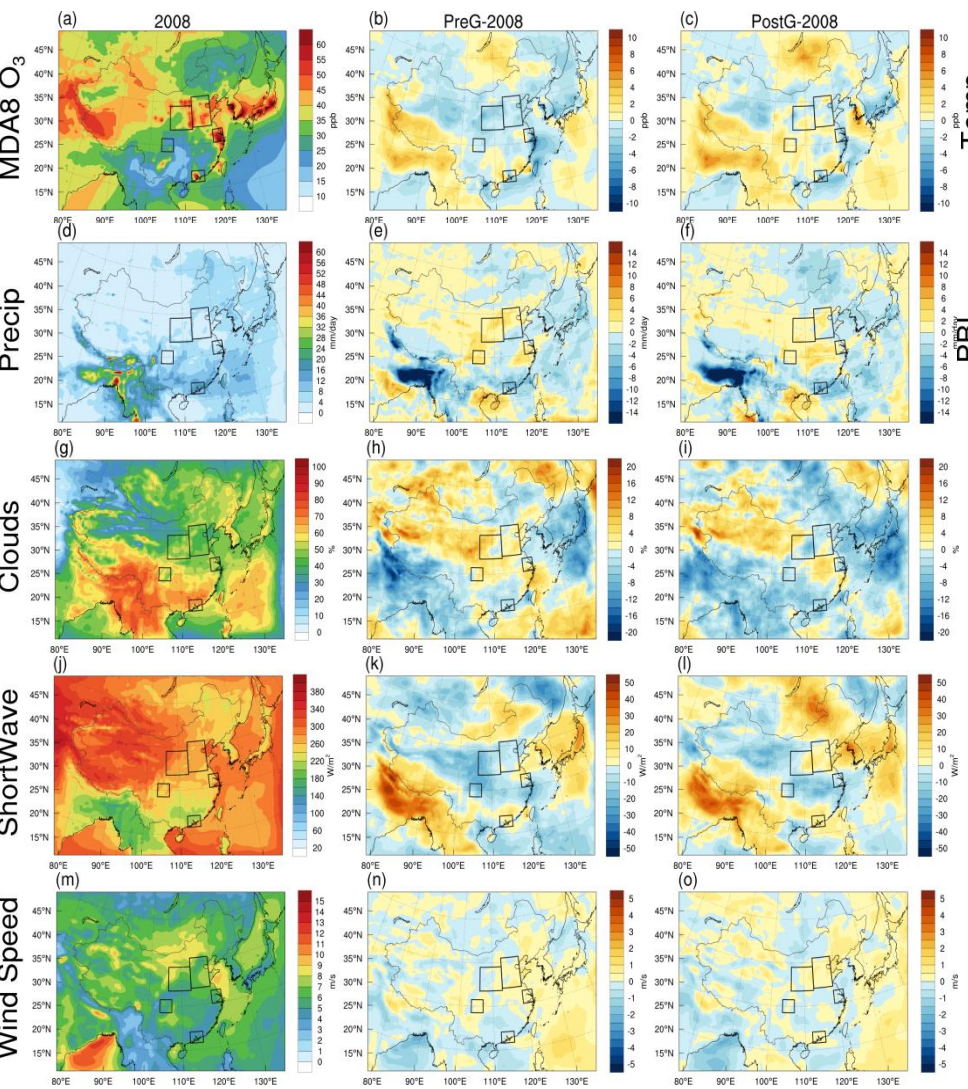

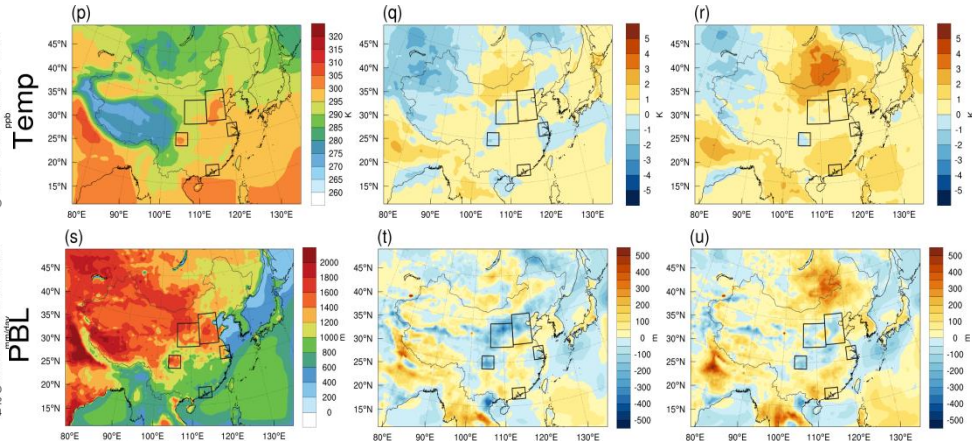

PreG：2009~2013

PostG：2014~2018

降水增加 **短波辐射减少**

云量增加 **风速增加**

温度增加 **边界层高度下降**

气象条件变化

PreG时期减少O_3，PostG时期使O_3增加的范围增大

CO_2排放变化对O_3浓度的影响

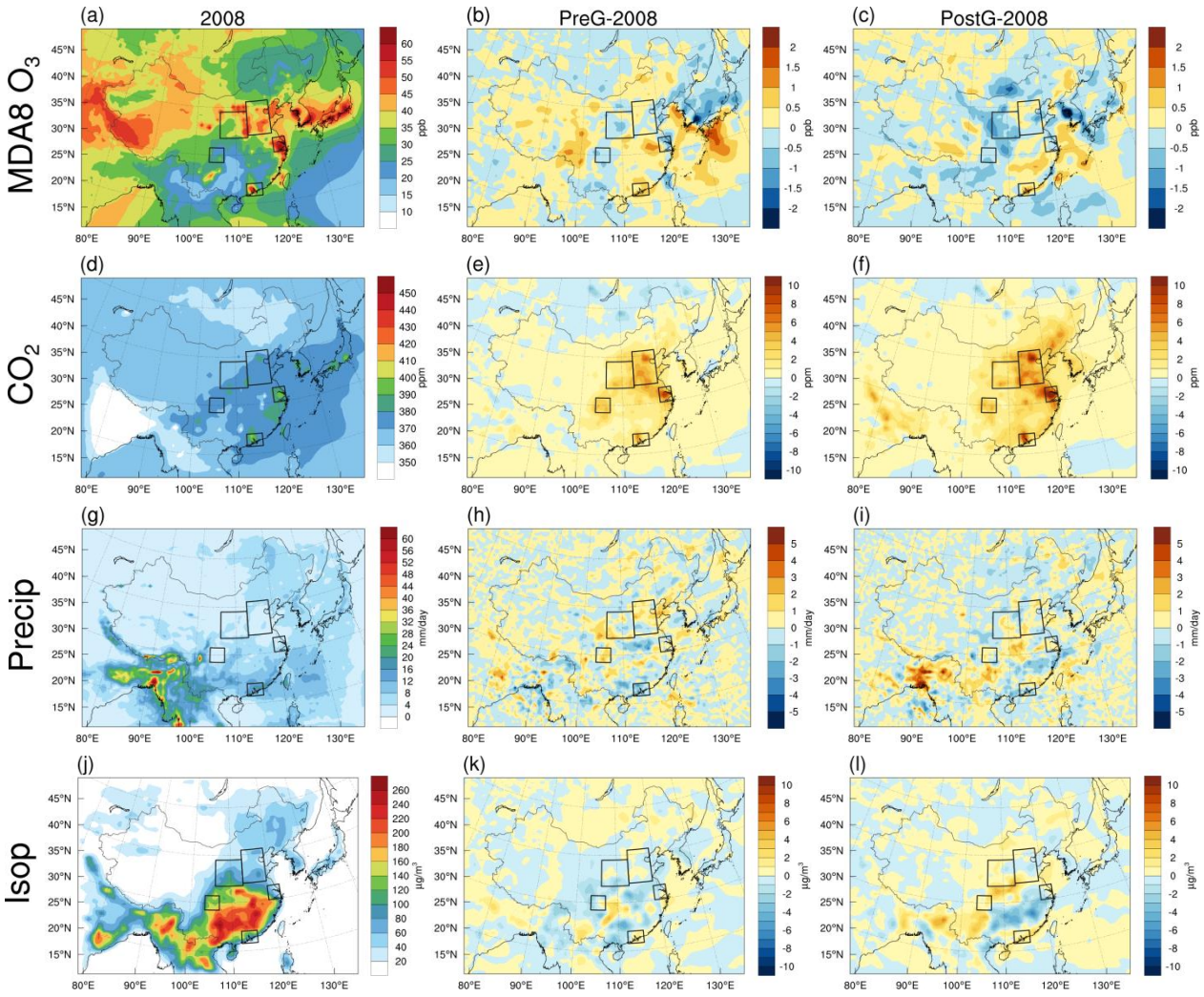

CO_2

辐射　　异戊二烯

降水　　BVOCs

CO_2排放变化

- 中国东南沿海的O_3增加0.28~0.46 ppb，而西南和中部地区减少0.51~0.11 ppb

人为排放变化对O_3浓度的影响

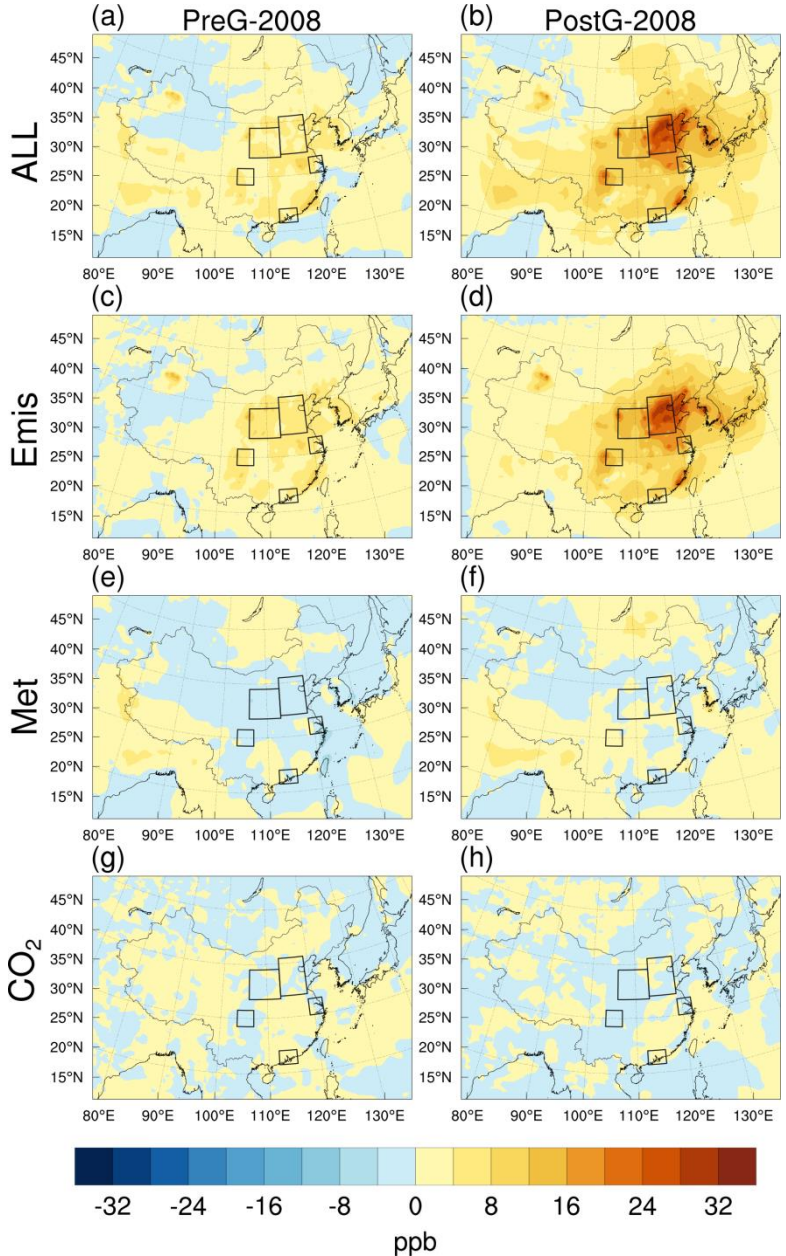

O_3浓度变化－气象条件的贡献－CO_2排放的贡献

↓

人为排放对O_3浓度的影响

Regions	Period	ALL (ppb)	Emis (ppb)	Met (ppb)	CO_2 (ppb)
NCP	PreG	3.27	4.08	-0.88	0.07
	PostG	18.42	18.51	-0.04	-0.05
FWP	PreG	3.63	5.15	-1.41	-0.11
	PostG	10.9	11.5	-0.09	-0.51
YRD	PreG	2.98	4.10	-1.03	-0.09
	PostG	10.07	11.17	-0.96	-0.14
PRD	PreG	2.56	2.33	-0.23	0.46
	PostG	4.94	5.74	-1.08	0.28
SCB	PreG	3.67	4.38	-0.41	-0.30
	PostG	11.21	10.80	0.71	-0.30

人为排放变化

- 人为排放是中国O_3浓度增加的主要原因，在华北平原引起了4.08~18.51 ppb的增加

2008-2018年O_3浓度变化归因

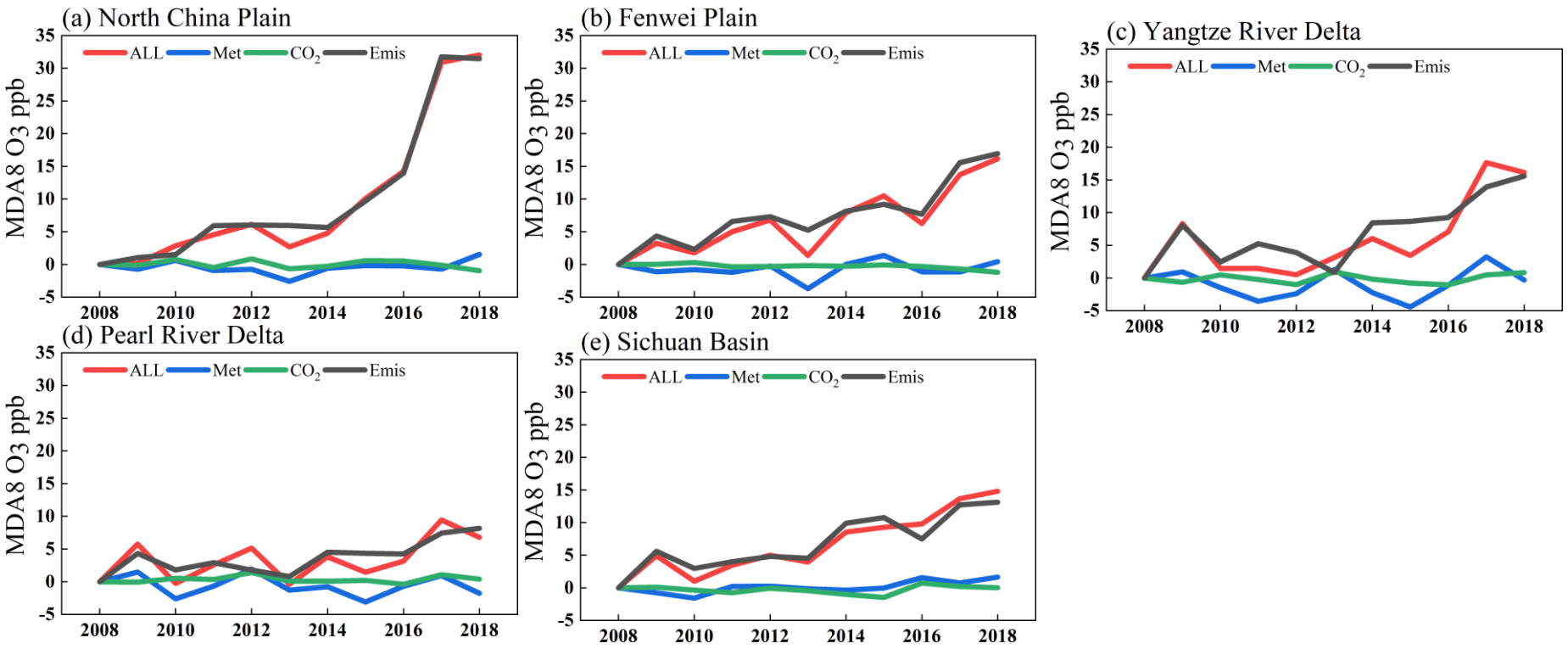

O_3浓度变化

- 人为排放：是O_3浓度增加的主要原因；
- 气象条件：在某些年份和地区与人为排放的影响相当，在YRD和PRD等沿海地区影响较大；
- CO_2排放：在植被茂盛的YRD和PRD地区影响更为显著，个别年份，比人为排放的影响更大。

报告提纲

- 研究背景
- 模式发展
- 应用研究
- 总结展望

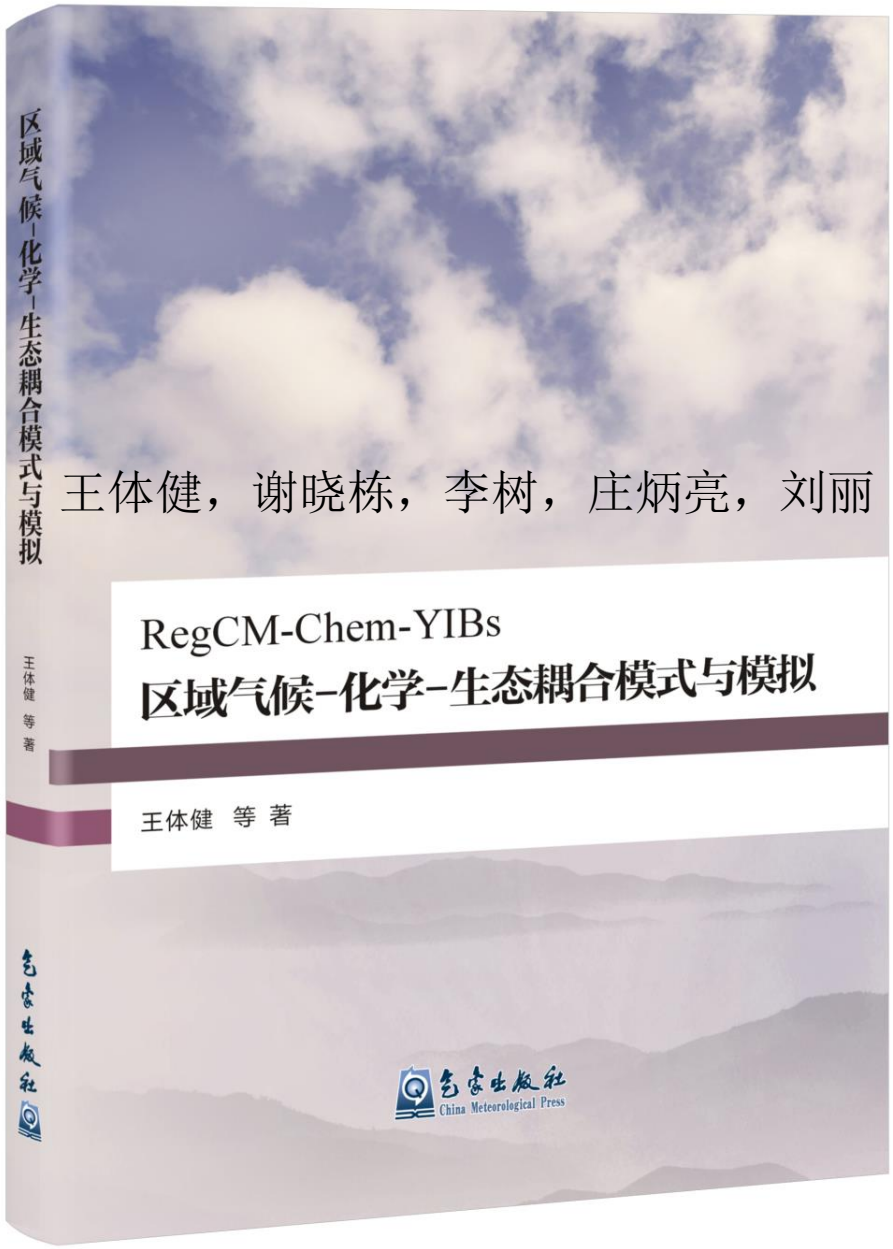

1.空气污染和气候变化
2.区域气候-化学耦合模式
3.区域气候-化学-生态耦合模式RegCM-Chem-YIBs
4.东亚地区大气气溶胶模拟
5.东亚地区大气臭氧模拟
6.东亚地区气溶胶和臭氧的气候效应
7.东亚地区二氧化碳模拟
8.臭氧和颗粒物对二氧化碳浓度的影响
9.全球/气候变化对我国空气污染的影响
10.RegCM-Chem-YIBs模式使用指南